Comparative Study of the PID, Nonlinear PID, and FOPID Controllers for a MIMO Distillation Column Process

Tewodros Asfaw Gebrtsadik

A Thesis Submitted to

The Department of Electrical Power and Control Engineering

School of Electrical Engineering and Computing

Presented in Partial Fulfillment of the Requirement for the Degree of Master's in Electrical Power and Control Engineering (Control)

Office of Graduate Studies

Adama Science and Technology University

September 2021

Adama, Ethiopia

Comparative Study of the PID, Nonlinear PID and FOPID Controllers for a MIMO Distillation Column Process

Tewodros Asfaw Gebrtsadik

Advisor: Prof. Gang Gyoo Jin
Co-advisor: Mr. Enderias Alemayehu (MSc)

A Thesis Submitted to

The Department of Electrical Power and Control Engineering School of Electrical Engineering and Computing

Presented in Partial Fulfillment of the Requirement for the Degree of Master's in Electrical Power and Control Engineering (Control)

Office of Graduate Studies
Adama Science and Technology University

September 2021

Adama, Ethiopia

DECLARATION

I hereby declare that this Master Thesis entitled "Comparative Study of the PID, Nonlinear PID, and FOPID Controllers for a MIMO Distillation Column Process" is my original work. That is, it has not been submitted for the award of any academic degree, diploma or certificate in any other university. All sources of materials that are used for this thesis have been duly acknowledged through citation

Tewodros Asfaw Gebrtsadik		**September 09, 2021**
Name of the student	Signature	Date

RECOMMENDATION

We, the advisors of this thesis, hereby certify that we have read the revised version of the thesis entitled "Comparative Study of the PID, Nonlinear PID, and FOPID Controllers for a MIMO Distillation Column Process" prepared under our guidance by **Tewodros Asfaw Gebrtsadik** submitted in partial fulfillment of the requirements for the degree of Mater's of Science in Control Engineering. Therefore, we recommend the submission of revised version of the thesis to the department following the applicable procedures.

Prof. Gang Gyoo Jin		**September 09, 2021**
Major Advisor	Signature	Date
Mr. Enderias Alemayehu		**September 09, 2021**
Co-advisor	Signature	Date

APPROVAL SHEET

We, the advisors of the thesis entitled "Comparative Study of the PID, Nonlinear PID, and FOPID Controllers for a MIMO Distillation Column Process" and developed by **Tewodros Asfaw Gebrtsadik Id No. PGR/19399/12,** hereby certify that the recommendation and suggestions made by the board of examiners are appropriately incorporated into the final version of the thesis.

Prof. Gang Gyoo Jin	________________	**September 09, 2021**
Major Advisor	Signature	Date
Mr. Enderias Alemayehu	________________	**September 09, 2021**
Co-advisor	Signature	Date

We, the undersigned, members of the Board of Examiners of the thesis by Tewodros Asfaw Gebrtsadik have read and evaluated the thesis entitled "Comparative Study of the PID, Nonlinear PID, and FOPID Controllers for a MIMO Distillation Column Process" and examined the candidate during open defense. This is, therefore, to certify that the thesis is accepted for partial fulfillment of the requirement of the degree of Master of Science in Control Engineering.

________________	________________	________________
Chairperson	Signature	Date
________________	________________	________________
Internal Examiner	Signature	Date
________________	________________	________________
Eternal Examiner	Signature	Date

Finally, approval and acceptance of the thesis is contingent upon submission of its final copy to the Office of Postgraduate Studies (OPGS) through the Department Graduate Council (DGC) and School Graduate Committee (SGC).

________________	________________	________________
Department Head	Signature	Date
________________	________________	________________
School Dean	Signature	Date
________________	________________	________________
Office of Postgraduate Studies, Dean	Signature	Date

ACKNOWLEDGEMENTS

First and foremost, I would like to thank God Almighty for giving me the strength, opportunity, and making it possible to undertake, and complete this thesis satisfactorily without his blessings, this achievement would not have been possible.

I would also like to thank **Adama Science and Technology University**, the School of Electrical Engineering and Computing along with Power and Control engineering chair for the opportunity they have given me to attend this Master's program.

It gives me a great pleasure to express my deepest gratitude to my advisor and mentor **Prof. Gang Gyoo Jin**, for his heartfelt support and guidance at all times. He has given me invaluable guidance, inspiration and suggestions throughout the course of doing this thesis, and I am so thankful.

Beside my advisor, my thanks are extended to my fellow colleagues in electrical Power and Control Engineering department, **Dr. Shubhashish Bhakta**, **Mr. Enderias Alemayehu**, and **Mr. Minyamer Gelawe** who built an academic and very friendly study environment that made my study at the university most enjoyable and skillful.

My acknowledgement would be incomplete without thanking the biggest source of my strength, my families and friends for all the love, support and encouragement. It would have been impossible without having you around.

Thank you.

Tewodros Asfaw Gebrtsadik

TABLE OF CONTENTS

LIST OF TABLES

LIST OF FIGURES

LIST OF ACRONYMS AND ABBREVIATION

BDC	Binary Distillation Column
CH_3OH (MeOH)	Methanol
C1	Controller one
C2	Controller two
DC	Distillation Column
DCP	Distillation Column Process
FOPID	Fractional Order Proportional Integral and Derivative
GA	Genetic Algorithm
H_2O	Water
IAE	Integral Absolute Error
LC	Level Controller
MIMO	Multiple Input and Multiple Output
NPID	None-linear Proportional Integral and Derivative
P	Proportional
PI	Proportional Integral
PID	Proportional Integral and Derivative
PSO	Particle Swarm Optimization
RGA	Relative Gain Array
RK4	Rang Kutta Fourth Order
RNGA	Relative Normalized Gain Array
SP	Set Point
SISO	Single Input and Single Output
TITO	Two Inputs and Two Outputs
WD	With Decoupler
WOD	Without Decoupler
WB	Wood and Berry
ZN	Ziegler Nicholas

ABSTRACT

Distillation column is one of the most important units in a chemical plant. The distillation column is a multiple input multiple output (MIMO) process that means all the inputs, and outputs are coupled to each other. Usually, MIMO system introduce challenges to design controller without decoupling. This thesis provides a comparative analysis of different control strategies used to control the top, and bottom product of a distillation column by considering the effect of decoupling. The Wood-Berry (WB) distillation column model is considered which separates methanol from water. The influence of the feed flow rate disturbance is considered for this model. In order to reduce or eliminate the cross interaction between the inputs and outputs, it is necessary to design a decoupler which enables the process to convert into two independent single input and single output system (SISO). The proportional-integral-derivative (PID), nonlinear PID (NPID), and fractional-order PID (FOPID) controllers are designed for the DC control and their parameters are optimally tuned using a genetic algorithm (GA). Performance evaluation of the corresponding controllers is done using MATLAB/Simulink. The simulation result reveals that the system with decoupling reduced total error compared with the system without decoupling in terms of SP tracking and disturbance rejection.

Keywords: *Distillation column, Wood and Berry model, Decoupling, PID controller, Nonlinear PID controller, FOPID controller, and Genetic Algorithm.*

CHAPTER 1

INTRODUCTION

1.1 Background

The separation of liquid mixtures into their various components is one of the major operations in the process industries. Distillation column is one of the most common unit operations used in most of the chemical and petroleum industries. It is used for the separation and the purification of mixtures containing two or more components in a typical process. Distillation has various applications such as the separation of crude oil into different oil cuts (e.g. diesel, gasoline, kerosene, etc.), water desalination and purification, the separation of air into its components (e.g. nitrogen, oxygen, and argon), and the production of distilled beverages or the distillation of fermented solutions with high alcohol content [1].

The vertical cylindrical column provides a large number of separate stages of vaporization and condensation in a compact form and with the minimum of ground requirements. Due to its highly nonlinear properties, its Multiple Inputs Multiple Outputs (MIMO) structure, and the occurrence of disturbances during operation, controlling the distillation column process presents certain challenges. The chemical process is challenging to model and regulate due to the system's relative uncertainty [2].

The quality and purity of the distillation column are critical, hence effective system control is required. Thus, predicting the behavior of multistage distillation columns has been the basis of many studies, including controlling top and bottom columns via control schemes. The internal and external flow of liquid and vapor in distillation columns has substantial time delays. The rate at which a change in reflux ratio is transmitted from tray to tray inside the column is determined by the hold-up on each tray and the down comer's capacity. A change in feed rate or composition, for instance, cannot be transmitted instantly via the column.

Long-time lags, particularly for quick input disturbances, have a significant impact on the column's controllability. The distillation column is a (MIMO) process that is more complicated to understand and operate than a single-input single-output (SISO) process. From a control aspect, these systems have a number of issues: delayed dynamic response, high order behavior, substantial dead times, nonlinearity, and multivariable interaction [3].

The safe and efficient operation of many plants depends on the consistent and reliable performance of one or more distillation columns. To control top concentration, bottom concentration, reboiler level, and reflux rate level, a distillation column has at least four feedback control loops. In processes where there are significant time lags between the measurements of the controlled variable and the result of the control action, the feed-back performs poorly. Suppose the lag is large and the controlled variable fluctuates quite rapidly by the time the control action takes effect. In that case, it may well augment the disturbance rather than reduce it. Even if the disturbance is subsequently decreased, the controlled variable may remain outside of specification limits for an extended period of time.

Decoupling control is another control approach that is used to control multivariable processes that include interaction between control loops. By constructing an appropriate decoupler for the loops, this strategy decreases or eliminates the effect of interaction. It necessitates a thorough understanding of the dynamic behavior of the controlled variables in order to detect changes in the disturbance and manipulated variables. [4] [5].

In process control methodologies the most widely used feedback control strategy are Proportional Integral Derivative (PID) controller. Because it is still the most efficient and has simple structure. The meaning of three parameters or gains, which can be easily understood by process operators. Many studies have been used various tuning methods of PID controller gains such as Ziegler and Nichols [2], Cohen and Coon [3], gain phase margin methods, and so on. These methods are based on trial and error and process reaction curve which may not give the required performance on the controlled variable.

After a time, many researchers introduced different forms of PID controllers such as Fractional-order PID (FOPID) and Nonlinear PID (NPID) controllers. The system is highly nonlinear, multivariable process with strong interactions with input and output pairs. This research work provides a comparative analysis of PID, FOPID, and NPID controllers used to control top and bottom product of distillation column using the Wood- Berry model. Moreover, to minimize the control interactions decoupling is considered. Optimal tuning of these controllers gain is needed for the best performance of the system. In order to determine the optimal gain set of these controllers a genetic algorithm (GA) is used. In line with this, objective functions such as integral absolute error, and control signal (IAEU), integral time absolute error, and control signal (ITAEU), and integral square error, and control signal (ISEU) are used in order to select the best optimal gains of the three controllers. The performances of the controllers in the proposed system are evaluated based on steady-state and transient state parameter performances under set-point tracking and disturbance rejecting capabilities.

1.2 Statement of the Problem

Distillation column is used in a typical process for the separation and the purification of mixtures containing two or more components by the application and removal of heat. It consumes a huge amount of energy in both heating and cooling operations. A proper control of distillation columns operation is important due to reduction of energy consumption during operation. However, designing a controller is a highly challenging task due to the interaction or coupling which exists between various control loops of the distillation column. In addition, distillation column is a highly complex and non-linear multivariable process, and it is subject to constraints and disturbances. The steady-state operation of the column is disturbed by the sudden change in the feed flow rate. Besides, the model uncertainty affects the performance of the distillation column process.

Adding a decoupler can improve the above problems to some extent by reducing or eliminating the controller's interaction effect. However, designing a decoupler is not enough in order to eliminate the disturbance effect and set-point tracking problems. Thus, to mitigate these problems feedback control is required. In this study, a comparative analysis using PID, FOPID, and NPID controllers are designed and decoupling control is employed based on genetic algorithm (GA) optimization technique. The three control systems are implemented using MATLAB software tool.

1.3 Objectives of the Study

1.3.1 General Objective

The general objective of this thesis work is to carry out the comparative study of the performance of the PID, Nonlinear PID, and FOPID controllers for a MIMO distillation column process.

1.3.2 Specific Objectives

The specific objectives are:

- ✓ To analyze the interaction of the input-output pairs of the process

- ✓ To design a decoupler for the DC process
- ✓ To design GA-tuned PID, NPID, and FOPID controllers for the top and bottom composition control of the DC process.
- ✓ To simulate the response of the DC process with the designed controllers using MATLAB/Simulink.
- ✓ To evaluate the performance of the PID, NPID, and FOPID controllers based on set point tracking and disturbance rejection.
- ✓ To compare the responses of the process with and without decoupling.

1.4 Scope of the Study

The scope of this thesis focuses on design the PID, NPID, and FOPID controllers for distillation columns in cooperation with genetic algorithm optimization techniques. The decoupling control, mathematical modeling, and simulation of GA-based top and bottom composition control of the distillation column using MATLAB/Simulink for the chemical industry application is implemented.

1.5 Limitation of the Study

Due to complex nature of the DC system, in this work the controller design of the reflux level and reboiler level are not considered. Also, the proposed plant structure is limited to only a 2×2 distillation column. The simulation data is gathered from related literatures, this is because of the engineers working in the Wonji sugar factory do not know the basic structure and actual data of the DC. Moreover, the distillation of the methanol and water using 8-tray and 9-inch DC in the industries is limited in the country.

1.6 Motivation of the Study

The use of distillation columns is very vast in process control industries, chemical industries, and oil refineries. It plays a significant role in separating the constituent of a mixture to make the process automatic. The process dynamics of the system are complex and nonlinear. A distillation column is applicable in different industries in order to separate two or more mixtures. The controlled variables and manipulated variables must be paired so that the necessary controlling action can be taken place. It has good research areas and can be implemented in different nonlinear control systems.

1.7 Significant of the Study

This research study is useful in the areas of chemical industries for the separation and the purification of mixtures containing two or more components. Distillation has various applications such as;

- The separation of crude oil into different oil cuts (e.g., diesel, gasoline, kerosene, etc.),
- Water desalination and purification,
- The separation of air into its components (e.g., nitrogen, oxygen, and argon) and,
- The production of distilled beverages or the distillation of fermented solutions with high alcohol content.

1.8 Thesis Organizations

This thesis is organized into six chapters.

Chapter 1: The first chapter includes introduction of the research work, statement of the problems, objectives, significance, scope, and limitation of the research area of application, methodology and definition of terms.

Chapter 2: Presents a literature review on the background of distillation column process, different control mechanisms, and working of distillation column to the application of methanol with water are discussed.

Chapter 3: Covers distillation column system modelling, computation of relative gain array, decoupler design, and the steady-state analysis of distillation column with and without decoupling.

Chapter 4: Present the design of the controllers, the optimization algorithm, and objective functions are designed.

Chapter 5: Summarizes the results of the simulation work and discusses them.

Chapter 6: Finally, conclusion and recommendation are made.

CHAPTER 2

THEORETICAL BACKGROUND AND LITERATURE REVIEW

In this chapter the background of distillation column and working principle of distillation column are discussed. Closely related works especially in top and bottom composition along with their merits and demerits are reviewed and discussed.

2.1 Distillation Column System

In the chemical and petroleum industries, distillation columns are used to separate various liquids based on their physical and chemical properties. The distillation column is the most common and significant process unit, and it has been extensively researched and examined in the chemical engineering field in recent years. [6] [7]. Distillation is a thermal separation technique for separating a combination of two or more liquid materials into their appropriate quality component fractions based on the components' volatility differences. It is worth noting that distillation is a single step in a physical separation process.

However, the combination of different distillation process operations leads to the introduction of new distillation processes such as a fractional column or with a chemical reaction, leading to the introduction of chemical reactive distillation and other chemical process operations.

In the petrochemical industry, distillation columns are one of the most common plant units, along with utilities. The feed enters from one side of the column, but the exact height of the input stream into the column varies depending on the application. Due to its lower boiling point, one liquid boil earlier than the other and transforms into vapor when the feed is heated. The light product is a vapor liquid that is collected from the top of the distillation column and condensed to return it to liquid distillate before being stored or fed into other downstream units for further processing. The heavier component of the feed that remains in a liquid form is collected from the bottom of the distillation column and is termed to as bottoms [8].

Because of the following factors, controlling the distillation column becomes challenging.

- Presence of number of interacting variables
- Extreme process interactions
- Dead times and non-linearity in the process
- The process variables are difficult to measure.

For a long time, researchers in both the academic and industry sectors have been interested in distillation column control systems because of all of the aforementioned reasons and additional industrial plant challenges. The most critical aspect of distillation column (DC) control is maintaining consistent product quality. Because the distillation column is a complex, highly nonlinear, and multivariable process, engineers and operators have found it difficult to regulate and operate. As a result, different control strategies have been developed to solve this difficult control problem [9]. Refining has different applications such as the separation of rough oil into different oil cuts (e.g., diesel, gasoline, lamp fuel, etc.), water desalination and refinement, the division of air into its components (e.g., nitrogen, oxygen, and argon), and the production of refined beverages or the refining of fermented arrangements with high alcohol substance.

2.2 The Working Principle and Components of a Distillation Column

2.2.1 Component of Distillation Column

A distillation column is a fundamental component of a refinery that separates a mixture of chemical products based on their boiling points. As can be seen in Figure 2.1, have a schematic of a distillation column. A distillation column is basically a long tower (Much long if a super fractionator considers). Trays are placed at various heights of the tower and are separated by a constant length throughout the tower. Furthermore, each tray features a bubble cap that allows for mass transmission. Then there's the feed, which is a mixture of several chemicals, in this case fractional distillation (only two components in the mixture), that must be separated using different temperature profiles.

The distillation column, reflux, and reboiler are the most important components. Consider how the reflux system works. It features a surge tank that stores the mixture's light key and the pressure of the distillation column is controlled by a condenser, and the level of the light key is controlled by a surge tank and acts as an input to the reflux which introduce the light key to the process and the level of the surge tank is controlled by the output valve. Only the quality or purity of the light and heavy key of the chemical mixture are considered in this case. Then there's the re-boiler, which works in the same way as the reflux only it has a boiler that heats up the hot key and acts as a heat source for the distillation column.

To govern distillate concentration, bottom concentration, reboiler level, and reflux rate, a distillation column has at least four feedback control loops [10]. As a reason, it is classified as a MIMO control issue. This work proposes a controller for controlling distillate and bottom concentrations. MIMO control can be accomplished by using two controllers, one for each variable. The detail working principle of the distillation column process depict below.

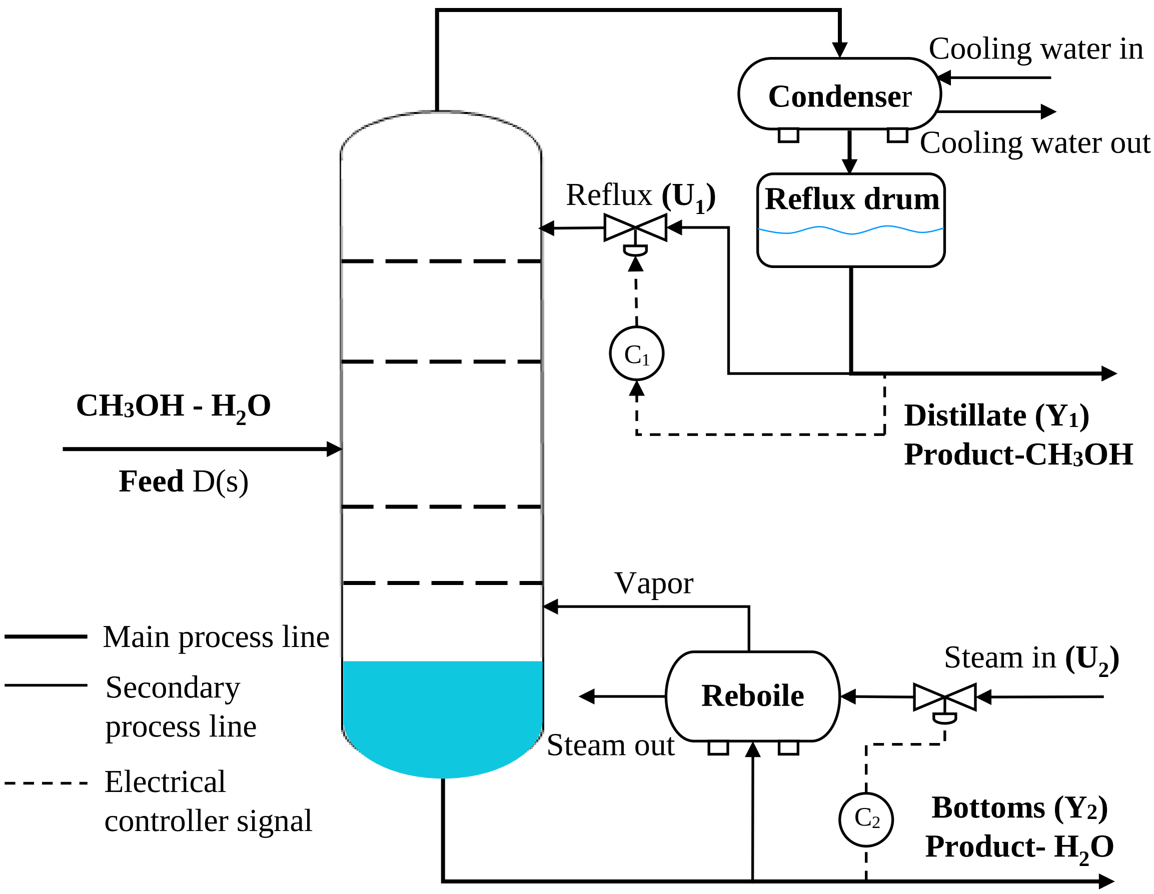

Figure 2. 1 Schematic diagram of the conventional two point distillation column control system [11] [L1].

2.2.2 Working of Distillation Column

A chemical plant contains a mixture of water (H_2O) and methanol (CH_3OH). In the sense that water has a greater boiling point than methanol and vice versa, water is a heavy key and methanol is a light key. When the mixture is entered into the column, the light key will heat up due to high temperature and go in to the form of the gas step by step and tray by tray in the distillation column and ends up at the highest point in the column in a gas phase then it got condense by the condenser and got store into the surge tank and due to high boiling point methanol stuck up at bottom and purity of the product depends on the boiler temperature of the distillation column. The reflux's function is to return the chemical that has been held in the reflux surge tank, which contains light key methanol and a little amount of heavy key water. Due to the continued reflux feedback process, the pure light key is now up to standards and within tolerance levels, and the process can now be seen from the perspective of the heavy key. Heavy key water will sink down in the distillation column due to its high boiling point and is collected at the bottom of the distillation column, which runs through the reboiler to heat up before being sent back to the column, which helps to keep the column at the proper temperature during the separation process. Now, the purity of the heavy key can be controlled utilizing feed flow, reflux flow rate, reboiler temperature, or feedback to the reboiler system. And the Light key is also subject to the same requirements. This is the coupling problem, which occurs when you try to control numerous outputs using multiple system inputs. This type of system is referred to as a coupled system since the outcome is dependent on multiple inputs.

2.3 Related Works on Distillation Column Control

Several research papers were reported on the distillation column control system by using different tuning and optimization algorithm approaches. Distillation column processes are MIMO systems and their parameters are co-related each other [2]. Hence such a system needs a decoupler for the interaction of system parameters in order to reduce the sluggish response of the controllers [5]. In this section the closely related works are reviewed and discussed.

Implementation of fuzzy logic control for FOPDT model of distillation column has been reported in literature [12]. PID, Fuzzy, and Fuzzy-PID controllers were compared in terms of dynamic performance parameters like settling time, rise time, and overshoot. Accordingly

Fuzzy-PID controller has better dynamic performance than other controllers. It is known that the system has disturbances due to the composition process and flow rate of the liquid mixture. The drawback is, the system is not decoupled in order to remove the effects of the systems inputs and outputs interaction.

In [13], authors implemented GA to optimize two simple PI controller gains with different sets of tuning parameters to control the top and bottom compositions of a binary distillation column. Also, the comparison of the proposed PI controller is made with the ZN method and the control systems dynamic performance is obtained in terms of settling times, output overshoot, control efforts and consumed power. Even though the proposed controller has good performance in case of set point tracking, the authors did not check the performance with decoupler and disturbance rejection capabilities.

A comparative analysis of the distillation column process control for the top and bottom composition of wood and berry model has been summarized in literature [14]. The Non-dimensional tuning (NDT) method and Particle Swarm Optimization (PSO) algorithms were used for tuning of the two PID top and bottom composition controller gains. For wide range of process operation, the simulation results shows that PSO algorithm provides the most efficient approach for tuning a controller and furthermore the response of the proposed controller is proved to be fast and stable than the controller tuned by NDT method. Besides, the PSO tuned PID controller reduces the overshoot, settling time, rise time and peak time. The gaps on the proposed controllers were simulated without considering the unsettling influence impact on the system.

In a similar manner, the comparative analysis using Active Disturbance Rejection Control (ADRC) and convectional PI controllers for distillation column process has been developed in literature [15]. The performance of ADRC was found that the ADRC scheme gives much better control performance than the PI controller in terms of set-point tracking, rejection of control loop interactions, and external disturbance rejection. However, decoupler are not incorporated for the controller study in distillate column.

In literature [16], FLC and PID controllers based on cuckoo search-based optimization algorithm for the control of top and bottom compositions in a binary distillation column have been proposed. In addition, an additive online FLC is also utilized for the plant subjected to the model parameter variations. The authors demonstrated that online controller is superior to offline in terms of performance index integral square error (ISE). For the implementation of control system, a decoupler is not considered in this literature.

The authors in [11], developed a comparative analysis of a binary distillation column using two PI controllers for the top and bottom systems. Ziegler Nicholas (ZN) and Skogestad Simple Internal Model Control (SIMC) tuning methods were used to optimize the gains of the two PI controllers. The result shows that SIMC tuned PI control system is better dynamic efficiency in terms of settling times, output overshoots, control effort and consumed power than ZN tuned PI controllers. The limitation is, decoupler are not considered for the controller interaction in the distillate column.

According to [9], a comparative analysis of various control algorithm under non-interactive situation are employed in order to control the distillate and bottom composition using four controllers. These controllers are internal model controller (IMC), lead lag IMC, feed-forward IMC, and smith predictor IMC. Considering the transient state performance, the simulation result found to be better for feed forward IMC controller compared to the rest of the controllers during disturbance at top and bottom product composition. Also, lead-lag IMC provides better response in set point regulation scenario for the same controller. However, decoupler are not incorporated for the controller study in distillate column.

In [2], model based predictive controller (MPC) is designed for a multivariable plant i.e., Distillation column to directly control the products composition, as an alternative indirect method of temperature control. The Distillation column considered is Wood and Berry Model and PID controller is designed and tuned by Biggest Log modulus Tuning (BLT) & ZN methods with and without decoupling elements. The simulation results confirm that the MPC has better tracking response in comparison to PID in terms of decline in rise time, number of overshoots and effective set point tracking subjected to set point changes for both bottom and distillate composition.

In general, the performances of the different controllers based on different optimization techniques are reviewed in this section. In addition, mainly the controllers were performed without disturbance rejection capabilities and decoupler in order to avoid the system parameter interactions in the control system.

This research study provides a comparative analysis of different controllers for the control of top and bottom products of distillation column with decoupler. Different controllers such as PID, NPID, and FOPID are designed and the performance of the controllers is evaluated based on steady state and transient state performance parameters. Set point regulation and disturbance rejection property of the controllers are also evaluated using simulation. The gains of each controller in top and bottom composition of distillation column are optimized using genetic algorithm (GA) optimizer.

CHAPTER 3

MATHEMATICAL MODEL OF THE SYSTEM

In this chapter, data collection inclusion with analysis, mathematical model of the distillation column (DC) system, and decoupling are presented in detail. The steady-state analysis of the distillation column with and without decoupling are discussed. While modeling the system components, the non-linear terms are linearized by using Francis-Weir equations.

3.1 Materials

In this research work, software such as MATLAB/2020a, Microsoft office 2016, Mendeley, and Math Type 6.9 equation editor are used. MATLAB is the computing software which consists of technical toolboxes and Simulink [L2]. Microsoft office is used for editing the thesis documentation. Mendeley is a free reference manager that may help us organize citations, collect references, and make bibliographies [L3]. Math Type 6.9 is used for editing mathematical equations in Microsoft offices word and PowerPoint presentation tools.

3.2 Methods

To analyses the specific objectives of the proposed research study, the following method is employed. First, the works that are closely linked are examined. After that, the relevant data for their work is gathered. Distillation column process specifications have taken from different literatures and related works. The acquired data is mathematically examined in order to comprehend and build system modeling. Then a wood and berry (WB) transfer function model with time delay of distillation column for a nine-inch diameter and eight trays is implemented.

Finally, the comparative relation of PID, NPID, and FOPID controllers for the top and bottom composition of distillation column using GA optimization are done in MATLAB/Simulink environment. The following flow chart, as illustrated in Figure 3.1, summarizes the method used throughout the research study.

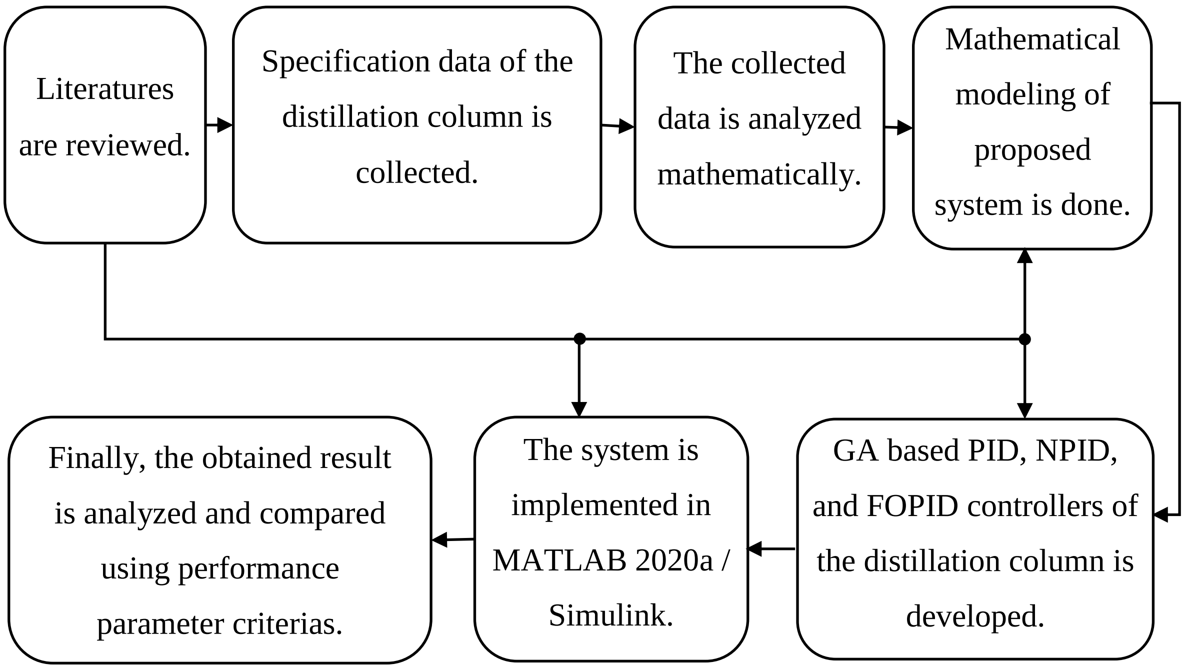

Figure 3. 1 Block diagram of the research methodology

3.3 Modeling of a Distillation Column Process

3.3.1 Structure of the DC Process

The proposed block diagram of the distillation column process for the top and bottom composition control is shown in Figure 3.2.

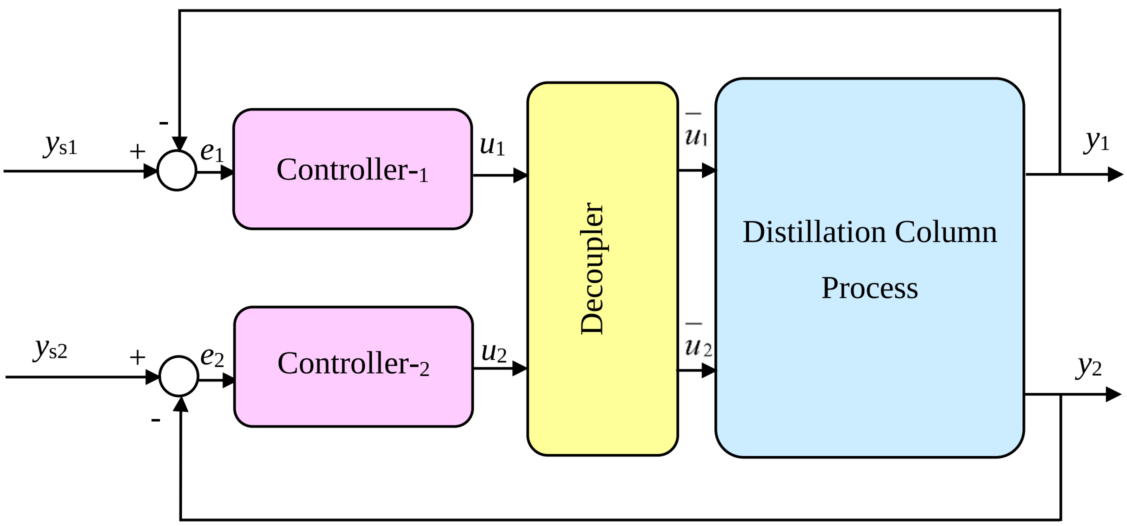

Figure 3. 2 Block diagram of a MIMO distillation column process

In a typical DC, trays are employed to improve component separations in a vertical column. [6]. The necessary vaporization from the bottom of the column is accomplished with the help of a reboiler. The vapor from the top of the DC is cooled and condensed by the condenser. The condensed vapor is stored in the reflux drum so that liquid reflux can be recycled from the top of the column. There are two product streams and one feed stream in the DC [7]. Mostly, for the MIMO system it is necessary to design a decoupler to minimize the interaction between the inputs and outputs effect in the feedback control system. The top and bottom composition of a DC system using different controllers are designed in Chapter four.

In order to study the control algorithms, a precise model of the DC process is required. In the present work, two-input and two-output DC system based on the Wood and Berry (WB) model is taken for case study. Figure 3.3 depicts the simplified process with inputs, outputs, and disturbances.

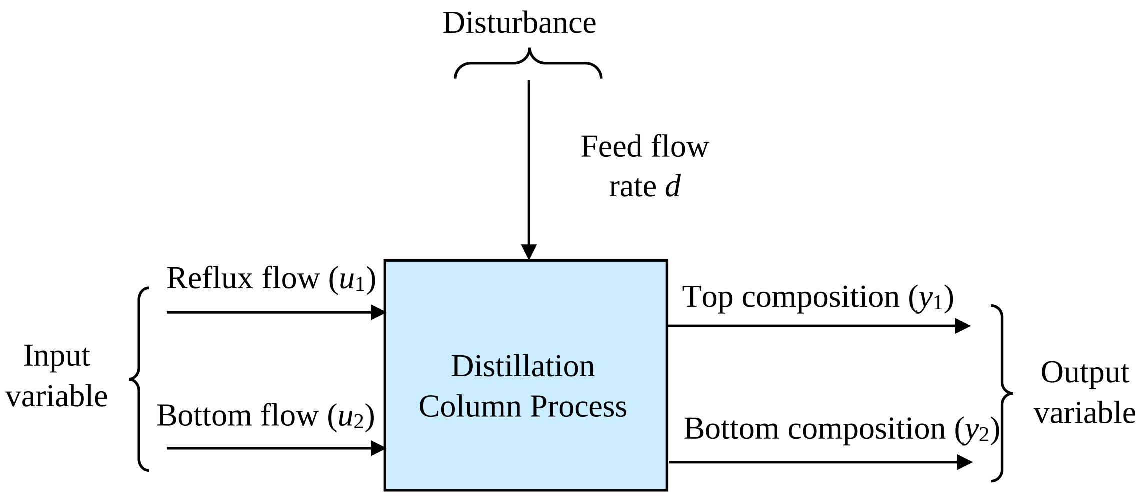

Figure 3. 3 I/O signals of the DC process [11].

3.3.2 Mathematical Modeling of the DC Process

The modeling of the DC process is helpful in comprehending the nature, properties, and operation of the column. It is a nonlinear, non-stationary, and MIMO system with strong interactions between inputs and outputs. There are many mathematical models that are proposed by different researchers, such as Tyreus stabilizer, Wood and Berry, Vinante and Luyben, Wardle and Wood, and Orgunnaike and Ray [4]. In this work the Wood and Berry (WB) model is considered. This is due to two reasons, the first is the WB model is experimentally implemented. Secondly, the 2×2 system model which contain eight trays DC of nine-inch diameter. WB modeled empirically by considering separating methanol from water using DC consisting of eight tray, condenser, basket type reboiler of nine inch diameter [17]. A mole percent of the component known as *xF* is present in the feed. The light component of the product stream at the top has a composition of y_1 (xD), whereas the heavy component of the product stream exiting the bottom has a composition of y_2 (xB). Every array of the distillation column assumes liquid holdup. Figure 3.4 depicts a 2x2 structure of a distillation column process.

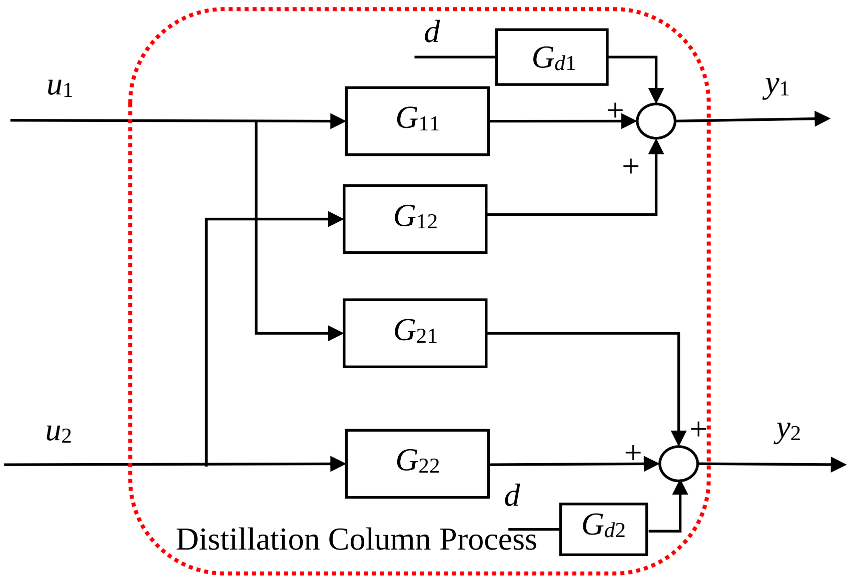

Figure 3. 4 Two-input and two-output representation of the distillation column

The differential equations related to the plant modelling are described in this section. For linearization and modelling the variable liquid hold up, the Francis-Weir formula is utilized, and it is stated as [5], [18], [19], [20].

$$L_n = L_{n0} + \frac{M_n - M_{n0}}{\beta} \tag{3.1}$$

where L_n, L_{n0}, and M_{n0} are internal liquid flow rate, reference value of internal liquid flow rate, and reference molar holdup for the nth tray, respectively.

For condenser and reflux drum the mathematical model can be given as:

$$\frac{dM_D}{dt} = V_{NT} - (R + D_L + D_V) \tag{3.2}$$

where M_D molar holdup in reflux drum, in mols, L_{N+1} reflux, mol/min, D distillate, mol/min, V vapor flow, mol/min.

Component mass balance is described by

$$\frac{dM_D X_D}{dt} = V_{NT} Y_{NT} - (R + D_L) X_D - D_V Y_D \tag{3.3}$$

where X_D component of liquid distillate.

The modeling for the top tray (NT) is given by Equations (3.4) - (3.5).

$$\frac{dM_{NT}}{dt} = R + V_{NT-1} - L_{NT} - V_{NT} \tag{3.4}$$

$$\frac{dM_{NT} X_{NT}}{dt} = RX_D - L_{NT} X_{NT} + V_{NT-1} Y_{NT-1} - V_{NT} Y_{NT} \tag{3.5}$$

The mathematical model for the nth tray is represented by

$$\frac{dM_n}{dt} = L_{n+1} - L_n + V_{n-1} - V_n \tag{3.6}$$

where M_n denotes liquid holdup on the nth tray, in moles, L_N liquid leaving tray n, mol/min.

Component mass balance is stated by

$$\frac{dM_n X_n}{dt} = L_{n+1} x_{n+1} - L_n x_n + V_{n-1} Y_{n-1} - V_n Y_n \tag{3.7}$$

For feed tray (at NF) the mathematical model is expressed by Equation (3.8)

$$\frac{dM_{NF}}{dt} = L_{NF+1} - L_{NF} + V_{NF-1} - V_{NF} + F_L \tag{3.8}$$

where M means liquid holdup on the feed tray in moles and L liquid leaving feed tray in mol/min

Component mass balance is stated by

$$\frac{dM_{NF} X_{NF}}{dt} = L_{NF+1} x_{NF+1} - L_{NF} x_{NF} + V_{NF-1} Y_{NF-1} - V_{NF} Y_{NF} + F_L Z_L \tag{3.9}$$

For bottom tray the mathematical model is

$$\frac{dM_1}{dt} = L_2 - L_1 + V_B - V_L \tag{3.10}$$

Component mass balance is stated by

$$\frac{dM_1 X_1}{dt} = L_2 X_2 - L_1 X_1 + V_B Y_B - V_1 Y_1 \tag{3.11}$$

The mathematical model for a reboiler and column base can be represented as:

$$\frac{dM_B}{dt} = L_1 - V_B - B \tag{3.12}$$

Component mass balance is stated by

$$\frac{dM_B X_B}{dt} = L_1 X_1 - L_B Y_B + V_B Y_B - B X_B \tag{3.13}$$

where M_B molar holdup in column base, in moles, B bottoms flow, mol/min, L_1 liquid leaving tray 1, mol/min, V vapor boil up in recoiled, mol/min.

The vapor liquid equilibrium is also utilized in the distillation process to relate the vapor phase composition to the liquid phase composition of the more volatile component.

$$Y_n = \frac{\alpha X_n}{1 + (\alpha - 1) X_n} \tag{3.14}$$

where Y_n is vapor phase composition, X_n is liquid phase composition for n^{th} tray in distillation column, and α is relative volatility respectively.

It is well known that variation in feed flow rate is the most common external disturbances in a distillation column [21]. The disturbances affecting the distillation column has a strong effect on the product composition. According to the Wood and Berry model in Equation (3.15), this disturbance models is considered. Usually, the disturbance magnitude of the distillation column is around 10–20% of the nominal value in the operating points [22]. In this study the design of the feed stream which means that feed entering into the column has to be stay constant to work properly.

The system has four transfer functions in the form of first order dynamics and significant time delays. Here the objective of the control system is to adjust the controlled variables y_1 and y_2 by manipulating the input variables u_1 and u_2. Therefore, the overall distillation column is described by mathematical model as given in Equation (3.15). It is a MIMO process with strong interaction between two input and two output pairs. The simplified dynamic model used in [14], [23] is defined as,

$$\begin{bmatrix} Y_1(s) \\ Y_2(s) \end{bmatrix} = \begin{bmatrix} G_{p11}(s) & G_{p12}(s) \\ G_{p21}(s) & G_{p22}(s) \end{bmatrix} \begin{bmatrix} U_1(s) \\ U_2(s) \end{bmatrix} + \begin{bmatrix} G_{d1}(s) \\ G_{d2}(s) \end{bmatrix} D(s) \tag{3.15a}$$

Based on the specifications data of the proposed system shown in Appendix F, the wood and berry model transfer function are given by the following equations [14], [23], [24].

$$\begin{aligned} G_{p11}(s) &= \frac{12.8e^{-s}}{16.7s+1}, \qquad G_{p12}(s) = \frac{-18.9e^{-3s}}{21s+1} \\ G_{p21}(s) &= \frac{6.6e^{-7s}}{10.9s+1}, \qquad G_{p22}(s) = \frac{-19.4e^{-3s}}{14.4s+1} \end{aligned} \tag{3.15b}$$

The disturbance transfer equations are given by

$$\begin{aligned} G_{d1}(s) &= \frac{3.8e^{-8s}}{14.9s+1} \\ G_{d2}(s) &= \frac{4.9e^{-3.4s}}{13.2s+1} \end{aligned} \tag{3.15c}$$

where u_1 and u_2 as the inputs denote reflux flow rate (*lb*/min) and steam flow rate (*lb*/min) respectively, y_1 and y_2 as the outputs distillate methanol (*mol*%) and water (*mol*%) respectively, and d as the disturbance of unmeasured flow rate (*lb*/min). Finally, the system in Equation (3.15) can be rewritten in the compact from as:

$$\boldsymbol{Y}(s) = \boldsymbol{G}_p(s)\boldsymbol{U}(s) + \boldsymbol{G}_d(s)D(s) \tag{3.16a}$$

$$\boldsymbol{Y}(s)=\begin{bmatrix}Y_1(s)\\Y_2(s)\end{bmatrix},\quad \boldsymbol{U}(s)=\begin{bmatrix}U_1(s)\\U_2(s)\end{bmatrix},$$

$$\boldsymbol{G}_p(s)=\begin{bmatrix}G_{11}(s) & G_{12}(s)\\G_{21}(s) & G_{22}(s)\end{bmatrix},\quad \boldsymbol{G}_d(s)=\begin{bmatrix}G_{DF}(s)\\G_{BF}(s)\end{bmatrix} \tag{3.16b}$$

where $Y_1(s)$ (*lb/min*) and $Y_2(s)$ (*lb/min*) are percentages of methanol in the distillate and bottom compositions, respectively. $U_1(s)$ and $U_2(s)$ are the reflux and reboiler vapor flow rates, respectively and $D(s)$ (*lb/min*) is the feed flow rate disturbance.

3.3.3 Calculation of Relative Gain Array (RGA)

Due to the existence of interactions between input and output variables, MIMO processes are more difficult to control than single-input single output (SISO) systems in general [25]. The Relative Gain Array (RGA) is the most often used interaction measure, and it provides a way for selecting a suitable pairing in a decentralized control structure. The input-output coupling with the largest positive value closest to one in the relative gain element should be chosen, while the pairing with a negative RGA element should be avoided [26].

The RGA is a numerical matrix. The array's *ij*th element is referred to as λ_{ij}. It is the ratio of the steady-state gain between the *j*th controlled variable and the *j*th manipulated variable when all other manipulated variables are constant. And then divided by the steady-state gain between the same two variables when all other controlled variables are constant. Dual composition control can be considered of as a time-delayed two-input two-output (TITO) multivariable system. [26]. From the input-output relations for the process without disturbances, is defined by Equations (3.17) and (3.18).

$$Y_1(s)=G_{p11}(s)U_1(s)+G_{p12}(s)U_2(s) \tag{3.17}$$

$$Y_2(s)=G_{p21}(s)U_1(s)+G_{p22}(s)U_2(s) \tag{3.18}$$

Using Equations (3.16) yields the steady-state gain matrix as [27] [28].

$$\begin{aligned}\boldsymbol{K} &= \lim_{s\to 0} \boldsymbol{G}_p(\mathrm{s})\\ &= \begin{bmatrix}K_{11} & K_{12}\\K_{21} & K_{22}\end{bmatrix}\end{aligned} \tag{3.19}$$

Based on the steady-state operation the input output equation is expressed as,

$$Y_1 = K_{11}U_1 + K_{12}U_2 \tag{3.20}$$

$$Y_2 = K_{21}U_1 + K_{22}U_2 \tag{3.21}$$

The open-loop gains can be obtained using Equation (3.15b) [27].

$$K_{11} = \frac{\partial y_1}{\partial u_1}\Big|_{U_2=0} = 12.8 \tag{3.22a}$$

$$K_{12} = \frac{\partial y_1}{\partial u_2}\Big|_{U_1=0} = -18.9 \tag{3.22b}$$

$$K_{21} = \frac{\partial y_2}{\partial u_1}\Big|_{U_2=0} = 6.6 \tag{3.22c}$$

$$K_{22} = \frac{\partial y_2}{\partial u_2}\Big|_{U_1=0} = -19.4 \tag{3.22d}$$

Once the open-loop gains K_{ij} have been obtained, evaluation of the closed-loop gains K^*_{ij} can be determined by assuming the outputs Y_1 and Y_2 zero independently,

Now let's find the expression of U_2 considering $Y_2 = 0$ in Equation (3.21).

$$U_2 = \frac{-K_{21}U_1}{K_{22}} \tag{3.23}$$

Substituting Equation (3.23) into Equation (3.20) yields the closed loop steady-state gain K^*_{11} as shown in Equation (3.24a) [29], [30].

$$K^*_{11} = \frac{\partial y_1}{\partial u_1}\Big|_{y_2=0} = K_{11} - \frac{K_{12}K_{21}}{K_{22}} \tag{3.24a}$$

The other steady state closed loop gains can be calculated by using the same approach used in K^*_{11}.

$$K^{*}_{12} = \frac{\partial y_1}{\partial u_2}\Big|_{y_2=0} = K_{12} - \frac{K_{11}K_{22}}{K_{21}} \tag{3.24b}$$

$$K^{*}_{21} = \frac{\partial y_2}{\partial u_1}\Big|_{y_1=0} = K_{21} - \frac{K_{22}K_{11}}{K_{12}} \tag{3.24c}$$

$$K^{*}_{22} = \frac{\partial y_2}{\partial u_2}\Big|_{y_1=0} = K_{22} - \frac{K_{21}K_{12}}{K_{11}} \tag{3.24d}$$

The relative gain (λ_{ij}) is the ratio of K_{ij} to K^{*}_{ij} and represented by Equation (3.25) [28].

$$\begin{aligned} \lambda_{ij} &= \frac{\text{Open-loop gain between } y_i \text{ and } u_j}{\text{Closed-loop gain between } y_i \text{ and } u_j} \\ &= \frac{K_{ij}}{K^{*}_{ij}} = \frac{\partial y_i}{\partial u_j}\Big|_u \Big/ \frac{\partial y_i}{\partial u_j}\Big|_y \end{aligned} \tag{3.25}$$

where the relative gain, λ_{ij} relates the ith controlled variable and the jth manipulated variable.

$$\lambda_{11} = \frac{1}{1 - \frac{K_{12}K_{21}}{K_{11}K_{22}}} = \frac{1}{1 - \frac{(-18.9)(6.6)}{(12.8)(-19.4)}} = 2.0094 \tag{3.26}$$

$$\lambda_{12} = \frac{1}{1 - \frac{k_{11}k_{22}}{k_{12}k_{21}}} = \frac{1}{1 - \frac{(12.8)(-19.4)}{(-18.9)(6.6)}} = -1.0094 \tag{3.27}$$

$$\lambda_{21} = \frac{1}{1 - \frac{k_{22}k_{11}}{k_{21}k_{12}}} = \frac{1}{1 - \frac{(-19.4)(12.8)}{(6.6)(-18.9)}} = -1.0094 \tag{3.28}$$

$$\lambda_{22} = \frac{1}{1 - \frac{k_{21}k_{12}}{k_{22}k_{11}}} = \frac{1}{1 - \frac{(6.6)(-18.9)}{(-19.4)(12.8)}} = 2.0094 \tag{3.29}$$

Finally, the overall RGA model of the system is obtained by combining all state equations of the sub-systems and given in Equation (3.30).

$$RGA = \begin{bmatrix} \lambda_{11} & \lambda_{12} \\ \lambda_{21} & \lambda_{22} \end{bmatrix} = \begin{bmatrix} \dfrac{1}{1-\dfrac{K_{21}K_{12}}{K_{22}K_{11}}} & \dfrac{1}{1-\dfrac{K_{11}K_{22}}{K_{12}K_{21}}} \\ \dfrac{1}{1-\dfrac{K_{22}K_{11}}{K_{21}K_{12}}} & \dfrac{1}{1-\dfrac{K_{21}K_{12}}{K_{22}K_{11}}} \end{bmatrix} \tag{3.30}$$

In the MIMO system, the array should be a matrix with one column for each input variable and one row for each output variable. This format is used to compare the relative gains associated with each input output variable pair, and to match the input and output variables that have the greatest impact on each other while minimizing unwanted side effects. The RGA can be evaluated from steady state gain matrix, therefore it is given in Equation (3.31).

$$RGA = \Lambda = \begin{array}{c c} & \begin{array}{cc} u_1 & \quad u_2 \end{array} \\ \begin{array}{c} y_1 \\ y_2 \end{array} & \begin{bmatrix} 2.0094 & -1.0094 \\ -1.0094 & 2.0094 \end{bmatrix} \end{array} \tag{3.31}$$

Generally, there are two rules to select the appropriate parings of the decoupler [31].

Pairing rule* 1*: Prefer pairings such that the rearranged system, with the selected pairings along the diagonal, has an RGA matrix close to identity at frequencies around the closed-loop bandwidth.

***Pairing rule* 2:** Avoid (if possible) pairing on negative steady-state RGA elements.

From the result of RGA matrix shown in Equation (3.31), the best pairs of manipulated and controlled variables are found based on the paring rules. Since only the pairing y_1-u_1 and y_2-u_2 has a positive relative gain value and the values are close to one. Thus, reflux flow with distillate composition and reboiler flow with bottom composition found to be best pairs.

3.3.4 Design of a Decoupler

Due to multiple variables, the control scheme needs a decoupler. In general, the better set point tracking and disturbance rejection response may not achieve using only decoupling. In order to achieve the best result, the system needs a feedback controller along with its tuning techniques. So, decoupling matrix M is designed and taken to decouple the proposed process with a transfer matrix as shown in Equation (3.36) [31][32]. In simplified decoupling the common choice is that $M_{11} = M_{22} = 1$ and the off-diagonal elements.

The block diagram of control scheme with decoupling is shown in Figure 3.5. They have a simple structure, and their design does not necessitate a detailed system description. The RGA is a normalized gain matrix that describes the impact of each control variable on the output as well as the impact of each control variable on other variables. The decoupler can be found out using the following Equations (3.32) - (3.35).

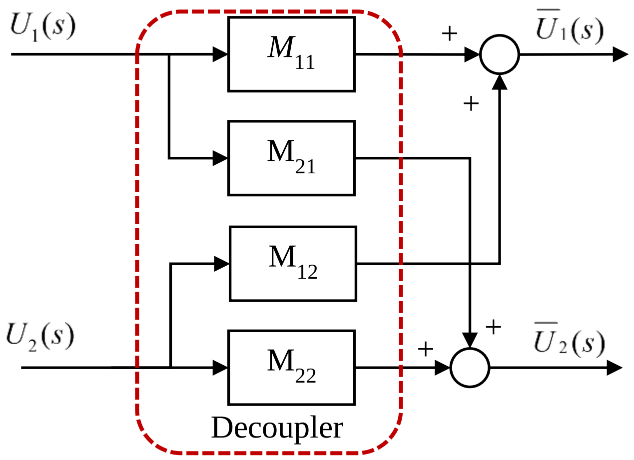

Figure 3. 5 TITO system with decoupling [26], [33].

From Equation (3.32), M_{12} is calculated by Equation (3.33) [7], [34].

$$M_{12}G_{P11}U_{22} + G_{P12}U_{22} = 0 \tag{3.32}$$

Since, $U_{22} \neq 0$ in general, then

$$M_{12} = -\frac{G_{P12}}{G_{P11}} \tag{3.33}$$

Similarly, using Equation (3.34), M_{21} is calculated and given in Equation (3.35).

$$M_{21}G_{P22}U_{11} + G_{P21}U_{11} = 0 \tag{3.34}$$

Since, $U_{11} \neq 0$ in general, then

$$M_{21} = -\frac{G_{P21}}{G_{P22}} \tag{3.35}$$

So, the final decoupler matrix is expressed by

$$\boldsymbol{M} = \begin{bmatrix} M_{11} & M_{12} \\ M_{21} & M_{22} \end{bmatrix} \tag{3.36a}$$

$$\begin{aligned} M_{11} &= 1 \\ M_{12} &= -\frac{G_{p12}}{G_{p11}} = \frac{24.66s + 1.48}{21s + 1} e^{-2s} \\ M_{21} &= -\frac{G_{p21}}{G_{p22}} = \frac{4.89s + 0.34}{10.9s + 1} e^{-4s} \\ M_{22} &= 1 \end{aligned} \tag{3.36b}$$

Therefore, the input-output relationship of the decoupler is described by

$$\bar{\boldsymbol{U}}(s) = \boldsymbol{M}(s)\boldsymbol{U}(s) \tag{3.37}$$

where $\bar{\boldsymbol{U}}(s) = \begin{bmatrix} \bar{U}_1(s) \\ \bar{U}_2(s) \end{bmatrix}$ denotes the output of the decoupler.

Figure 3.6 shows the block diagram of the TITO system with decoupling and considering disturbances.

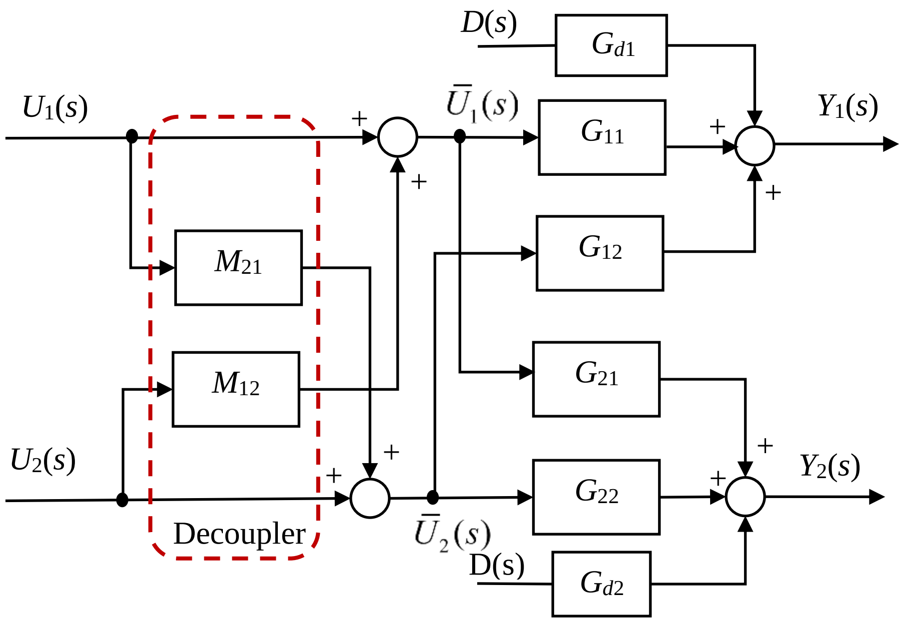

Figure 3. 6 TITO system with decoupling and disturbance

Recalling that $\boldsymbol{U}$(s) in Equation (3.16) becomes $\bar{\boldsymbol{U}}$(s) when the decoupler is used, the overall open-loop transfer function becomes as follows:

$$\boldsymbol{Y}(s) = \boldsymbol{G}_p(s)\boldsymbol{M}(s)\boldsymbol{U}(s) + \boldsymbol{G}_d(s)D(s) \tag{3.38a}$$

where

$$\begin{aligned}\boldsymbol{G}_p(s)\boldsymbol{M}(s) &= \begin{bmatrix} G_{11}(s) & G_{12}(s) \\ G_{21}(s) & G_{22}(s) \end{bmatrix}\begin{bmatrix} M_{11}(s) & M_{12}(s) \\ M_{21}(s) & M_{22}(s) \end{bmatrix} \\ &= \begin{bmatrix} G_{11}(s)M_{11}(s)+G_{12}(s)M_{21}(s) & G_{11}(s)M_{12}(s)+G_{12}(s)M_{22}(s) \\ G_{21}(s)M_{11}(s)+G_{22}(s)M_{21}(s) & G_{21}(s)M_{12}(s)+G_{22}(s)M_{22}(s) \end{bmatrix}\end{aligned} \tag{3.38b}$$

Finally, the overall system transfer function for distillate and bottom compositions becomes

$$\begin{aligned}Y_1(s) = {}&(G_{11}(s)M_{11}(s)+G_{12}(s)M_{21}(s))U_1(s)+(G_{11}(s)M_{12}(s) \\ &+G_{12}(s)M_{22}(s))U_2(s)+G_{d1}(s)D_1(s)\end{aligned} \tag{3.39a}$$

$$\begin{aligned}Y_2(s) = {}&(G_{21}(s)M_{11}(s)+G_{22}(s)M_{21}(s))U_1(s)+(G_{21}(s)M_{12}(s) \\ &+G_{22}(s)M_{22}(s))U_2(s)+G_{d2}(s)D_2(s)\end{aligned} \tag{3.39b}$$

3.4 Steady-State Analysis of Distillation Column

In this section the steady-state analysis has been done for both with and without decoupling.

3.4.1 DC Process without a Decoupler

As can be seen in Equation (3.16), when disturbance is not considered, the output of the DC process becomes:

$$\boldsymbol{Y}(s) = \boldsymbol{G}_p(s)\boldsymbol{U}(s) \tag{3.40}$$

The input-output relationship in the steady-state without any change in the input/output signals, that is, the gain matrix can be obtained as follows:

$$\boldsymbol{Y}_0 = \boldsymbol{K}\boldsymbol{U}_0 \tag{3.41a}$$

$$\boldsymbol{K} = \begin{bmatrix} K_{11} & K_{12} \\ K_{21} & K_{22} \end{bmatrix} = \lim_{s\to 0}\boldsymbol{G}_p(s) \tag{3.41b}$$

where

$$K_{11} = \frac{y_{10}}{u_{10}} = \lim_{s\to 0} G_{p11}(s) = \quad 12.8$$
$$K_{12} = \frac{y_{10}}{u_{10}} = \lim_{s\to 0} G_{p12}(s) = -18.9$$
$$K_{21} = \frac{y_{10}}{u_{10}} = \lim_{s\to 0} G_{p21}(s) = \quad 6.6$$
$$K_{22} = \frac{y_{10}}{u_{10}} = \lim_{s\to 0} G_{p22}(s) = -19.4 \tag{3.41c}$$

From Equation (3.41), when $\boldsymbol{U}_0$ is given, $\boldsymbol{Y}_0$ can be known and conversely, when $\boldsymbol{Y}_0$ is given and the gain matrix $\boldsymbol{K}$ is nonsingular, $\boldsymbol{U}_0$ can be obtained by

The steady-state TITO distillation column system is showed in Figure 3.7.

$$\boldsymbol{U}_0 = \boldsymbol{K}^{-1}\boldsymbol{Y}_0 \tag{3.42}$$

Based on Figure 3.7 the outputs y_{10} and y_{20} are derived as shown in Equation (3.43).

$$y_{10} = u_{10}g_{11} + u_{20}g_{12} \tag{3.43a}$$

$$y_{20} = u_{20}g_{22} + u_{10}g_{21} \tag{3.43b}$$

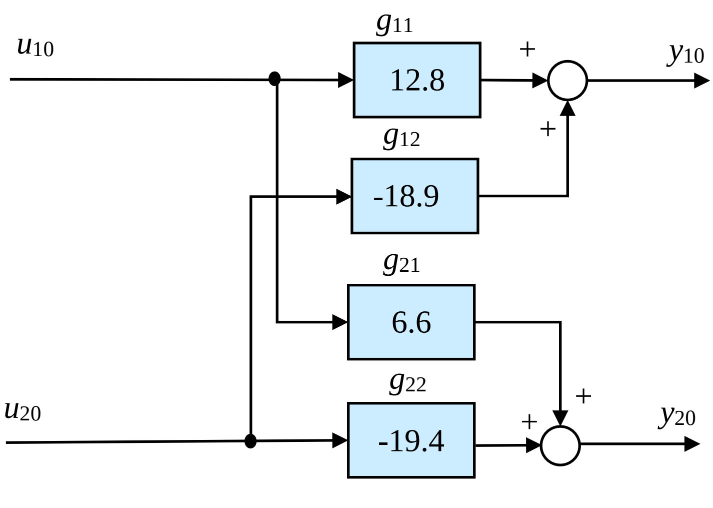

Figure 3. 7 Steady-state of the TITO system without decoupling

The effects of the inputs on the outputs at steady-state without decoupler can be analyzed by taking random data of the inputs. As an example, the two conditions are considered which are (a) and (b) cases in Equation (3.47).

$$\text{(a)}\ \begin{bmatrix} u_{10} \\ u_{20} \end{bmatrix} = \begin{bmatrix} 0.1 \\ 0 \end{bmatrix}, \qquad \text{(b)}\ \begin{bmatrix} u_{10} \\ u_{20} \end{bmatrix} = \begin{bmatrix} 0 \\ 0.1 \end{bmatrix} \tag{3.47}$$

For the above inputs, the outputs are

$$\text{(a)}\ \begin{bmatrix} y_{10} \\ y_{20} \end{bmatrix} = \begin{bmatrix} 1.2 \\ 0.66 \end{bmatrix}, \qquad \text{(b)}\ \begin{bmatrix} y_{10} \\ y_{20} \end{bmatrix} = \begin{bmatrix} -1.89 \\ -1.94 \end{bmatrix} \tag{3.48}$$

It can be seen at the calculated two outputs that one input is simultaneously affecting the two outputs.

3.4.2 DC Process with a Decoupler

Based on Figure 3.8 the outputs y_{10} and y_{20} are derived as shown in Equations (3.46) and (3.47).

$$y_{10} = g_{11}u_{10} + m_{21}g_{12}u_{10} + g_{12}u_{20} + m_{12}g_{11}u_{20} \tag{3.46}$$

$$y_{20} = g_{22}u_{20} + m_{12}g_{21}u_{20} + g_{21}u_{10} + m_{21}g_{22}u_{10} \tag{3.47}$$

The steady-state TITO distillation column system is showed in Figure 3.8.

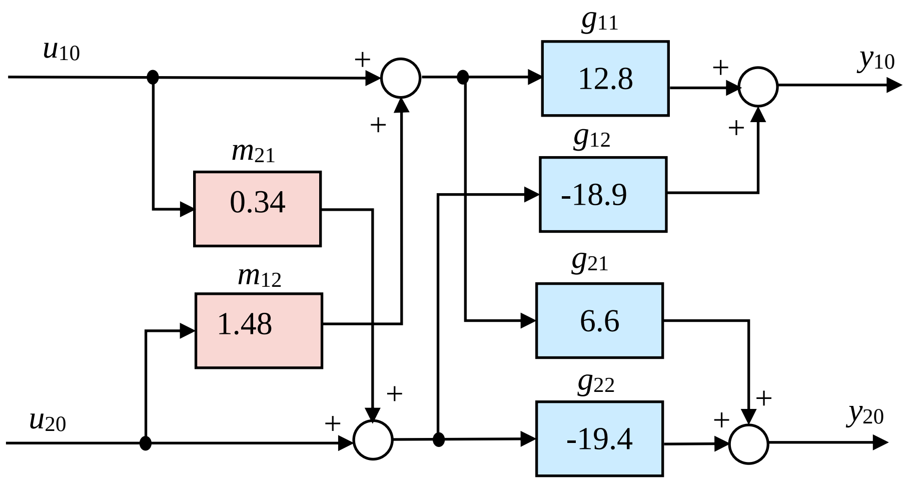

Figure 3. 8 Steady-state of the TITO system with decoupling

The effects of the inputs on the outputs at steady state with decoupler can be analyzed by taking random data of the inputs. As an example, the two conditions are considered which are (a) and (b) cases in Equation (3.48).

$$\text{(a)} \begin{bmatrix} u_{10} \\ u_{20} \end{bmatrix} = \begin{bmatrix} 0.1 \\ 0 \end{bmatrix}, \qquad \text{(b)} \begin{bmatrix} u_{10} \\ u_{20} \end{bmatrix} = \begin{bmatrix} 0 \\ 0.1 \end{bmatrix} \tag{3.48}$$

Based on the above inputs, the outputs are shown

$$\text{(a)} \begin{bmatrix} y_{10} \\ y_{20} \end{bmatrix} = \begin{bmatrix} 0.6374 \\ 0 \end{bmatrix}, \qquad \text{(b)} \begin{bmatrix} y_{10} \\ y_{20} \end{bmatrix} = \begin{bmatrix} 0 \\ -0.9632 \end{bmatrix} \tag{3.49}$$

As expected from this example, by using a decoupler, it can be seen that u_{10} affects only y_{10}, and similarly, u_{20} affects only y_{20}.

3.4.3 Steady-State Responses of the DC Process with and without a Decoupler

In this section the open-loop DC responses are analyzed graphically using the examples computed in the previous section. Based on the examples, the responses without and with decoupling are drawn as shown in Figures 3.8 and 3.9 and Figures 3.10 and 3.11, respectively. In both cases i.e., with and without decoupling the open-loop DC system is stable. Figure 3.8 is drawn when $u_{10} = 0.1$ and $u_{20} = 0$ in case (*a*) of the previous examples considering without decoupling. As a result, input u_{10} has an interaction with the outputs both y_{10} and y_{20} and at the same time u_{20} has also an interaction with the output both y_{10} and y_{20}. The interaction between the inputs and the outputs in case of (*b*) are also the same in case of (*a*) i.e., the two inputs have an interaction on each output of the controlled variable.

When $u_{10} = 0.1$ and $u_{20} = 0$ in case (a) of the previous examples with decoupler design, the response is shown in Figure 3.10. Therefore, input u_{10} has an interaction with only output y_{10} and at the same time u_{20} has also an interaction with only output y_{20} and the same with case (b).

Generally, as it can be seen from the previous mathematical analysis and the graphical result shown in Figures 3.10-11, the decoupler can eliminate the controller interaction between u_{10} with y_{20} and u_{20} with y_{10}. The only interacting manipulated variable of output y_{10} is u_{10} and output y_{20} is u_{20}. Therefore, decoupler design is necessary for any MIMO system.

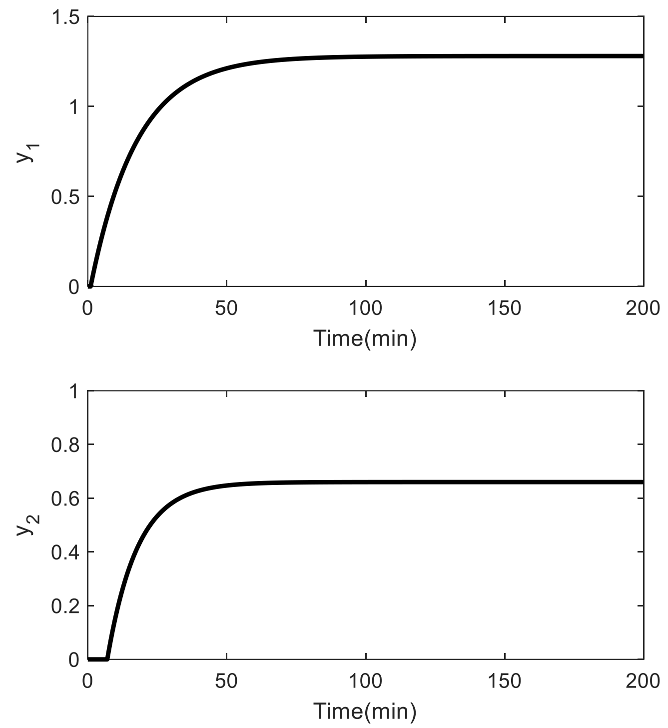

Figure 3. 9 Open-loop responses y_1 and y_2 of the process without decoupling to 10% step change of u_1

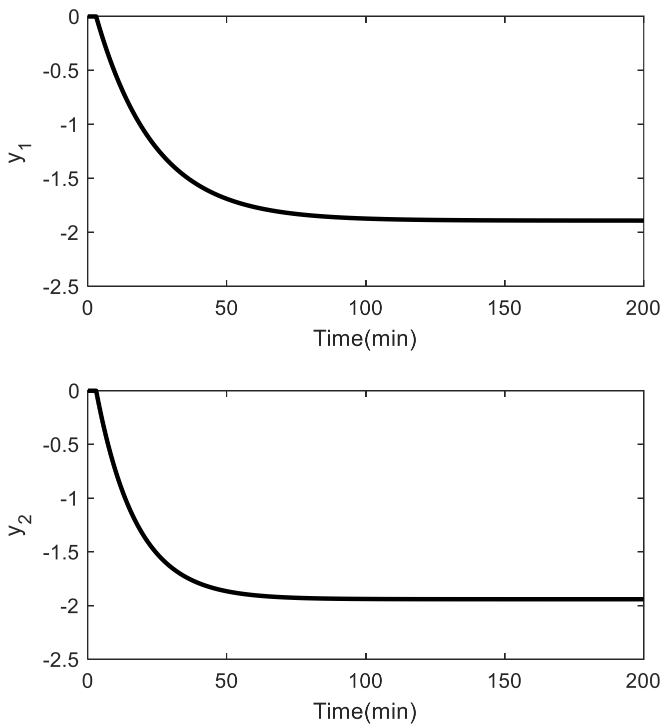

Figure 3. 10 Open-loop responses y_1 and y_2 of the process without decoupling to 10% step change of u_2

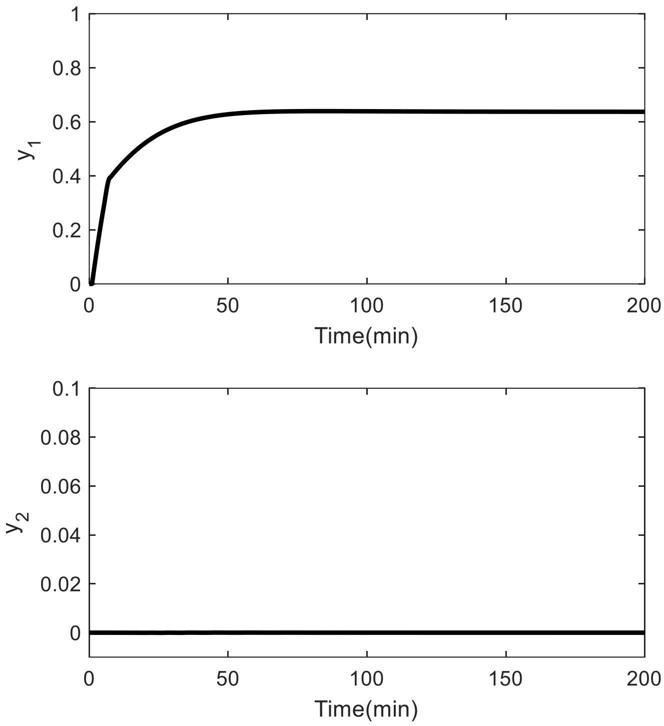

Figure 3. 11 Open-loop responses y_1 and y_2 of the process with decoupling to 10% step change of u_1

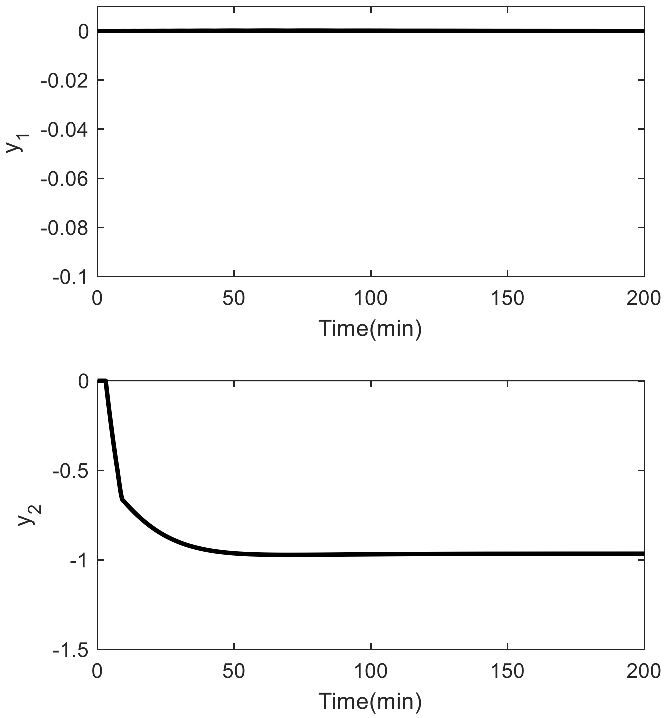

Figure 3. 12 Open-loop responses y_1 and y_2 of the process with decoupling to 10% step change of u_2

CHAPTER 4

CONTROLLER DESIGN

In this chapter, the mathematical modeling and design for the comparative relation of (PID), Nonlinear (NPID), and (FOPID) controllers for MIMO distillation column is done. In this research work, a genetic algorithm (GA) optimization is considered for tuning of these controllers and its effectiveness is analyzed based on the performance index of object functions. Figure 4.1 shows the proposed control system composing the controllers, the decoupler and the process.

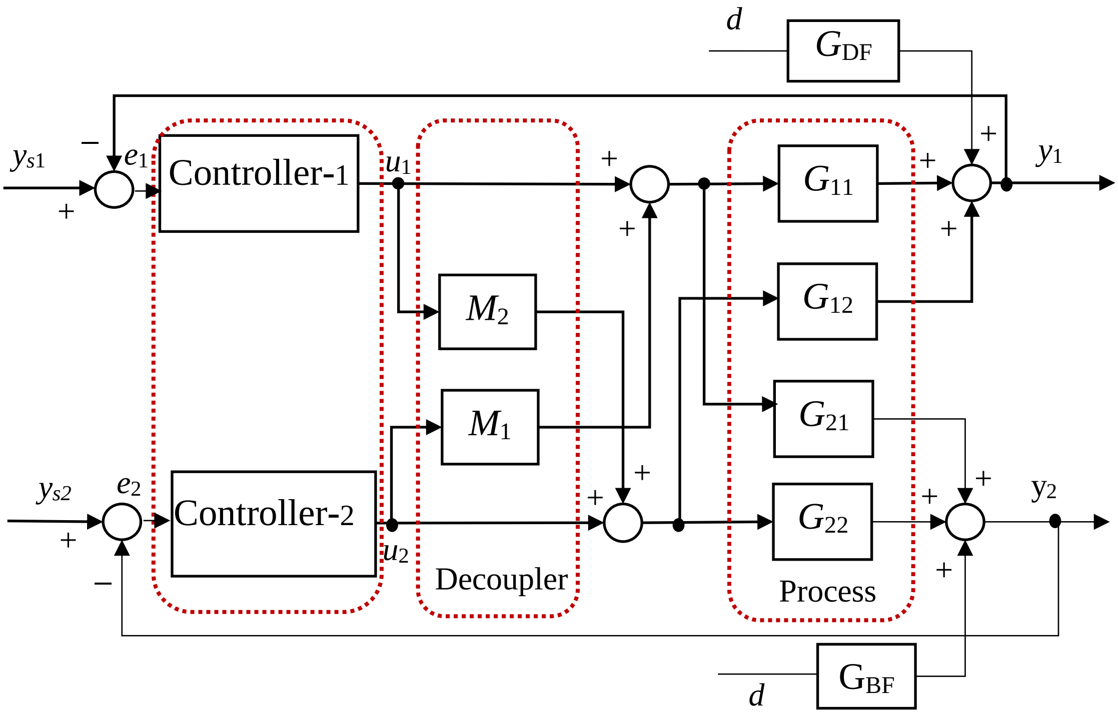

Figure 4. 1 The proposed control system of the MIMO process with decoupling

4.1 Design of a PID Controller

The traditional PID controller can be considered as the controller in Figure 4.2. The PID control is the commencement controlling strategy of every industrial process control system due to the advantage of less cost, simple structure, good stability, and high reliability [35], [36]. The time-domain equations of the PID controller are shown below in Equations (4.1) and (4.2).

Standard form:

$$u(t) = K_p[e(t) + \frac{1}{T_i}\int_0^t e(\tau)d\tau + T_d \frac{de(t)}{dt}] \tag{4.1}$$

Parallel form:

$$u(t) = K_p e(t) + \mathrm{K}_i \int_0^t e(\tau)d\tau + K_d \frac{de(t)}{dt} \tag{4.2}$$

where K_p is the proportional gain, T_i is the integral time, T_d is the derivative time, K_i is the integral gain with $K_i = K_p/T_i$, and K_d is the integral gain with $K_d = K_p T_d$.

And the frequency domain equations of the PID controller are given by

Standard form:

$$U(s) = K_p(1 + \frac{1}{T_i s} + T_d s)E(s) \tag{4.3}$$

Parallel form:

$$U(s) = (K_p + \frac{K_i}{s} + K_d s)E(s) \tag{4.4}$$

The structure of the parallel-form PID controller is shown in Figure 4.2..

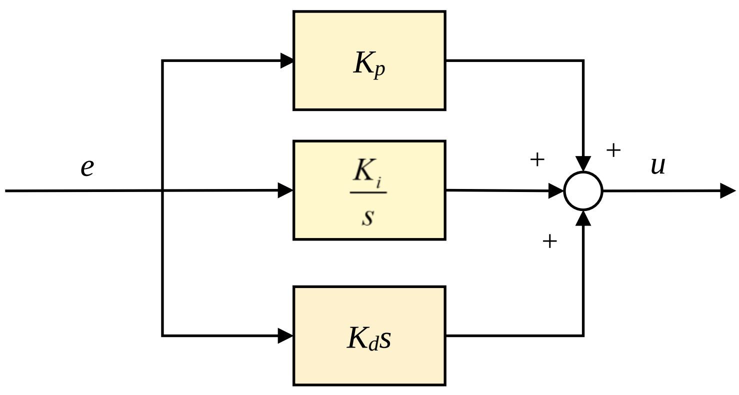

Figure 4. 2 Schematic of the PID controller

4.1.1 Role of PID Controller

PID controller maintains the error between the process variable and the set point zero by closed-loop operations. It is the composition of proportional, integral, and derivative actions that are explained below [14], [L4].

Proportional action (P): It gives a yield that is relative to current error e(t). When used alone, P-action requires biasing or manual reset. This is due to the fact that it never achieves the steady-state condition. It provides stable operation while maintaining the steady-state error.

Integral action (I): Due to the restriction of P-action where there continuously exists an offset between the method variable and set point, I-action is required, which provides the necessary activity to resolve the steady-state error. When a negative error occurs, integral control reduces its output. It slows down the system's response time and affects its stability. The response speed is enhanced by lowering the integral gain, Ki.

Derivative action (D): I-action does not have the capability to predict error behavior in the future. So, it reacts normally once the set point is changed. D-action solves this problem by predicting the error's future behavior. It increases system response by providing a kick start for the output.

As discussed in the previous chapter, since the system is a 2-input-2-output MIMO system. Therefore, two PID controllers are needed to control each variable. The PID controller for controlling each variable is as follows:

$$e_k(t) = y_{sk} - y_k \tag{4.5a}$$

$$u_k(t) = K_{pk} e_k(t) + K_{ik} \int_0^t e_k(\tau) d\tau + K_{dk} \frac{de_k(t)}{dt} \quad (k = 1, 2) \tag{4.5b}$$

where *k* represents the number of controllers used in the distillation column process.

4.2 Design of a Nonlinear PID Controller

Although a fixed parameter PID controller discussed in Section 4.1 gives good response characteristics in an operating range, its performance may degrade and become unstable in some cases when it is out of the range. Several nonlinear PID (NPID) controllers have been proposed to compensate for the disadvantages of the PID controller.

4.2.1 Existing Nonlinear PID Controllers

NPID controllers proposed so far introduce nonlinear functions in the platform of the PID controller. They can be broadly classified into two types. One is the nonlinear PID controller introduced by the previous works in [37], [38], and [39]. Whose gains are gradually changed based on error and/or error rate. The time-domain equation of one typical NPID controller is described by

$$u(t) = K_p(e)e(t) + K_i(e)\int_0^t e(\tau)d\tau + K_d(e,\dot{e})\frac{de(t)}{dt} \tag{4.6}$$

Figure 4.3 shows the block diagram of the NPID controller proposed by [37].

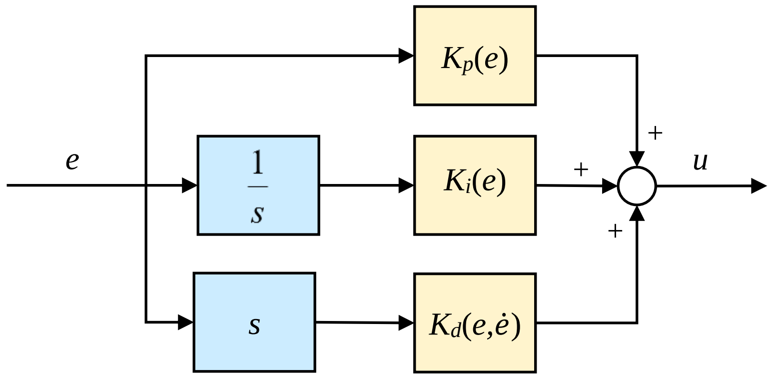

Figure 4. 3 Structure of the NPID controller

The other type is the NPID controller introduced in literature [40], [41], and [42], where a nonlinear gain in cascade with a linear PID controller produces the scaled error. The time domain equation of one typical NPID controller is described by:

$$v(t) = k(e)e(t) \tag{4.7a}$$

$$u(t) = K_p v(t) + K_i\int_0^t v(\tau)d\tau + K_d\frac{dv(t)}{dt} \tag{4.7b}$$

where $v(t)$ denotes the scaled error with $v(t) = k(e).e(t)$, $k(e)$ denotes a nonlinear gain function of $e(t)$ with $e(t) = y_s(t) - y(t)$. The scaled error $v(t)$ is then applied to the PID controller which generates the control input $u(t)$ as shown in Figure 4.4.

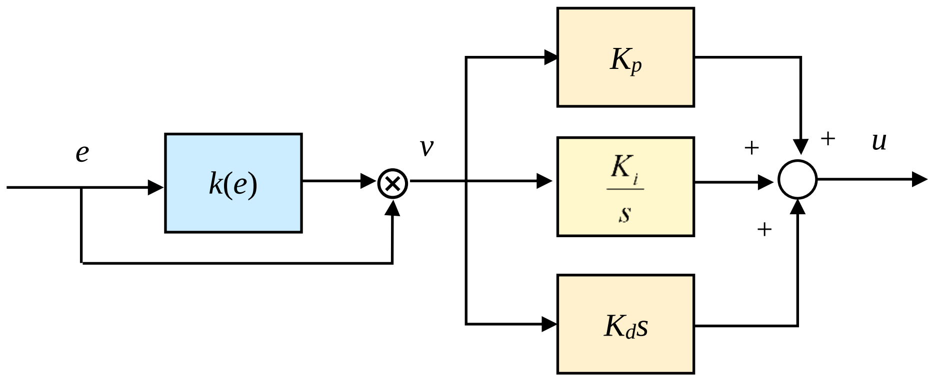

Figure 4. 4 Structure of the NPID controller introduced by [40].

Two nonlinear gains, the sigmoidal function and the hyperbolic function, are proposed in [41] and [43].

$$k(e) = k_0 + k_1[\frac{2}{1+\exp(-k_2 e)} - 1] \tag{4.8}$$

$$\begin{aligned} k(e) &= k_0 + k_1[1 - \frac{2}{\exp(k_2 e) + \exp(-k_2 e)}] \\ &= k_0 + k_1[1 - \sec h(k_2 e)] \end{aligned} \tag{4.9}$$

Figure 4.5 depicts the shapes of the two nonlinear gains.

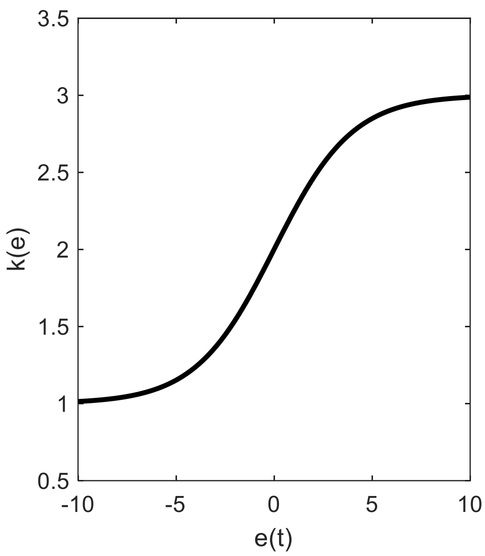

(a) $k(e)$ of Equation (4.8)

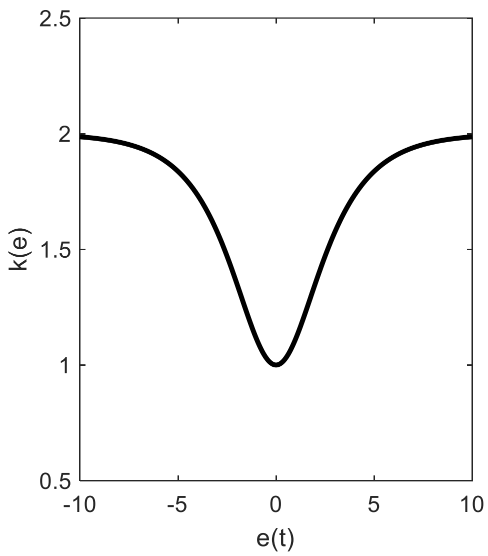

(b) $k(e)$ of Equation (4.9)

Figure 4. 5 Two nonlinear gains

where k_0, k_1, and k_2 are user-defined positive constants. The gain k is now upper-bounded by $k_{max} = k_0 + k_1$ when $e = \pm\infty$, and lower-bounded by $k_{min} = k_0$ when $e = 0$. Thus, k_0 defines the minimum value, k_1 denotes the range of variation, and k_2 specifies the rate of variation of k. Figure 4.5b shows a typical variation of k versus e when k_0=1, k_1 =1, and k_2 = 0.5. It is seen that k is an "inverted bell-shaped" curve, and is an even function of e, that is $k(-e) = k(e)$. This class of nonlinear gains is applicable when k is required to be a function of the error magnitude $|e|$.

The previously proposed methods produce satisfactory results in a variety of control contexts, but they have some disadvantages. When compared to the traditional PID controller, they are process dependent and, in most circumstances, have their own limitation due to the increased number of tuning parameters.

4.2.2 Nonlinear PID Controller Employed in This Study

In this work, as an alternative, the NPID controller proposed in [44], [45], and [46] is considered. The block diagram of the NPID controller is shown in Figure 4.6. Its structure is similar with the conventional PID controller, but only the integral action contains a nonlinear function while the other actions are linear. Hence, the error input to the integral action is scaled by a nonlinear function in the form of the product of the error and a nonlinear gain.

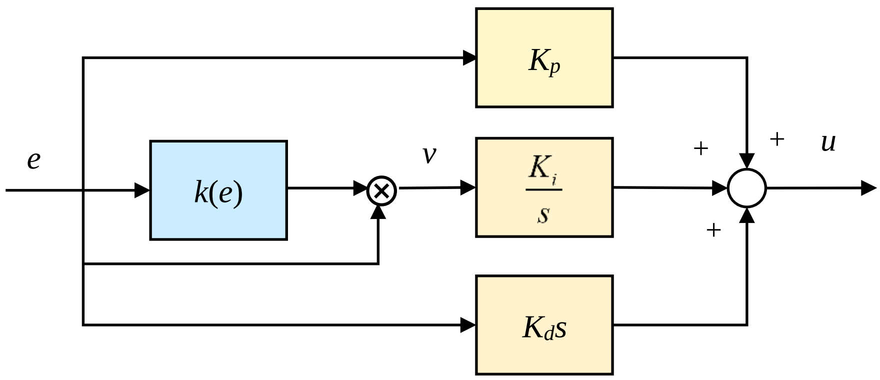

Figure 4. 6 Structure of the nonlinear PID controller employed in this study [46].

The time-domain equation is expressed by

$$v(t) = k(e)e(t) \tag{4.10a}$$

$$u(t) = K_p e(t) + K_i \int_0^t v(\tau)d\tau + K_d \frac{de(t)}{dt} \tag{4.10b}$$

where e denotes the error, that is, the difference between the set point and the output. v is a scaled error and $k(e)$ a nonlinear gain which provides a nonlinearly-scaled error according to e. $k(e)$ is given by

$$k(e) = \exp(-\frac{e^2}{2\Delta y_s^2}) \tag{4.11}$$

where Δy_s ($\neq 0$) is the set point change.

Figure 4.7 shows typical shapes of $k(e)$ versus e according to the change of Δys.

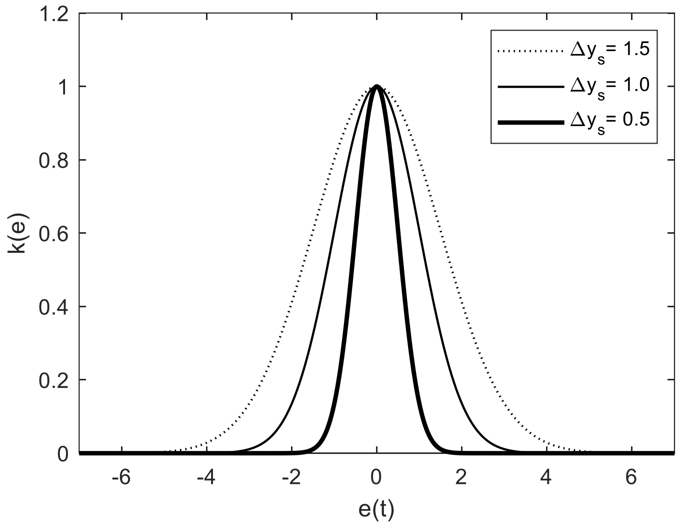

Figure 4. 7 For varying Δy_s, the shapes of k(e) relative e

Note that $k(e)$ is an even function. Given the input e, the shape of the nonlinear gain $k(e)$ depends on e and Δy_s. The lower the magnitude of Δys, the narrower the width becomes, and the larger the magnitude of Δys, the wider the width. Moreover, it can also be noticed that $k(e)$ converges to the lower limit 0 when e goes to infinity, and converges to the upper limit 1 when e approaches 0.

It is clearly seen from Figure 4.8 that, for large e which is caused by the set point change or/and disturbances, the nonlinear function $k(e)$ scales down the error in order to avoid excessive control effort. This favorable property of $k(e)$ produces good transient responses.

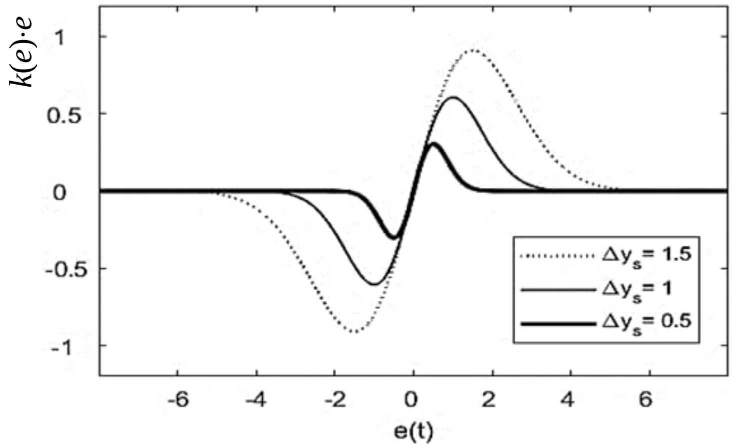

Figure 4. 8 For different Δy_s, the shapes of k(e)·e versus e

As two controllers are used for control like the PID controller in the previous section, each NPID controller is expressed as follows:

$$v_k(t) = k(e_k)e_k(t) \tag{4.12a}$$

$$u_k(t) = K_{pk}e_k(t) + K_{ik}\int_0^t v_k(\tau)d\tau + K_{dk}\frac{de_k(t)}{dt} \quad (k=1,2) \tag{4.12b}$$

where $e_k(t) = y_{sk} - y_k(t)$ and k represents the number of the controllers used in the distillation column process.

4.3 Design of a Fractional-Order PID Controller

In this work, like the previous two controllers, the Fractional-Order PID (FOPID) controller is used as an alternative control scheme. The FOPID controller is described by fractional-order differential equations. The expansion of integer-order control is the FOPID controller. The performance of controllers constructed with fractional order derivatives and integrals is superior to that of integer order controllers [4][6].

The derivatives and integrals of fractional calculus can be any real number. The basic operator of fractional calculus is denoted as ${}_a\mathrm{D}_t^r$, where a is the lower limit and t is the upper limit of the operation, and r is the order of operation. r is generally a real number, $r \in R$ but could be a complex number. The operator can be defined as follows [47], [48].

$$
{}_aD_t^r = \begin{cases} \dfrac{d^r}{dt}, & \text{for } r > 0 \\ 1, & \text{for } r = 0 \\ \int (d\tau)^{-r}, & \text{for } r < 0 \end{cases} \tag{4.13}
$$

There are three commonly used definitions for the general fractional order differential-integral such as the Grunwald-Letnikov, Riemann-Liouville, and the Caputo definitions for $n-1<r<n$. Riemann-Liouville definition of fractional calculus for differentiation and integration is also formulated in form of Laplace transformation for $n-1<r<n$ and $s \equiv j\omega$ which is the Laplace transform variable, since this method is commonly used in engineering problems solving [49], [50].

<u>Grunwald-Letnikov definition</u>:

$$
{}_aD_t^r f(t) = \lim_{h\to 0} h^{-r} \sum_{j=0}^{\left[\frac{t-a}{h}\right]} (-1)^j \binom{r}{j} f(t-jh) \tag{4.14}
$$

<u>Caputo definition</u>:

$$
{}_aD_t^r f(t) = \frac{1}{\Gamma(n-r)} \int_a^t \frac{f^n(\tau)}{(t-\tau)^{r-n+1}} d\tau \tag{4.15}
$$

<u>Riemann-Liouville definition:</u>

$$
{}_aD_t^r f(t) = \frac{1}{\Gamma(n-r)} \frac{d^n}{dt^n} \int_a^t \frac{f(\tau)}{(t-\tau)^{r-n+1}} d\tau \tag{4.16}
$$

where $\Gamma(\cdot)$ is gamma function, and referring to it is expressed as:

$$
\Gamma(x) = \int_0^\infty t^{x-1} e^{-t} dt \tag{4.17}
$$

where the real part of $R(x) > 0$.

The Reimann-Liouville definition of fractional order operation in the form of Laplace transformation under zero initial conditions is given as follows:

$$\int_0^\infty e^{-st}\,{}_aD_t^r f(t)dt = s^r F(s) \tag{4.18}$$

The fractional derivatives have the following rules.

$$\frac{d^n}{dt^n}({}_{t0}D_t^\lambda f(t)) = {}_{t0}D_t^{\lambda+n} f(t) \tag{4.19}$$

$$\frac{d^n}{dt^n}({}_{t0}D_t^\mu f(t)) = {}_{t0}D_t^{\mu+n} f(t) \tag{4.20}$$

The time-domain equation of the FOPID controller is represented by

$$u(t) = K_p e(t) + K_i[{}_0D_t^{-\lambda} e(t)] + K_d[{}_0D_t^{\mu} e(t)] \tag{4.21}$$

The generalized transfer function is shown by

$$U(s) = (K_P + \frac{K_i}{s^\lambda} + K_d s^\mu)E(s) \tag{4.22}$$

where e and u are the error signal and the control input, respectively; K_p, K_i, *and* K_d are the proportional, integral, and derivative gains, respectively; λ and μ are the integral and derivative orders, respectively, satisfying $0 < \lambda, \mu < 2$.
The structure of the FOPID controller is shown in Figure 4.9.

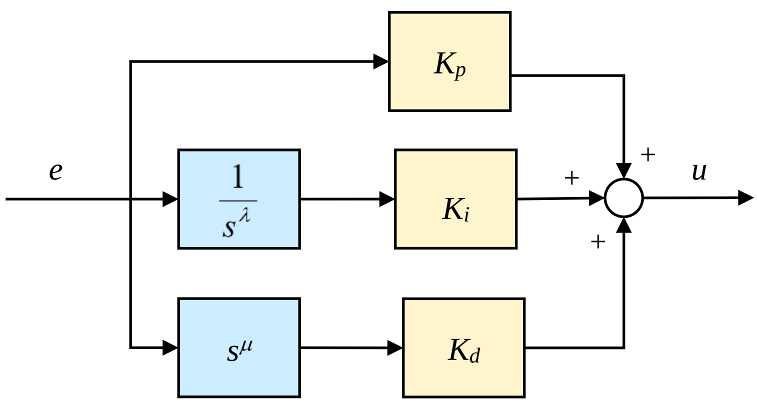

Figure 4. 9 Structure of the FOPID controller

Note that the FOPID controller generalizes the conventional integer-order PID controller. In other words, it can be said that it is the expansion of point to plane. For λ = 1 and μ = 1, the

FOPID controller becomes the standard PID controller. In the PID controller there are three design parameters but in the fractional-order PID controller there are five design parameters. However, the extra two degrees of freedom gives more flexibility to improve the performance of the FOPID controller [4], [6]. The control possibilities using PID and FOPID are shown in Figure 4.10.

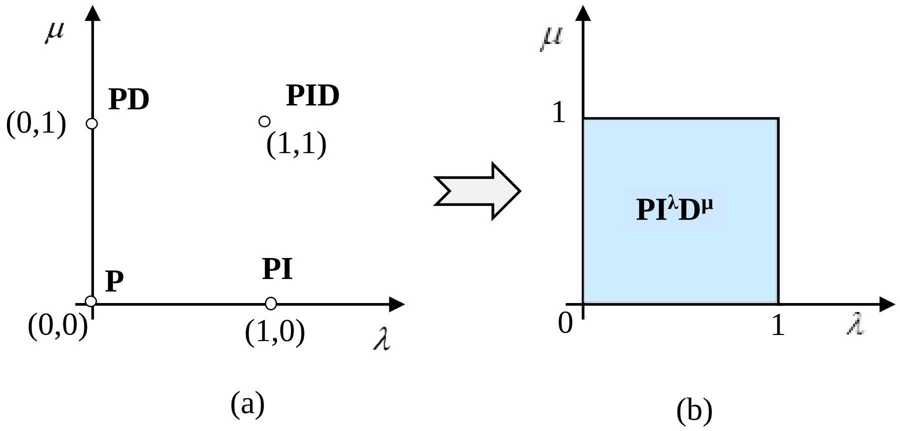

Figure 4. 10 FOPID controller areas with λ and μ tuning parameters [51].

As in the previous two controllers, two FOPID controllers are applied to the distillation column MIMO system. Each controller output u(t) in time domain is:

$$e_k(t) = y_{sk} - y_k \tag{4.23a}$$

$$u_k(t) = K_{pk} e_k(t) + K_{ik}[{}_0D_t^{-\lambda_k} e_k(t)] + K_{dk}[{}_0D_t^{\mu_k} e_k(t)] \tag{4.23b}$$

where *k* represents the number of controllers used in the distillation column process.

4.4 Tuning of the Controllers

The PID, NPID, and FOPID controllers discussed in the previous three sections have 3, 3, and 5 parameters, respectively. They need to be optimally tuned to achieve satisfactory response performance. At this time, a performance evaluation function based on these parameters is introduced and when this evaluation function is minimized, a multivariate optimization problem occurs. To solve this problem, considered a genetic algorithm as a global optimizer.

4.4.1 Genetic Algorithm (GA) Optimizer

In order to solve complex optimization problems, several evolutionary algorithms based on the principles of natural phenomena have been proposed. In this study, the GA is considered to have optimal controller parameters. The GA is an algorithm developed by mimicking the principles of natural selection and evolution of living organisms [52]. Figure 4.11 shows the pseudo code of a genetic algorithm.

Set k= 0;
Initialize a population $\boldsymbol{P}(k)$;
Evaluate each individual in $\boldsymbol{P}(k)$;
do while < stop conditions are not satisfied >
    set k= k+1;
    Select individuals from $\boldsymbol{P}(k\text{-}1)$ to set up a tentative population $\widehat{\boldsymbol{P}}(k)$;
    Crossover individuals in $\widehat{\boldsymbol{P}}(k)$;
    Mutate individuals in $\widehat{\boldsymbol{P}}(k)$;
    Evaluate each individual in the new population $\boldsymbol{P}(k)$;
end while
Output the best individual in $\boldsymbol{P}(k)$ as the solution;

Figure 4. 11 Pseudo code of a genetic algorithm

GA starts with an initial population containing a number of chromosomes where each individual chromosome represents a solution of the problem and its performance is evaluated by a fitness function. Genetic algorithm consists of three main stages: Selection (reproduction), Crossover and Mutation. Selection retains a fit set of chromosomes in the given population. Crossover and mutation involve swapping between two parent strings and flipping a random bit in the set of chromosomes respectively [53], [54]. The application of these three basic operations allows the creation of new individuals which may be better than their parents. This algorithm is repeated for many generations and finally stops when reaching individuals that represent the optimum solution to the problem.

The complete response of the system for each controller parameter value and initial fitness value of integral absolute error, and control signal (IAEU), integral time absolute error, and control signal (ITAEU), and integral square error, and control signal (ISEU) is computed and optimized using GA. This process should be repeated every generation until the end of the generations where the best fitness value is achieved.

4.4.2 Objective Functions

Tuning of a controller is performed by minimizing the objective function. There are many types of performance measures are available. The three commonly used performance measures in tuning controller parameters are the integral of absolute error (IAE), the integral of time multiplied absolute error (ITAE), and the integral of squared error (ISE) [4], [55], which are based on the error as:

$$IAE = \int_0^{t_f} |e(t)|dt \tag{4.24}$$

$$ITAE = \int_0^{t_f} t\,|e(t)|dt \tag{4.25}$$

$$ISE = \int_0^{t_f} e^2(t)dt \tag{4.26}$$

Each of the above measures is calculated over some interval of time $0 \le t \le t_f$ where t_f is a time long enough for the error to settle down.

These performance criteria have advantages as well as disadvantages. For example, ISE tuning makes large errors larger and small errors smaller and often leads to a fast response with low amplitude oscillation. IAE does not add any weight to the errors and tends to provide slower response than ISE tuning. ITAE imposes small time penalty for the initial large error and gives higher time weight to the absolute error at later times.

Due to the effect of time penalty, ITAE tuning produces an initial slow response. Another disadvantage of these three methods is that they tune the controller for the control input to be excessively large in order to quickly reduce the error. This causes saturation in the actuator and can ultimately lead to integrator wind-up problems [56].

Therefore, in this work, not only the time integral of absolute error is employed as a part of the performance index to achieve the satisfactory dynamic characteristics in the transition process but also the absolute controlled variable is adopted to avoid the large control input.

Three performance criteria (Integral of Absolute Error and Control Signal: IAEU) are defined as follows:

$$J_1 = IAEU = \int_0^{t_f} \sum_{k=1}^{2} [|e_k(t)| + w_k |\Delta u_k(t)|] dt \tag{4.27}$$

$$J_2 = ITAEU = \int_0^{t_f} \sum_{k=1}^{2} t[|e_k(t)| + w_k |\Delta u_k(t)|] dt \tag{4.28}$$

$$J_3 = ISEU = \int_0^{t_f} \sum_{k=1}^{2} [e_k^2(t) + w_k \Delta u_k^2(t)] dt \tag{4.29}$$

where $e_k(t)$ is the error signal between the output y_k and the corresponding set point; the deviation of control input $\Delta u_k(t) = u_k - u_{k0}$; w_k is the weighting factor. By appropriately changing the weighting factors, the design specifications can be achieved.

4.4.3 Controller Tuning Using a GA

In this subsection for the comparison purpose, the GA-based PID, NPID and FOPID top and bottom composition controllers are implemented. It is considered the same objective functions for tuning the three controllers. In order to assess the performance of each controller, all the controllers have been run ten times, and the best, worst, and average results have been discussed in detail at chapter five. The top and bottom distillation column of the PID and NPID controllers have six parameters (K_{p1}, K_{i1}, K_{d1}, K_{p2}, K_{i2}, and K_{d2}) while the FOPID has ten parameters (K_{p1}, K_{i1}, K_{d1}, λ_1, μ_1, K_{p2}, K_{i2}, K_{d2}, λ_2, and μ_2). The GA parameters settings used in the simulation for the tuning of the PID, NPID and FOPID controllers of distillation column control are shown in Table 4.1.

Table 4. 1 Parameter settings of the genetic algorithm

Parameter	PID/NPID controllers	FOPID controller
Maximum Generation	50	50
Population Size	20	20
No of Parameter	6	10
Lower Boundary	[0 0 0 -0.5 -0.5 -0.5]	[0 0 -0.5 -0.5 -0.5 -0.5 0 0 0 0]
Upper Boundary	[1 1 1 1 1 1]	[1 1 1 1 1 1 1 1 1 1]

The details of the parameters of the PID, NPID, and FOPID top and bottom composition based on GA with and without decoupler are obtained. The selection of the best optimized parameters is done with the help of less fitness values of IAEU, ITAEU, and ISEU as shown in the Appendix: E1-E6.

CHAPTER 5

RESULTS AND DISCUSSIONS

In the previous sections the details of the mathematical modeling of distillation column based on wood and berry model were done. For controlling DC, the PID, NPID, and FOPID controllers are designed and their parameters are tuned using the GA in MATLAB 2020a/Simulink software**.** In order to obtain the performance of each controller, the feedback system is simulated based on the set point tracking and disturbance rejection conditions with and without decoupling.

5.1 Performance of Distillation Column without Decoupling

5.1.1 Controllers Parameter Tuning Result

In this section all the implemented controllers are tuned based on GA optimization without considering decoupling. The optimal tuned controller gain parameters of top and bottom compositions of distillation column without decoupling is presented in Table 5.1a and Table 5.1b. The objective functions of controllers are subjected to minimization.

Table 5. 1**a** Optimum settings of the PID, NPID, and FOPID controllers for top composition without decoupling via minimizing J_1, J_2, and J_3

Tuning Methods	**Controller Type**	**Parameters**				
		K_{p1}	K_{i1}	K_{d1}	λ_1	μ_1
J_1 = ***IAEU***	PID	0.1580	0.0039	0.1265	-	-
	NPID	0.5339	0.0039	0.7891	-	-
	FOPID	0.3748	0.0362	0.7398	0.7500	0.4851
J_2 = ***ITAEU***	PID	0.4734	0.0020	0.6016	-	-
	NPID	0.9595	0.2886	0.1954	-	-
	FOPID	0.2091	0.8434	0.9669	0.3664	0.7274
J_3 = ***ISEU***	PID	0.2826	0.0223	0.3611	-	-
	NPID	0.3125	0.0156	0.3301	-	-
	FOPID	0.2106	0.0156	0.1006	1.0000	0.6455

Table 5. 1**b** Optimum settings of the PID, NPID, and FOPID controllers for bottom composition without decoupling via minimizing J_1, J_2, and J_3

Tuning Methods	**Controller Type**	**Parameters**				
		K_{p2}	K_{i2}	K_{d2}	λ_2	μ_2
	PID	-0.2233	-0.0105	-0.3695	-	-
J_1 = *IAEU*	NPID	-0.1161	-0.0099	-0.2992	-	-
	FOPID	0.0320	-0.0214	-0.2835	0.7415	0.8583
	PID	-0.3221	-0.0110	-0.1085	-	-
J_2 = *ITAEU*	NPID	-0.0198	-0.0082	-0.0073	-	-
	FOPID	-0.0451	-0.0133	-0.0059	0.8467	0.9500
	PID	-0.4540	-0.0063	-0.2359	-	-
J_3 = *ISEU*	NPID	-0.4951	-0.0080	-0.2332	-	-
	FOPID	-0.2912	-0.1036	0.0293	0.2970	0.6317

5.1.2 Set Point Tracking Performance Results

The set point tracking result for the top (distillate) and bottom composition is shown in Figure 5.1 and Figure 5.2.

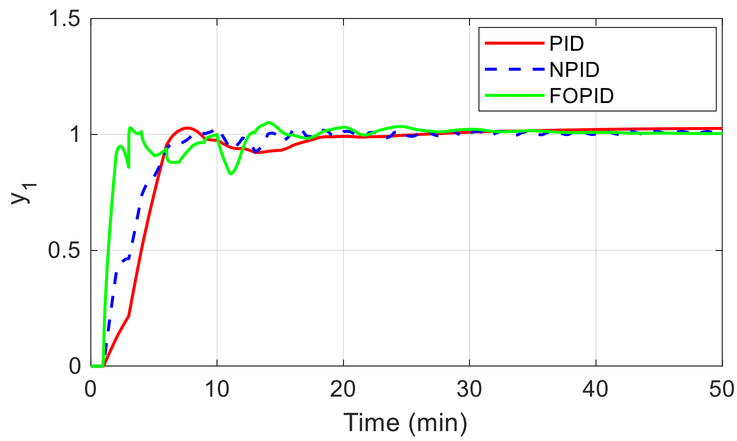

(a) IAEU

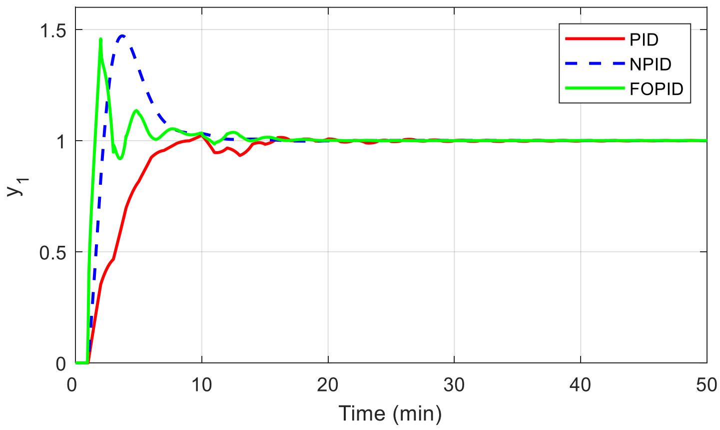

(b) ITAEU

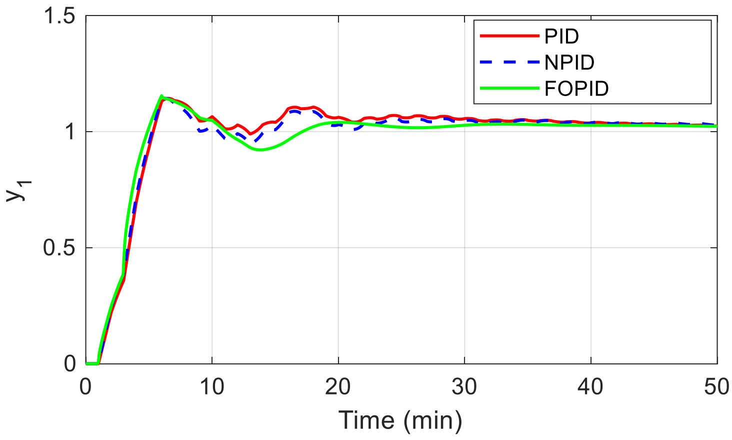

(c) ISEU

Figure 5. 1 Step responses of the PID, NPID and FOPID controllers for distillation column without decoupling

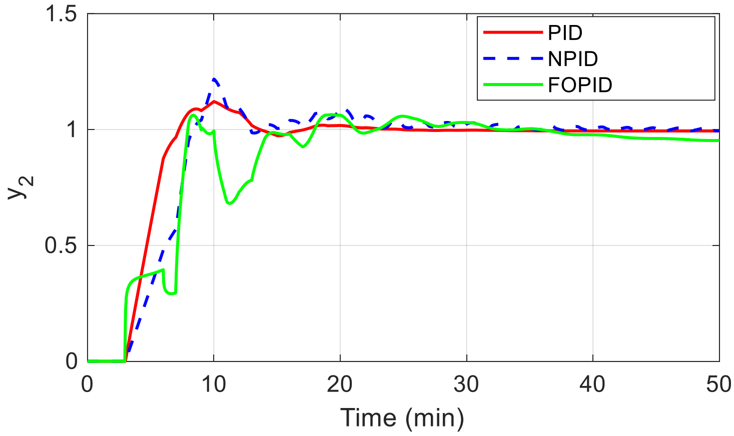

(a) IAEU

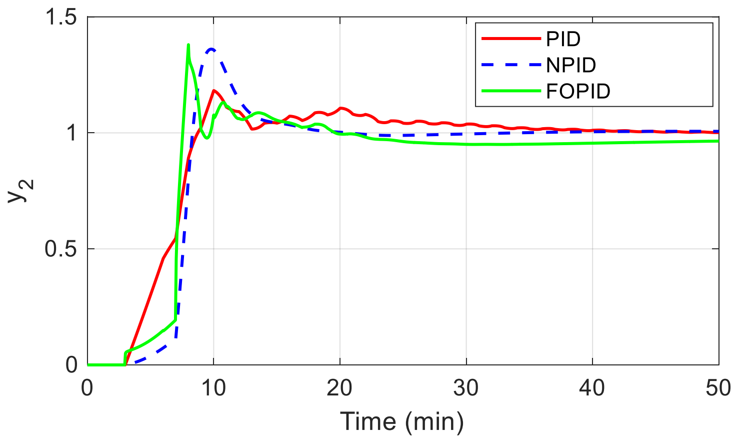

(b) ITAEU

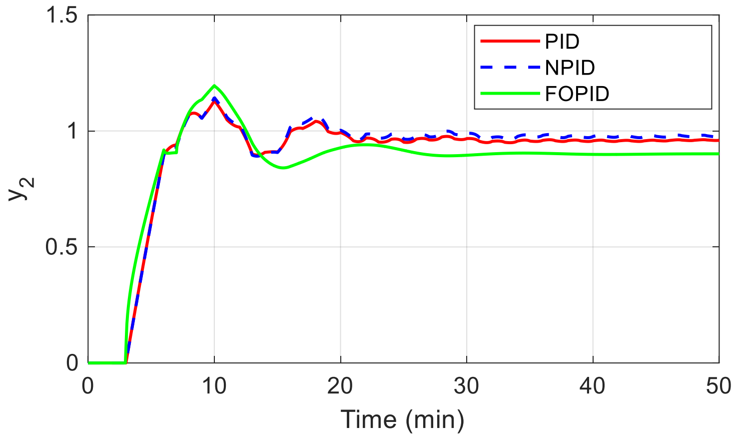

(c) ISEU

Figure 5. 2 Step responses of the PID, NPID, and FOPID controllers for distillation column without decoupling

5.1.3 Discussion of Set point Tracking Results

Table 5.2a and Table 5.2b presents the performance index IAE, optimum time indices parameters, and objective functions of top composition and bottom composition of distillation column. Considering the top composition and corresponding objective function J_1, the FOPID controller provides the least IAE value and high M_p value compared to other controllers. For the FOPID controller there is no t_s value determined but for PID and NPID, t_s values found to be 103.815 (min) and 16.647 (min), respectively. The t_r values for PID, NPID, and FOPID are 6.586 (min), 8.163 (min), and 7.944 (min), respectively. The highest t_r value is observed in the NPID controller.

In the case of bottom composition, the least IAE value is observed in PID compared to other controllers. The NPID controller yield highest M_p values and least corresponding value found in FOPID controller. In PID and NPID, the t_s values are 15.741 (min) and 32.707 (min), respectively, whereas no ts value found in FOPID controller. The t_r values for PID, NPID and FOPID are 7.232 (min), 8.356 minute and 7.944 (min), respectively. It may be noticed that the t_r values for top and bottom compositions is same.

Table 5. 2**a** Quantitative performance comparisons of the top composition (y_1) of the DC without decoupling

Tuning Methods	Controller Type	SP tracking performance			
		M_p (%)	t_s	t_r	*IAE*
	PID	2.7213	103.814	6.5862	6.9873
J_1 = IAEU	NPID	2.6442	16.6472	8.1626	4.4803
	FOPID	6.4088	-	7.9435	**3.0200***
	PID	2.4379	13.9618	9.0335	3.8476
J_2 = ITAEU	NPID	47.160	10.9108	2.2273	**3.2430***
	FOPID	38.021	107.270	7.5445	10.9867
	PID	14.355	55.4841	5.3229	6.2856
J_3 = ISEU	NPID	14.369	67.3647	5.2325	6.1854
	FOPID	19.538	-	7.3859	**5.3583***

∗ mean the best ***IAE***

Considering the top composition and corresponding objective function J_2, the least IAE value is obtained for NPID compared to other controllers. The highest and lowest M_p value found in NPID and PID controllers, respectively. The least t_s value is 10.911 (min) for NPID and 107.270 (min) for FOPID while in PID, the t_s value obtained is 13.962 (min). The t_r values for PID, NPID, and FOPID are found to be 9.034 (min), 2.227 (min), and 7.545 (min), respectively.

In the case of bottom composition, the least IAE value obtained in PID controller. The maximum M_p is seen in FOPID controller and the less M_p observed in PID controller. The highest t_s is 107.270 (min) for FOPID and lowest value for NPID controller. The t_r values for PID, NPID, and FOPID are found to be 8.730 (min), 8.314 (min) and 7.545 minute, respectively. It may be notice that for FOPID controller, the t_s values are same for top and bottom composition of distillation column.

Table 5. 2**b** Quantitative performance comparisons of the bottom composition (y_2) of the DC without decoupling

Tuning Methods	**Controller Type**	**SP tracking performance**			
		M_p **(%)**	t_s	t_r	***IAE***
	PID	12.081	15.7411	7.2323	**5.7525***
J_1 **= *IAEU***	NPID	21.797	32.7067	8.3560	7.2468
	FOPID	6.4088	-	7.9435	10.8945
	PID	18.225	34.8352	8.7302	**7.8619***
J_2 **= *ITAEU***	NPID	36.081	17.2230	8.3140	8.9890
	FOPID	38.021	107.270	7.5445	10.9780
	PID	12.994	87.2021	7.3820	8.3907
J_3 **= *ISEU***	NPID	14.356	59.9524	7.4274	**7.0877***
	FOPID	19.538	-	7.3859	17.3521

∗ mean the best ***IAE***

Acknowledging the top composition and corresponding objective function J_3, the least IAE value is obtained for FOPID compared to other controllers while for PID and NPID, these values are 6.286 and 6.185, respectively. The maximum M_p is found in FOPID followed by PID and NPID. No t_s is found for FOPID, however, for PID and NPID, these values are 55.484 (min) and 67.365 (min), respectively. The t_r values for PID, NPID, and FOPID are 5.3229 (min), 5.2325 (min), and 7.3859 (min), respectively.

In the case of bottom composition, the least IAE value obtained in NPID controller. Maximum M_p observed in case of FOPID followed by PID and NPID. No t_s is found for FOPID, however, t_s values estimated for PID and NPID are 87.202 (min) and 59.952 (min), respectively. The t_r values for PID, NPID, and FOPID are found to be 7.382 (min), 7.427 (min) and 7.386 (min), respectively. It can be noticed that for FOPID controller, the M_p values are same for top and bottom composition of DC.

Figure 5.1 and Figure 5.2 show the set point tracking performance of top and bottom composition of DC, respectively. The order of controllers based on least IAE with respect to top composition of DC found to be FOPID for J_1, NPID for J_2 and FOPID for J_3. In bottom composition, the corresponding controllers order obtained are PID for J_1 and J_2 while NPID for J_3.

5.1.4 Disturbance Rejection Responses

In order to assess the robustness of three controllers to disturbance changes, 0.2 input feed rate are used at a time of 80 (min). Figure 5.3 and Figure 5.4 show the disturbance rejection responses for the top (distillate) and bottom composition, respectively.

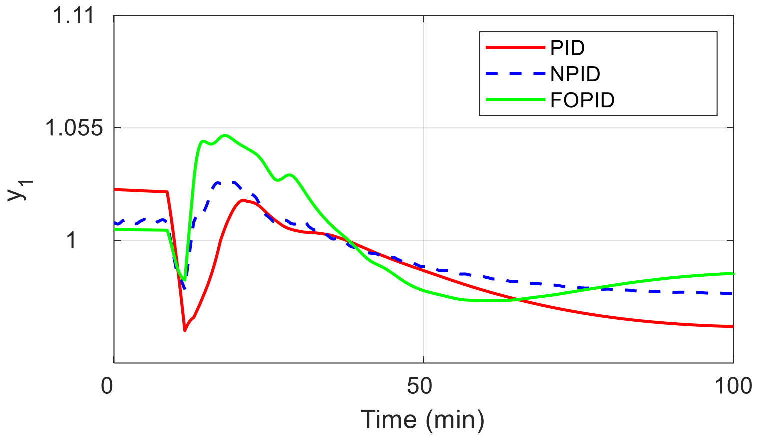

(a) IAEU

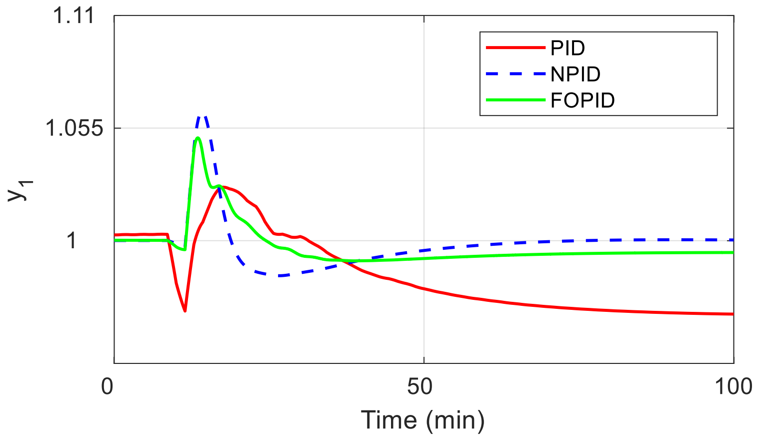

(b) ITAEU

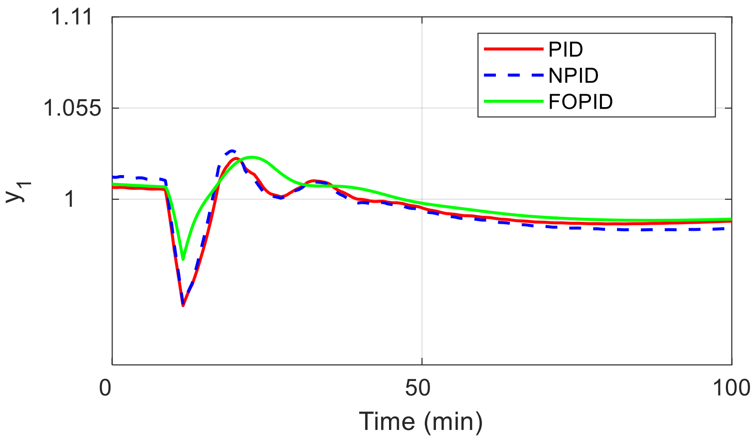

(c) ISEU

Figure 5. 3 Top composition responses using the three controllers for distillation column without decoupling to step-type change of input feed rate

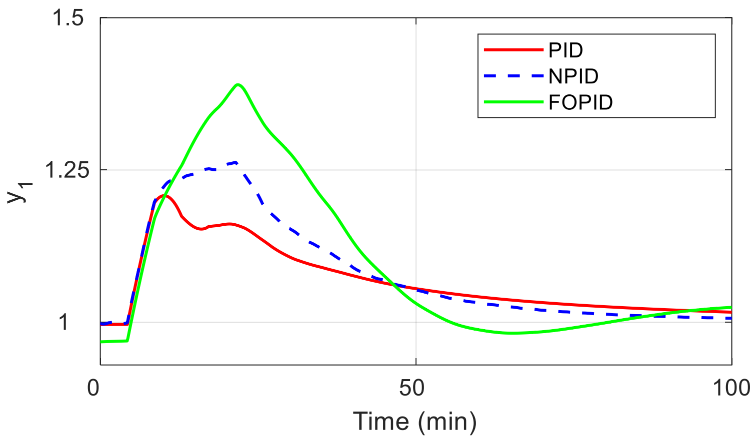

(a) IAEU

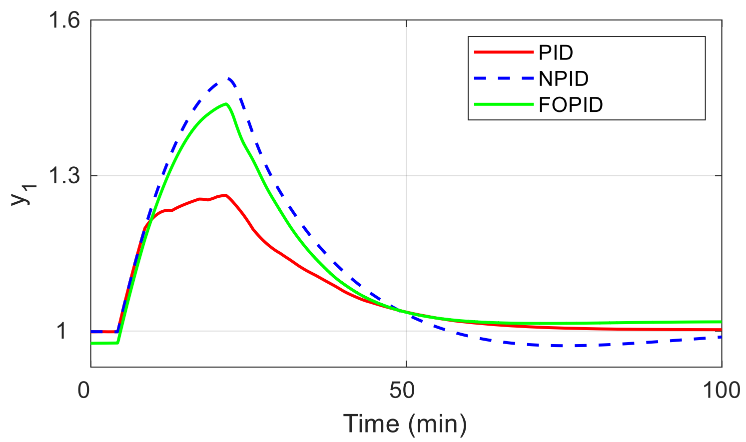

(b) ITAEU

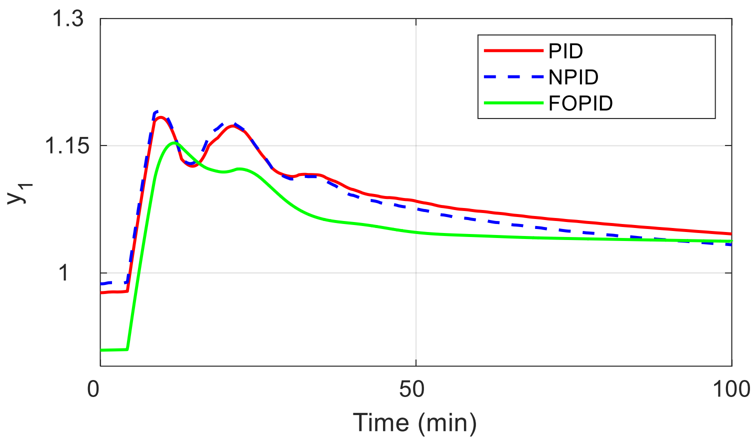

(c) ISEU

Figure 5. 4 Bottom composition responses using the three controllers for distillation column without decoupling to step-type change of input feed rate

5.1.5 Discussion of Disturbance Rejection Results

Table 5. 3**a** Top composition (y_1) of the optimum time indices parameter and objective function for J_1, J_2, and J_3 for *DC* without decoupling considering 0.2 input feed rate disturbance

Tuning Methods	Controller Type	Disturbance rejection performance			
		t_p	M_p (%)	t_s	*IAE*
	PID	8	0.0441	-	1.6283
J_1 = IAEU	NPID	13.4500	0.0284	-	**1.1566***
	FOPID	12.5290	0.0512	-	1.5726
	PID	70	0.0359	-	1.5408
J_2 = ITAEU	NPID	9.9100	0.0630	44.87	**0.4714***
	FOPID	9.4420	0.0502	-	0.5640
	PID	8	0.0643	-	0.8526
J_3 = ISEU	NPID	8	0.0632	-	0.9895
	FOPID	8	0.0363	-	**0.7257***

∗ mean the best ***IAE***

Table 5.3a and Table 5.3b presents an optimum time indices parameter and objective function for J_1, J_2, and J_3 for distillation column without decoupling considering 0.2 step input disturbance. Considering J_1, in top and bottom composition the least IAE value obtained 1.157 for NPID controller and 4.848 for PID controller. The lowest M_p values are 0.025% for *NPID* and 0.208% for PID in top and bottom composition of DC, respectively. In t_p, the least value estimated as 8 (min) for PID controller and highest value found in NPID controller for top composition, whereas least and maximum t_p values for bottom composition are 7.09 (min) and 15.251 (min) for PID and FOPID, respectively. However, no values are found for t_s in all controllers. In the case of objective function J_2, the least IAE value found in NPID controller for top composition and PID for bottom composition. In top and bottom composition, the lowest M_p value is PID controller. The corresponding maximum M_p value is 0.063% and 0.4875% for NPID controller, in order with respect to composition.

Table 5. 3**b** Bottom composition (y_2) of the optimum time indices parameter and objective function for J_1, J_2, and J_3 for *DC* without decoupling considering 0.2 input feed rate disturbance

Tuning Methods	**Controllers Type**	**Disturbance rejection performance**			
		t_p	M_p **(%)**	t_s	***IAE***
	PID	7.0900	0.2079	-	**4.8479***
J_1 **=** ***IAEU***	NPID	15	0.2628	-	5.7427
	FOPID	15.2510	0.3900	-	7.3966
	PID	15	0.2620	53.576	**5.2031***
J_2 **=** ***ITAEU***	NPID	15.0700	0.4875	-	8.5141
	FOPID	15.0030	0.4381	-	7.5386
	PID	6.7100	0.1835	-	6.1448
J_3 **=** ***ISEU***	NPID	6.5400	0.1906	-	5.7039
	FOPID	8.1800	0.1532	-	**4.5309***
* mean the best ***IAE***					

The t_p values for PID, NPID, and FOPID controllers for top composition are obtained as 70 (min), 9.91 (min) and 9.442 (min), respectively and the corresponding values for bottom composition are 15 (min), 15.07 (min) and 15.003 (min), in order. The t_s values for top composition are 44.87 (min) for NPID controller and 53.574 (min) for PID controller in bottom composition only.

Considering objective function J_3, the least IAE values found in FOPID controller for both top and bottom composition compared to other controllers. For top composition, the M_p

values obtained as 0.064% for PID, 0.063% for NPID and 0.036% for FOPID. For bottom composition, M_p values found to be 0.184% for *PID*, 0.191% for NPID and 0.153% for FOPID. In all the controllers for top composition, the t_p value is 8 (min), while the t_p values in bottom composition are obtained as 6.71 (min) for PID, 6.54 (min) for NPID and 8.18 (min) for FOPID. There is no t_s value found in all controllers. Figure 5.3 shows the dynamic responses for 0.2 step input disturbance using *PID*, *NPID*, and *FOPID* controllers for the top composition of distillation column without decoupler.

Figure 5.4 shows the dynamic responses for 0.2 step input disturbance using PID, NPID, and FOPID controllers for the bottom composition of DC decoupler. The order of controllers based on least IAE with respect to top composition of distillation column found to be NPID for J_1 and J_2 and FOPID for J_3. In bottom composition, the corresponding controllers order obtained are PID for J_1 and J_2 while FOPID for J_3.

5.2 Performance of Distillation Column with Decoupling

5.2.1 Controllers Parameter Tuning Result

Table 5. 4**a** Optimum settings of the PID, NPID, and FOPID controllers for top composition with decoupling via minimizing J_1, J_2, and J_3

Tuning Methods	**Controllers Type**	**Parameters**				
		K_{p1}	K_{i1}	K_{d1}	λ_1	μ_1
J_1 = IAEU	PID	0.4924	0.1316	0.5372	-	-
	NPID	0.6846	0.0863	0.5417	-	-
	FOPID	0.4740	0.1026	0.3629	0.9154	0.7456
J_2 = ITAEU	PID	0.4796	0.1679	0.5191	-	-
	NPID	0.4406	0.2228	0.5024	-	-
	FOPID	0.0985	0.1878	0.4485	0.8736	0.5002
J_3 = ISEU	PID	0.5302	0.0812	0.7214	-	-
	NPID	0.6009	0.1057	0.6995	-	-
	FOPID	0.3713	0.0656	-0.0003	0.9976	0.9958

In this section all the implemented controllers are tuned based on GA optimization with considering decoupler. The optimally tuned parameters of top and bottom compositions of distillation column with decoupler is presented in Table 5.4a and Table 5.4b.

Table 5. 4**b** Optimum settings of the PID, NPID, and FOPID controllers for top composition with decoupling via minimizing J_1, J_2, and J_3

Tuning Methods	Controllers Type	Parameters				
		K_{p2}	K_{i2}	K_{d2}	λ_2	μ_2
$J_1 = IAEU$	PID	-0.1705	-0.0233	-0.2717	-	-
	NPID	-0.1426	-0.0355	-0.2167	-	-
	FOPID	-0.0610	-0.0808	-0.2865	0.7037	0.9516
$J_2 = ITAEU$	PID	-0.1158	-0.0196	-0.0617	-	-
	NPID	-0.1271	-0.0304	-0.0397	-	-
	FOPID	-0.0700	-0.0436	-0.0981	0.7817	0.7133
$J_3 = ISEU$	PID	-0.1809	-0.0237	-0.3249	-	-
	NPID	-0.1737	-0.0433	-0.2727	-	-
	FOPID	0.2663	-0.1688	-0.4284	0.4809	0.4262

5.2.2 Set point Tracking Performance Results

The set point tracking responses for the top (distillate) and bottom composition are shown in Figure 5.5 and Figure 5.6.

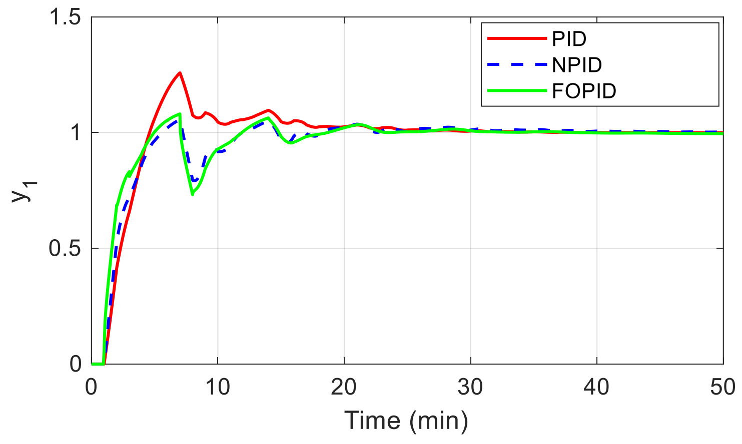

(a) IAEU

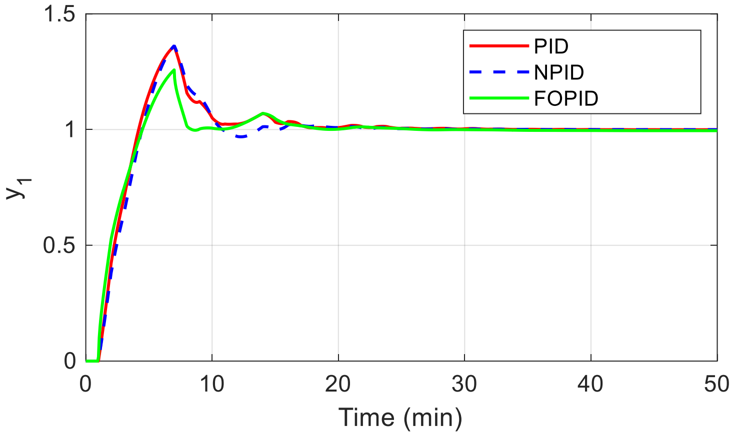

(b) ITAEU

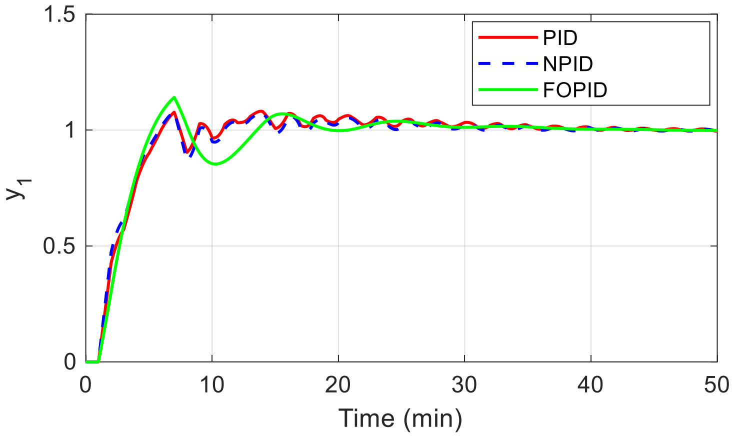

(c) ISUE

Figure 5. 5 Step responses of the PID, NPID, and FOPID controllers for distillation column with decoupling

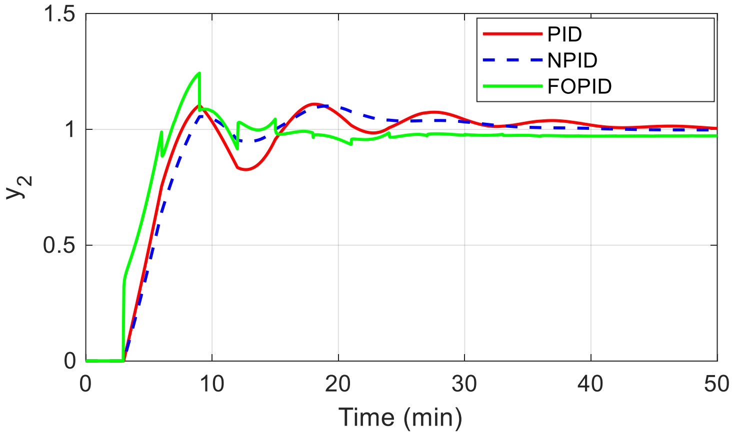

(a) IAEU

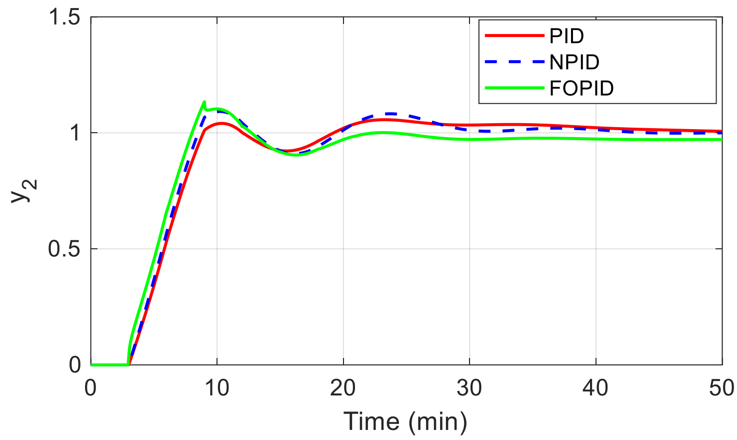

(b) ITAEU

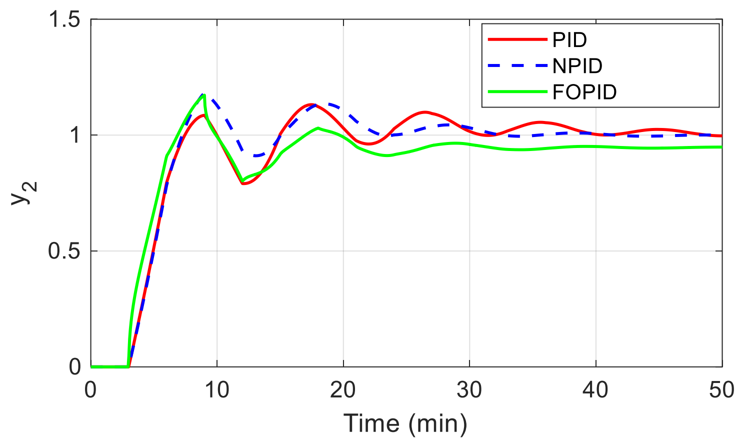

(c) ISEU

Figure 5. 6 Step responses of the PID, NPID, and FOPID controllers for distillation column with decoupling

5.2.3 Discussion of Set point Trucking Results

In Table 5.5a and Table 5.5b, considering the objective function J_1 the least IAE value obtained in FOPID controller for top and bottom composition. The maximum M_p found in PID controller is same compared to NPID and FOPID. The t_s values in top composition are 23.794 (min) for PID, 28.731 (min) for NPID and 22.106 (min) for FOPID. The corresponding values for bottom composition as 39.870 (min) for PID, 32.099 (min) for NPID and no t_s values found in FOPID. The PID controller shows highest t_s value compared to other controllers. The minimum t_r values estimated as 4.5856 minute for PID in top composition and 6.790 (min) for FOPID in bottom composition.

Considering objective function J_2, the least IAE values found in FOPID for both top and bottom composition. The maximum M_p values obtained in top and bottom composition are 36.253% for NPID and 13.417% for FOPID, respectively. The t_s estimated as 16.989 (min) for PID, 16.936 (min) for NPID and 16.470 (min) for FOPID in top composition while for bottom composition, t_s values are 40.928 (min) for PID and 37.645 (min) for NPID. No t_s value found for FOPID in bottom composition. The t_r values in top composition are 4.174 (min) for *PID*, 4.438 (min) for NPID and 4.479 (min) for FOPID whereas in bottom composition these values obtained as 8.902 (min) for PID, 8.502 (min) for NPID and 8.011 minute for FOPID.

Concerning to objective function J_3, the least IAE value found in NPID controller for top and bottom composition. The maximum M_p valued found in FOPID for top composition and NPID for bottom composition. The minimum t_s values as 27.725 (min) for FOPID and 30.862 (min) for NPID in top and bottom composition respectively. The *tr* values estimated in top composition are 5.9494 minute for PID, 5.8161 minute for NPID and 5.243 (min) for FOPID while in bottom composition, t_r values estimated as 7.4364 (min) for PID, 7.232 (min) for NPID and 6.879 (min) for FOPID.

Table 5. 5**a** Quantitative performance comparisons of the top composition (y_1) of the DC with decoupling

Tuning Methods	**Controllers Type**	**SP tracking performance**			
		M_p **(%)**	t_s	t_r	***IAE***
J₁ = IAEU	PID	25.7899	23.7939	4.5856	3.8477
	NPID	5.5280	28.7310	5.5914	3.3406
	FOPID	8.0539	22.1059	4.9528	**2.9959***
J₂ = ITAEU	PID	35.9477	16.9885	4.1736	3.8927
	NPID	36.2532	16.9360	4.4381	3.8856
	FOPID	25.7880	16.4697	4.4787	**3.0680***
J₃ = ISEU	PID	8.1474	35.0187	5.9494	3.9275
	NPID	7.9706	32.8856	5.8161	**3.5569***
	FOPID	14.1198	27.7254	5.2427	4.1200

∗ mean the best ***IAE***

The dynamic responses for top composition and bottom composition with the optimally tuned PID, NPID and FOPID controllers based on the genetic algorithm are shown in Figure 5.5 and Figure 5.6, respectively. The order of controllers based on least IAE with respect to top composition of distillation column found to be FOPID for J_1 and J_2 and NPID for J_3. In bottom composition, the corresponding controllers order obtained are FOPID for J_1 and J_2 while NPID for J_3.

Table 5. 5**b** Quantitative performance comparisons of the bottom composition (y_2) of the DC with decoupling

Tuning Methods	Controllers Type	SP tracking performance			
		M_p (%)	t_s	t_r	*IAE*
J_1 = IAEU	PID	25.789	39.8692	7.6015	6.9335
	NPID	10.110	32.0989	8.4362	6.6746
	FOPID	24.343	-	6.7899	**5.6153***
J_2 = ITAEU	PID	5.6726	40.9283	8.9022	7.2121
	NPID	9.2137	37.6445	8.5015	7.0460
	FOPID	13.417	-	8.0110	**6.7270***
J_3 = ISEU	PID	13.146	46.2388	7.4364	7.0515
	NPID	18.208	30.8621	7.2322	**6.5426***
	FOPID	17.242	-	6.8790	7.0807

∗ mean the best ***IAE***

5.2.4 Disturbance Rejection Response

In order to assess the robustness of three controllers to disturbance changes, 0.2 input feed rate are used at a time of 50 (min). Figure 5.7 and Figure 5.8 show the disturbance rejection responses for the top (distillate) and bottom composition, respectively.

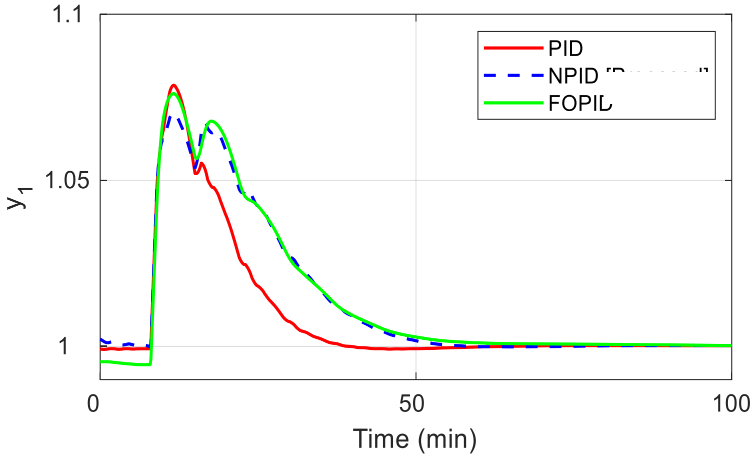

(a) IAEU

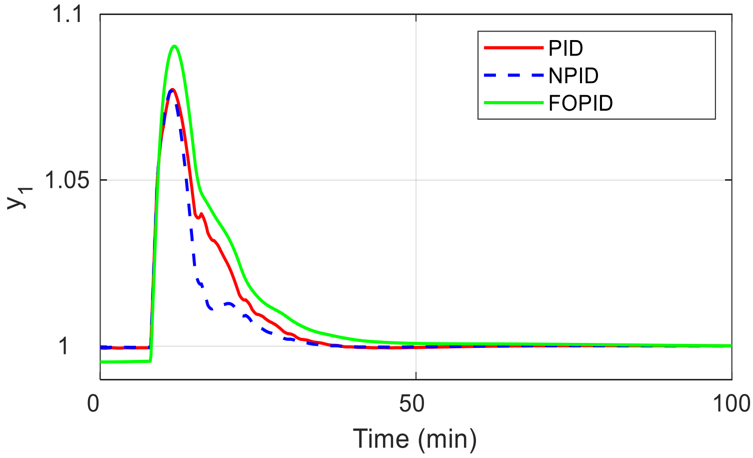

(b) ITAEU

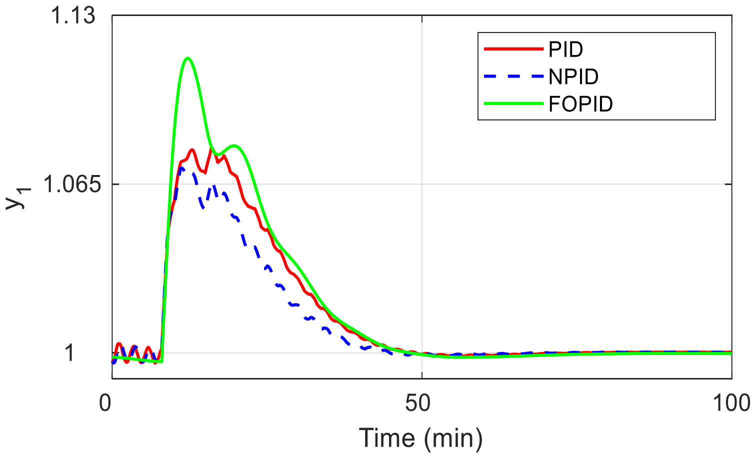

(c) ISEU

Figure 5. 7 Top composition responses using the three controllers for distillation column with decoupler to step-type change of input feed rate

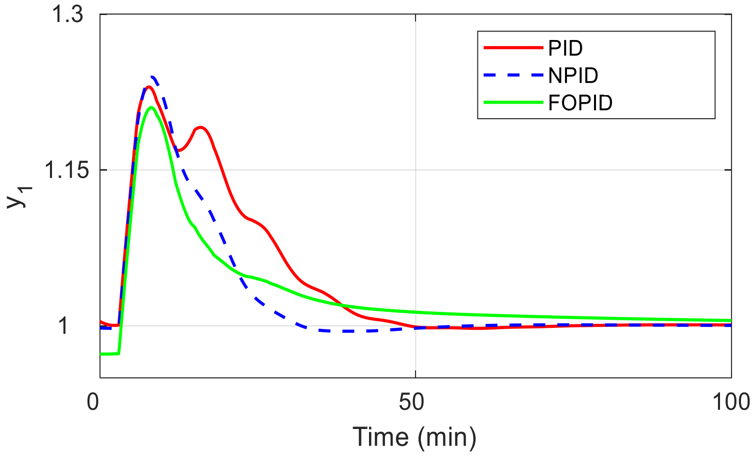

(a) IAEU

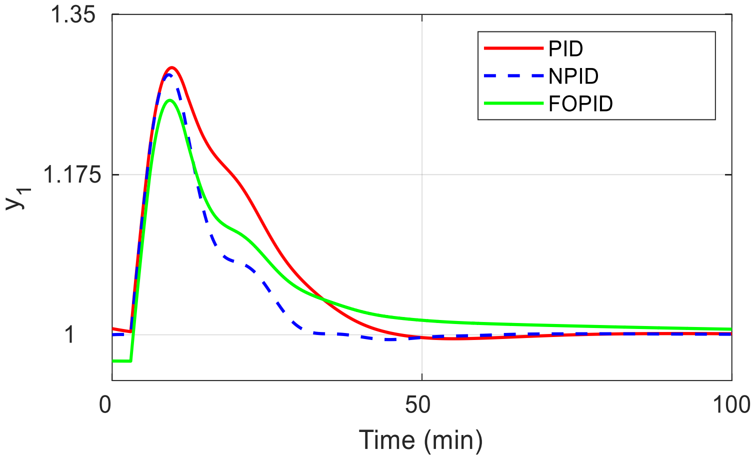

(b) ITAEU

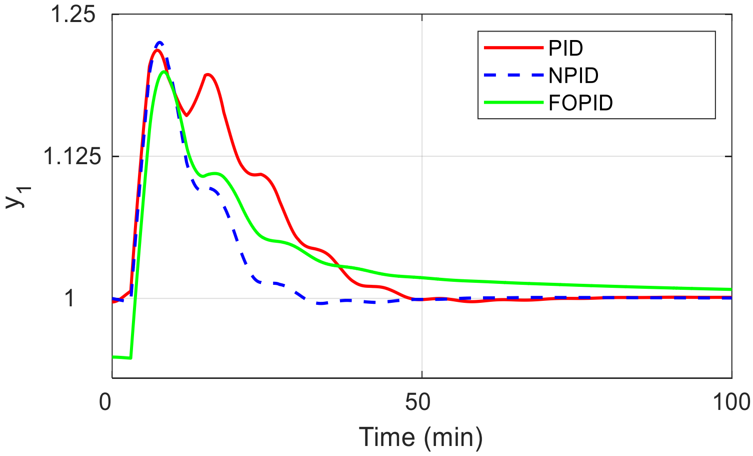

(c) ISEU

Figure 5. 8 Bottom composition responses using the three controllers for distillation column with decoupling to step-type change of input feed rate

5.2.5 Discussion of Disturbance Rejection Results

Table 5.6a and Table 5.6b presents an optimum time indices parameter and objective function for J_1, J_2, and J_3 for distillation column without decoupling considering 0.2 step input disturbance. Considering the objective function J_1, the least IAE value found in PID and NPID for top and bottom composition respectively. In considered controllers, the least M_p observed in top composition compared to bottom composition. The t_p values are 11.64 (min) for PID, 11.62 (min) for NPID and 11.603 (min) for FOPID in top composition, while in bottom composition, t_p values are 7.75 (min) for PID, 8.21 (min) for NPID and 8.13 (min) for FOPID. The t_s values are 35.746 (min) for PID, 50.649 (min) for NPID and 55.308 (min) for FOPID in top composition, whereas in bottom composition, t_s values found to be 45.5579 (min) for PID and 43.1064 (min) for NPID. No t_s value found for FOPID in bottom composition.

Table 5. 6**a** Top composition of the optimum time indices parameter and objective function for J_1, J_2, and J_3 for DC with decoupling considering 0.2 step input disturbance

Tuning Methods	**Controllers Type**	**Disturbance rejection performance**			
		t_p	M_p (%)	t_s	*IAE*
J_1 = IAEU	PID	11.6400	0.0786	35.7487	**0.9239∗**
	NPID	11.6200	0.0704	50.6494	1.3739
	FOPID	11.6030	0.0761	55.3076	1.4792
J_2 = ITAEU	PID	11.4400	0.0773	33.2516	0.7202
	NPID	11.2100	0.0768	31.0444	**0.5406 ∗**
	FOPID	11.7350	0.0903	40.8500	0.9836
J_3 = ISEU	PID	16.0200	0.0792	44.8112	1.4870
	NPID	11.2200	0.0712	42.1929	**1.1510 ∗**
	FOPID	12.1880	0.1135	44.1850	1.8053

∗ mean the best ***IAE***

Table 5. 6**b** Bottom composition (y_2) of the optimum time indices parameter and objective function for J_1, J_2, and J_3 for DC with decoupling considering 0.2 step input disturbance

Tuning Methods	Controllers Type	Disturbance rejection performance			
		t_p	M_p (%)	t_s	*IAE*
J₁ = IAEU	PID	7.7500	0.2299	45.5579	4.3564
	NPID	8.2100	0.2393	43.1064	**3.0126** ∗
	FOPID	8.1300	0.2100	-	3.4275
J₂ = ITAEU	PID	9.6200	0.2918	42.6537	5.2411
	NPID	9.1400	0.2840	30.8504	**3.4600** ∗
	FOPID	9.3020	0.2561	-	4.7723
J₃ = ISEU	PID	7.2900	0.2182	46.1228	4.2857
	NPID	7.6700	0.2251	29.7990	**2.4363** ∗
	FOPID	8.3450	0.1993	-	3.9872

∗ mean the best ***IAE***

Considering the objective function J_2, the least IAE value observed in NPID for top and bottom composition. In considered controllers, the least M_p observed in top composition compared to bottom composition. The t_p values are 11.44 (min) for PID, 11.21 (min) for NPID and 11.735 (min) for FOPID in top composition, while in bottom composition, t_p values are 9.62 (min) for PID, 9.14 (min) for NPID and 9.302 (min) for FOPID. The t_s values are 33.2516 (min) for PID, 31.044 (min) for NPID and 40.85 (min) for *FOPID* in top composition, whereas in bottom composition, t_s values found to be 42.654 (min) for PID and 30.850 (min) for NPID. No t_s value found for FOPID in bottom composition.

Choosing objective function J_3, the least IAE value observed in NPID for top and bottom composition. In considered controllers, the least M_p observed in top composition compared to bottom composition. The t_p values are 16.02 (min) for PID, 11.22 (min) for NPID and 12.188 (min) for FOPID in top composition, while in bottom composition, t_p values are 7.29 (min) for PID, 7.67 (min) for NPID and 8.345 (min) for FOPID. The t_s values are 44.811 (min) for PID, 42.193 (min) for NPID and 44.185 (min) for FOPID in top composition, whereas in bottom composition, *ts* values found to be 46.123 (min) for PID and 29.799 (min) for NPID. No t_s value found for FOPID in bottom composition.

The dynamic responses of the top composition and bottom composition for an instantaneous 0.2 step input variation are presented in Figure 5.7 and Figure 5.8, respectively. The order of controllers based on least IAE with respect to top composition of distillation column found to be PID for J_1 and NPID for J_2 and J_3. In bottom composition, the corresponding controllers order obtained are NPID for all considered objective functions.

6. CONCLUSIONS AND RECOMMENDATIONS

6.1 Conclusions

In the work presented, the TITO distillation column process has been studied, analyzed, and simulated. It's pairing analysis between control variables and manipulated variables were employed. The DC process steady-state analysis has been carried out. The main problem of the DC is the interaction between inputs and outputs. This has been eliminated with the help of appropriate decoupling, which made the MIMO process into two simple SISO system. Then, the three PID, NPID, and FOPID controllers were designed independently to control distillate top composition (y_1) and bottom composition (y_2) of the DC process. For tuning of the controller parameters, a genetic algorithm was used. Their performance analysis was carried out based on the chosen objective functions such as IAEU, ITAEU, and ISEU. For the quantitative comparison of the responses, the performance indices such as overshoot M_p, 2 % settling time t_s, rise time t_r, and integral of absolute error (IAE) were used to measure the performance of the controllers. Moreover, the set point tracking and disturbance rejection responses were obtained for all the controllers.

From the simulation results it was observed that the controllers for the distillation column process (DCP) with decoupling shows the least IAE values in terms of SP tracking and disturbance rejection as compared to DCP without decoupling. Thus, the DCP needs to be decoupled before designing the controllers.

The set point tracking performance of the controllers for the DCP with decoupling shows slight inconsistency with respect to the three fitness functions. Based on the obtained least time indices parameter and IAE values in fitness functions J_1 and J_2, the FOPID shows superior results. For fitness function J_3 NPID shows the best result compared to the other controllers for both top composition and bottom composition of the DC.

Considering the disturbance rejection performance, it is obtained that NPID controller shows the least time indices parameter and IAE values in fitness functions $J_{1,}$ $J_{2,}$ and J_3 in both top and bottom composition of the DCP, except the fitness function J_1 case in top composition of the DCP in which PID shows a superior performance.

Generally, as can be seen in the result for set point tracking FOPID shown better result and for the disturbance rejection NPID has superior result.

6.2 Recommendations

Distillation column dynamics are nonlinear and multivariable. Linearization of distillation columns is a huge area of research. If taking account of optimization of distillation column, it would be an interesting research field to work on. This thesis work has been done 2x2 WB distillation column process, so 3x3, 4x4 distillation column process may be future scope of work. Incorporating the reflux and reboiler levels may help to maintain the unit's overall material balance. Adding adaptive, and cascade control of two or more feedback control loop strategies can be further improve the performance of the distillation column.

Acknowledgements

The research for this paper was financially supported by Adama Science and Technology University under the grant number of **ASTU/SM-R/169/20**, Adama, Ethiopia.

REFERENCES

[1] M. Y. Hassan and S. S. Ezzaten, “PI-Like Interval Type-2 Fuzzy Logic Control Based Social Spider Optimization for distillation column,” in *2018 3rd Scientific Conference of Electrical Engineering, IEEE 2018*, 2018, pp. 67–71, doi: 10.1109/SCEE.2018.8684171.

[2] S. Chavan, N. Birnale, and A. S. Deshpande, “Design and simulation of model predictive control for multivariable distillation column,” in *2018 3rd IEEE International Conference on Recent Trends in Electronics, Information and Communication Technology, IEEE 2018 - Proceedings*, 2018, pp. 764–768, doi: 10.1109/RTEICT42901.2018.9012517.

[3] P. Manikandan, P. Thangaganapathy, and D. Manamalli, “Selection of control structure and dual composition control for ethanol-water distillation column,” 2017, doi: 10.1109/TIMA.2017.8064814.

[4] V. Haji Haji and C. A. Monje, “Fractional-order PID control of a MIMO distillation column process using improved bat algorithm,” *Soft Comput.*, vol. 23, no. 18, 2019, doi: 10.1007/s00500-018-3488-z.

[5] Y. Cheng, Z. Chen, M. Sun, and Q. Sun, “Decoupling control of a binary distillation column with measurement noise,” in *Chinese Control Conference, CCC*, 2018, vol. 2018-July, doi: 10.23919/ChiCC.2018.8482851.

[6] R. Kumar, S. Anand, A. Khulbey, and A. Nath Jha, “Design of Fractional Order Controller for Wood-Berry distillation column,” 2020, doi: 10.1109/INDICON49873.2020.9342220.

[7] N. Alawad and A. Alseady, “Fuzzy controller of model reduction distillation column with minimal rules,” *Appl. Comput. Sci.*, vol. 16, no. 2, 2020, doi: 10.23743/acs-2020-14.

[8] V. S. Bhat, I. Thirunavukkarasu, V. I. George, and C. Sreelatha, “Controller Design and Implementation for a Pilot Plant Binary Distillation Column,” 2019, doi: 10.1109/DISCOVER.2018.8674066.

[9] G. Dumpa, P. Acharya, and T. K. Dan, “Comparative analysis of different control

techniques for a distillation column," in *2016 International Conference on Computation of Power, Energy, Information and Communication, ICCPEIC 2016*, 2016, pp. 52–57, doi: 10.1109/ICCPEIC.2016.7557222.

[10] P. Acharya, G. Dumpa, and T. K. Dan, "Modelling and control of distillation column," 2016, doi: 10.1109/ICCPEIC.2016.7557236.

[11] A. S. Baiesu and M. Carbureanu, "A binary distillation column top and bottom compositions control using two PI controllers tuned with SIMC," *Rev. Chim.*, vol. 70, no. 6, pp. 1960–1966, 2019, doi: 10.37358/rc.19.6.7254.

[12] S. Chavan, V. Rathi, and N. Birnale, "Implementation of fuzzy logic control for FOPDT model of distillation column," 2019, doi: 10.1109/RTEICT46194.2019.9016877.

[13] A. S. Baiesu and N. Paraschiv, "Binary distillation column top and bottom compositions control using two PI controllers tuned with GA," in *Proceedings of the 2017 IEEE 9th International Conference on Intelligent Data Acquisition and Advanced Computing Systems: Technology and Applications, IDAACS 2017*, 2017, vol. 1, doi: 10.1109/IDAACS.2017.8095139.

[14] R. N. Pawar and S. P. Jadhav, "Design of NDT and PSO based decentralised PID controller for wood-berry distillation column," 2018, doi: 10.1109/ICPCSI.2017.8391808.

[15] F. Al-Kalbani, S. M. Al Hosni, and J. Zhang, "Active Disturbance Rejection Control of a methanol-water separation distillation column," 2015, doi: 10.1109/IEEEGCC.2015.7060045.

[16] A. N. Fard, M. Shahbazian, and M. Hadian, "Adaptive fuzzy controller based on cuckoo optimization algorithm for a distillation column," 2016, doi: 10.1109/ICCIA.2016.17.

[17] M. Hamdy, A. Ramadan, and B. Abozalam, "A novel inverted fuzzy decoupling scheme for MIMO systems with disturbance: a case study of binary distillation column," *J. Intell. Manuf.*, vol. 29, no. 8, 2018, doi: 10.1007/s10845-016-1218-x.

[18] P. Mendis, C. Wickramasinghe, M. Narayana, and C. Bayer, "Adaptive Model Predictive Control with Successive Linearization for Distillate Composition Control

in Batch Distillation," 2019, doi: 10.1109/MERCon.2019.8818777.

[19] A. S. Handoko, H. R. Pranoto, S. R. Arief, and E. M. I. Hidayat, "Mini Distillation Column Control Using Model Predictive Control," 2019, doi: 10.1109/IC3INA.2018.8629541.

[20] P. Acharya, G. Dumpa, and T. K. Dan, "Modelling and control of distillation column," in *2016 International Conference on Computation of Power, Energy, Information and Communication, ICCPEIC 2016*, 2016, pp. 123–128, doi: 10.1109/ICCPEIC.2016.7557236.

[21] S. A. Ammar Taqvi, H. Zabiri, L. D. Tufa, S. A. Fatima, and A. H. Shah Maulud, "Distillation Column: Review of Major Disturbances," 2019, doi: 10.1109/ICCSCE47578.2019.9068539.

[22] F. Al-Kalbani and J. Zhang, "Inferential active disturbance rejection control of a heat integrated distillation column using dynamic principal component regression models," 2018, doi: 10.1109/IEEEGCC.2017.8447917.

[23] J. Ramyashree, M. R. Roja, G. Sivagurunathan, and R. Kotteeswaran, "Firefly algorithm based multivariable PID controller design for MIMO process," *Int. J. Eng. Technol.*, vol. 7, no. 2, 2018, doi: 10.14419/ijet.v7i2.31.13394.

[24] R. K. Wood and M. W. Berry, "Terminal composition control of a binary distillation column," *Chem. Eng. Sci.*, vol. 28, no. 9, 1973, doi: 10.1016/0009-2509(73)80025-9.

[25] J. Berner, K. Soltesz, T. Hägglund, and K. J. Åström, "Autotuner identification of TITO systems using a single relay feedback experiment," in *IFAC-PapersOnLine*, 2017, vol. 50, no. 1, doi: 10.1016/j.ifacol.2017.08.922.

[26] M. Hamdy and A. Ramadan, "Design of Smith Predictor and Fuzzy Decoupling for Mimo Chemical Processes with Time Delays," *Asian J. Control*, vol. 19, no. 1, 2017, doi: 10.1002/asjc.1338.

[27] A. P. V. Anna Paula, G. Acioli, and P. R. Barros, "Evaluation and Redesign of the Inverted Decoupler: Open and Closed-loop Approaches," *Int. J. Control. Autom. Syst.*, vol. 18, no. 6, 2020, doi: 10.1007/s12555-019-0371-3.

[28] felipesanabria_19, "Process Dynamics and Control Seborg (2nd edition).pdf." pp.

598–601, 2014, [Online]. Available: https://www.scribd.com/doc/243147548/Process-Dynamics-and-Control-Seborg-2nd-edition-pdf.

[29] N. H. Ceaglske, *Fundamentals of Automatic Process Control*, vol. 48, no. 6. 1956.

[30] R. Hanuma Naik, D. V. Ashok Kumar, and P. Sujatha, “Independent controller design for MIMO processes based on extended simplified decoupler and equivalent transfer function,” *Ain Shams Eng. J.*, vol. 11, no. 2, 2020, doi: 10.1016/j.asej.2017.10.011.

[31] P. B. Nevetha and M. Suresh, “Design of decoupler and performance analysis of distillation column,” *Int. J. Innov. Res. Electr. Electron. Instrum. Control Eng.*, vol. 4, no. 6, pp. 40–43, 2016, doi: 10.17148/IJIREEICE.2016.4610.

[32] M. Ben Hariz and F. Bouani, “Design of controllers for decoupled TITO systems using different decoupling techniques,” in *2015 20th International Conference on Methods and Models in Automation and Robotics, MMAR 2015*, Sep. 2015, pp. 1116–1121, doi: 10.1109/MMAR.2015.7284035.

[33] J. P. Sutikno, Z. Azizah, R. Handogo, R. A. Hikmadiyar, and A. Hisyam, “Inverted decoupling 2DoF internal model control for MIMO processes,” *Int. J. Technol.*, vol. 10, no. 3, 2019, doi: 10.14716/ijtech.v10i3.2922.

[34] G. Gurumurthy and D. K. Das, “An FO–[PI] λ controller for inverted decoupled two-input two-output coupled tank system,” *Int. J. Syst. Sci.*, vol. 50, no. 2, pp. 392–402, Jan. 2019, doi: 10.1080/00207721.2018.1552772.

[35] Y. Wang, Y. Chen, Q. Liu, and Y. Zhang, “Research on temperature cascade control of distillation column based on Smith-Fuzzy-PID,” *Pap. Asia*, no. COMPENDIUM 2, 2018.

[36] W. Sekar Ayu, P. Hidaya Rusmin, and E. M. I. Hidayat, “Robust PID Control Design in CPS-based Batch Distillation Column,” *Proceeding Electr. Eng. Comput. Sci. Informatics*, vol. 6, no. 1, 2019, doi: 10.11591/eecsi.v6.1999.

[37] M. Korkmaz, Ö. Aydoğdu, and H. Doğan, “Design and performance comparison of variable parameter nonlinear PID controller and genetic algorithm based PID controller,” 2012, doi: 10.1109/INISTA.2012.6246935.

[38] B. M. Isayed and M. A. Hawwa, “A nonlinear PID control scheme for hard disk drive servosystems,” 2007, doi: 10.1109/MED.2007.4433790.

[39] B. M. Isayed and M. A. Hawwa, “A nonlinear PID control scheme for hard disk drive servosystems,” 2007, doi: 10.1109/MED.2007.4433790.

[40] H. Seraji, “A new class of nonlinear PID controllers with robotic applications,” *J. Robot. Syst.*, vol. 15, no. 3, 1998, doi: 10.1002/(SICI)1097-4563(199803)15:3<161::AID-ROB4>3.0.CO;2-O.

[41] H. Seraji, “A New Class of Nonlinear PID Controllers,” *IFAC Proc. Vol.*, vol. 30, no. 20, pp. 65–71, Sep. 1997, doi: 10.1016/s1474-6670(17)44245-5.

[42] G. Zaidner, S. Korotkin, E. Shteimberg, A. Ellenbogen, M. Arad, and Y. Cohen, “Non linear PID and its application in process control,” 2010, doi: 10.1109/EEEI.2010.5662155.

[43] H. Seraji, “Nonlinear and adaptive control of force and compliance in manipulators,” *Int. J. Rob. Res.*, vol. 17, no. 5, pp. 467–484, 1998, doi: 10.1177/027836499801700501.

[44] G. B. So and G. G. Jin, “Fuzzy-based nonlinear PID controller and its application to CSTR,” *Korean J. Chem. Eng.*, vol. 35, no. 4, 2018, doi: 10.1007/s11814-017-0329-1.

[45] Y. Son and G. G. Jin, “A nonlinear PD controller design and its application to MOV actuators,” *Stud. Informatics Control*, vol. 28, no. 1, 2019, doi: 10.24846/v28i1y201901.

[46] G. G. Jin and Y. D. Son, “Design of a nonlinear PID controller and tuning rules for first-order plus time delay models,” *Stud. Informatics Control*, vol. 28, no. 2, 2019, doi: 10.24846/v28i2y201904.

[47] L. Poletto and F. Frassetto, “Cost-effective plane-grating monochromator design for extreme-ultraviolet application,” *Appl. Opt.*, vol. 57, no. 5, 2018, doi: 10.1364/ao.57.001202.

[48] J. Morsali, K. Zare, and M. Tarafdar Hagh, “Applying fractional order PID to design TCSC-based damping controller in coordination with automatic generation control of

interconnected multi-source power system," *Eng. Sci. Technol. an Int. J.*, vol. 20, no. 1, 2017, doi: 10.1016/j.jestch.2016.06.002.

[49] F. M. Zaihidee, S. Mekhilef, and M. Mubin, "Fractional Order SMC for Speed Control of PMSM," 2018, doi: 10.1109/IEECON.2018.8712281.

[50] F. M. Zaihidee, S. Mekhilef, and M. Mubin, "Application of Fractional Order Sliding Mode Control for Speed Control of Permanent Magnet Synchronous Motor," *IEEE Access*, vol. 7, 2019, doi: 10.1109/ACCESS.2019.2931324.

[51] S. P. Arunachalam, S. Kapa, S. K. Mulpuru, P. A. Friedman, and E. G. Tolkacheva, "Intelligent fractional-order PID (FOPID) heart rate controller for cardiac pacemaker," 2016, doi: 10.1109/HIC.2016.7797708.

[52] T. Dutta, S. Bhattacharyya, S. Dey, and J. Platos, "Border Collie Optimization," *IEEE Access*, vol. 8, pp. 109177–109197, 2020, doi: 10.1109/ACCESS.2020.2999540.

[53] L. T. Popoola, G. Babagana, and A. A. Susu, "A Review of an Expert System Design for Crude Oil Distillation Column Using the Neural Networks Model and Process Optimization and Control Using Genetic Algorithm Framework," *Adv. Chem. Eng. Sci.*, vol. 03, no. 02, 2013, doi: 10.4236/aces.2013.32020.

[54] S. Li and D. Li, "Genetic Algorithms," in *Springer Series in Materials Science*, vol. 312, 2021.

[55] I. M. A. Nahrendra, P. H. Rusmin, and E. M. I. Hidayat, "Adaptive Control of Cyber-Physical Distillation Column using Data Driven Control Approach," in *Proceedings of the International Conference on Electrical Engineering and Informatics*, 2019, vol. 2019-July, pp. 93–98, doi: 10.1109/ICEEI47359.2019.8988821.

[56] L. Angel, J. Viola, and M. Paez, "Evaluation of the windup effect in a practical PID controller for the speed control of a DC-motor system," 2019, doi: 10.1109/CCAC.2019.8921219.

[57] P. Mishra, V. Kumar, and K. P. S. Rana, "A fractional order fuzzy PID controller for binary distillation column control," *Expert Syst. Appl.*, vol. 42, no. 22, 2015, doi: 10.1016/j.eswa.2015.07.008.

REFERENCE LINKS

[L1] https://www.researchgate.net/figure/Schematic-of-a-typical-binary-distillation-column_fig1_282652155

[L2] https://www.mathworks.com/help/matlab/matlab_prog/create-functions-in-iles.html

[L3] https://www.mendeley.com/guides/mendeley-reference-manager

[L4] https://www.elprocus.com/the-working-of-a-pid-controller/

APPENDIXES

Appendix A: Appendixes related to tuning of controllers gain with and without decoupling.

Appendix A1: MATLAB code for Tuning of the PID controller gains with decoupling (WD) using GA.

```
function Tune_PIDModel

clear all

options= optimoptions('ga','PlotFcn',@gaplotbestf);

options.PopulationSize= 20;

options.MaxGenerations= 50; % Increase value if needed

nvar= 6; % Number of parameters

LB= [0 0  0 -0.5 -0.5 -0.5]; % Lower bound of tuning parameters

UB= [1 1 1 1 1 1]; % Upper bound of tuning parameters

[x,fval]= ga(@EvalObj,nvar,[],[],[],[],LB,UB,[],options)

% EvalObj measures a performance index from the simulink model for tuning

% obj= EvalObj(x) returns the objective function value obj calculated using

% the gain vector, x= [Kp1 Ki1 Kd1 Kp2 Ki2 Kd2].

function obj= EvalObj(x)

% Updates the values of Kp, Ki and Kd in Simulink model workspace

simulink_model= 'PID_WD1_Wd';

simulink_model= 'PID_WD1_Wod';

load_system(simulink_model);

gains= get_param(simulink_model,'modelworkspace'); %PID gains

gains.assignin('Kp1', x(1));

gains.assignin('Ki1', x(2));

gains.assignin('Kd1', x(3));

gains.assignin('Kp2', x(4));

gains.assignin('Ki2', x(5));

gains.assignin('Kd2', x(6));
```

```
% Simulates the Simulink model to get the outputs
simOut= sim(simulink_model,'SaveOutput','on');
% Retrieves time t and error e
t= simOut.find('t');
e1= simOut.find('e1'); e2= simOut.find('e2'); u1= simOut.find('u1'); u2= simOut.find('u2');
% Calculate a performance index using the trapezoidal integration rule
n= length(e1); wt= 1;
obj= 0;
ae= abs(e1)+abs(e2)+wt*abs(u1-0.1486)+wt*abs(u2+0.1038); %IAEU
% ae= t.*abs(e1)+abs(e2)+wt*abs(u1-0.1486)+wt*abs(u2+0.1038); %ITAEU
% ae= e1.^2+e2.^2+wt*(u1-0.1486).^2+wt*(u2+0.1038).^2; % ISEU
for i= 2:n
   stepsize= t(i)-t(i-1);
   obj= obj+0.5*(ae(i-1)+ae(i))*stepsize;
end
```

Appendix A2: MATLAB code for Tuning of the NPID controller with decoupling (WD) using GA.

```
function Tune_NPIDModel
clear all
options= optimoptions('ga','PlotFcn',@gaplotbestf);
options.PopulationSize= 20;
options.MaxGenerations= 50;  % Increase value if needed
nvar= 6; % Number of parameters
LB= [0 0  0 -0.5 -0.5 -0.5]; % Lower bound of tuning parameters
UB= [1 1 1 1 1 1]; % Upper bound of tuning parameters
[x,fval]= ga(@EvalObj,nvar,[],[],[],[],LB,UB,[],options)
% EvalObj measures a performance index from the simulink model for tuning
% obj= EvalObj(x) returns the objective function value obj calculated using
% the gain vector, x= [Kp1 Ki1 Kd1 Kp2 Ki2 Kd2].
```

```
function obj= EvalObj(x)
% Updates the values of Kp, Ki and Kd in Simulink model workspace
simulink_model= 'NPID_WD1_Wd';
simulink_model= 'NPID_WD1_Wod';
load_system(simulink_model);
gains= get_param(simulink_model,'modelworkspace'); % NPID gains,
gains.assignin('Kp1', x(1));
gains.assignin('Ki1', x(2));
gains.assignin('Kd1', x(3));
gains.assignin('Kp2', x(4));
gains.assignin('Ki2', x(5));
gains.assignin('Kd2', x(6));
% Simulates the simulink model to get the outputs
simOut= sim(simulink_model,'SaveOutput','on');
% Retrieves time t and error e
t= simOut.find('t');
e1= simOut.find('e1');
e2= simOut.find('e2');
u1= simOut.find('u1');
u2= simOut.find('u2');
% Calculate a performance index using the trapezoidal integration rule
n= length(e1); wt= 1;
obj= 0;
% ae= abs(e1)+abs(e2)+wt*abs(u1-0.1486)+wt*abs(u2+0.1038); %IAUE
ae= t.*abs(e1)+abs(e2)+wt*abs(u1-0.1486)+wt*abs(u2+0.1038); %ITAEU
% ae= e1.^2+e2.^2+wt*(u1-0.1486).^2+wt*(u2+0.1038).^2; % ISUE
for i= 2:n
   stepsize= t(i)-t(i-1);
   obj= obj+0.5*(ae(i-1)+ae(i))*stepsize;
```

end

Appendix A3: MATLAB code for Tuning of the FOPID controller with decoupling (WD) using GA.

```
function Tune_FOPIDModel

clear all

options= optimoptions('ga','PlotFcn',@gaplotbestf);

options.PopulationSize= 20;

options.MaxGenerations= 50; % Increase value if needed

nvar= 10; % Number of parameters

LB= [0 0 -0.5 -0.5 -0.5 -0.5 0 0 0 0]; % Lower bound of tuning parameters

UB= [1 1 1 1 1 1 1 1 1 1]; % Upper bound of tuning parameters

[x,fval]= ga(@EvalObj,nvar,[],[],[],[],LB,UB,[],options)

function obj= EvalObj(x)

simulink_model= 'FOPID_WD1_Wd';

simulink_model= 'FOPID_WD1_Wod';

load_system(simulink_model);

gains= get_param(simulink_model,'modelworkspace'); % FOPID gains

gains.assignin('Kp1', x(1));

gains.assignin('Ki1', x(2));

gains.assignin('Kd1', x(3));

gains.assignin('Kp2', x(4));

gains.assignin('Ki2', x(5));

gains.assignin('Kd2', x(6));

gains.assignin('lam1', x(7));

gains.assignin('lam2', x(8));

gains.assignin('mu1', x(9));

gains.assignin('mu2', x(10));

% Simulates the simulink model to get the outputs

simOut= sim(simulink_model,'SaveOutput','on');
```

```
% Retrieves time t and error e
  t= simOut.find('t');
e1= simOut.find('e1');
e2= simOut.find('e2');
u1= simOut.find('u1');
u2= simOut.find('u2');
% Calculate a performance index using the trapezoidal integration rule
n= length(e1); wt= 1;
obj= 0;
ae= abs(e1)+abs(e2)+wt*abs(u1-0.1486)+wt*abs(u2+0.1038); % IAEU
%ae= t.*abs(e1)+abs(e2)+wt*abs(u1-0.1486)+wt*abs(u2+0.1038); %ITAEU
%ae= (e1).^2+(e2).^2+wt*(u1-0.1486).^2+wt*(u2+0.1038).^2; % ISEU
for i= 2:n
   stepsize= t(i)-t(i-1);
   obj= obj+0.5*(ae(i-1)+ae(i))*stepsize;
end
```

Appendix A4: MATLAB code for Tuning of the PID controller without decoupling (WoD) using GA.

```
function Tune_PIDModel
clear all
options= optimoptions('ga','PlotFcn',@gaplotbestf);
options.PopulationSize= 20;
options.MaxGenerations= 50; % Increase value if needed
nvar= 6; % Number of parameters
LB= [0 0  0 -0.5 -0.5 -0.5]; % Lower bound of tuning parameters
UB= [1 1 1 1 1 1]; % Upper bound of tuning parameters
[x,fval]= ga(@EvalObj,nvar,[],[],[],[],LB,UB,[],options)
function obj= EvalObj(x)
simulink_model= 'PID_WoD1_Wd';
```

```
simulink_model= 'PID_WoD1_Wod';
load_system(simulink_model);
% Call PID gains
simOut= sim(simulink_model,'SaveOutput','on');
t= simOut.find('t');
e1= simOut.find('e1');
e2= simOut.find('e2');
u1= simOut.find('u1');
u2= simOut.find('u2');
n= length(e1); wt= 1;
obj= 0;
ae= abs(e1)+abs(e2)+wt*abs(u1-0.1486)+wt*abs(u2+0.1038); %IAEU
% ae= t.*abs(e1)+abs(e2)+wt*abs(u1-0.1486)+wt*abs(u2+0.1038); %ITAEU
% ae= e1.^2+e2.^2+wt*(u1-0.1486).^2+wt*(u2+0.1038).^2; % ISEU
for i= 2:n
   stepsize= t(i)-t(i-1);
   obj= obj+0.5*(ae(i-1)+ae(i))*stepsize;
end
```

Appendix A5: MATLAB code for Tuning of the NPID controller without decoupling (WoD) using GA.

```
function Tune_NPIDModel
clear all
options= optimoptions('ga','PlotFcn',@gaplotbestf);
options.PopulationSize= 20;
options.MaxGenerations= 50; % Increase value if needed
nvar= 6; % Number of parameters
LB= [0 0  0 -0.5 -0.5 -0.5]; % Lower bound of tuning parameters
UB= [1 1 1 1 1 1]; % Upper bound of tuning parameters
[x,fval]= ga(@EvalObj,nvar,[],[],[],[],LB,UB,[],options)
```

```
function obj= EvalObj(x)
simulink_model= 'NPID_WoD1_Wd';
simulink_model= 'NPID_WoD1_Wod';
load_system(simulink_model);
% Call NPID gains
simOut= sim(simulink_model,'SaveOutput','on');
t= simOut.find('t');
e1= simOut.find('e1');
e2= simOut.find('e2');
u1= simOut.find('u1');
u2= simOut.find('u2');
n= length(e1); wt= 1;
obj= 0;
% ae= abs(e1)+abs(e2)+wt*abs(u1-0.1486)+wt*abs(u2+0.1038); %IAEU
ae= t.*abs(e1)+abs(e2)+wt*abs(u1-0.1486)+wt*abs(u2+0.1038); %ITAEU
% ae= e1.^2+e2.^2+wt*(u1-0.1486).^2+wt*(u2+0.1038).^2; % ISEU
for i= 2:n
   stepsize= t(i)-t(i-1);
   obj= obj+0.5*(ae(i-1)+ae(i))*stepsize;
end
```

Appendix A6: MATLAB code for Tuning of the FOPID controller without decoupling (WoD) using GA.

```
function Tune_FOPIDModel
clear all
options= optimoptions('ga','PlotFcn',@gaplotbestf);
options.PopulationSize= 20;
options.MaxGenerations= 50; % Increase value if needed
nvar= 10; % Number of parameters
LB= [0 0 -0.5 -0.5 -0.5 -0.5 0 0 0 0]; % Lower bound of tuning parameters
```

```
UB= [1 1 1 1 1 1 1 1 1 1]; % Upper bound of tuning parameters
[x,fval]= ga(@EvalObj,nvar,[],[],[],[],LB,UB,[],options)
function obj= EvalObj(x)
simulink_model= 'FOPID_WoD1_Wd';
simulink_model= 'FOPID_WoD1_Wod';
load_system(simulink_model);
% Call FOPID gains
simOut= sim(simulink_model,'SaveOutput','on');
  t= simOut.find('t');
e1= simOut.find('e1');
e2= simOut.find('e2');
u1= simOut.find('u1');
u2= simOut.find('u2');
n= length(e1); wt= 1;
obj= 0;
ae= abs(e1)+abs(e2)+wt*abs(u1-0.1486)+wt*abs(u2+0.1038); % IAEU
%ae= t.*abs(e1)+abs(e2)+wt*abs(u1-0.1486)+wt*abs(u2+0.1038); %ITAEU
%ae= (e1).^2+(e2).^2+wt*(u1-0.1486).^2+wt*(u2+0.1038).^2; % ISEU
for i= 2:n
   stepsize= t(i)-t(i-1);
   obj= obj+0.5*(ae(i-1)+ae(i))*stepsize;
end
```

Appendix B: Appendixes related to the simulation of the DC system

Appendix B1: MATLAB code for Simulate the top and bottom composition of distillation column process using PID controller with decoupling (WD).

```
clear all
% With decoupling
x= [0.4924 0.1316   0.5372  -0.1705  -0.0233  -0.2717]; %fval = 12.7566 IAEU
% x= [0.4796 0.1679   0.5191  -0.1158  -0.0196  -0.0617]; %fval =  25.8887ITAEU
```

```
% x= [0.5302 0.0812   0.7214  -0.1809  -0.0237  -0.3249]; %fval = 6.7631 ISEU
 simulink_model= 'PID_WD2_Wd';
 simulink_model= 'PID_WD2_Wod';
load_system(simulink_model);
% Call PID gains
simOut= sim(simulink_model,'SaveOutput','on');
data= simOut.find('data');
t= data.Time;
y1= data.Data(:,1);
y2= data.Data(:,2);
u1= data.Data(:,3);
u2= data.Data(:,4);
subplot 211
plot(t,y1,'b')
stepinfo(y1,t,1,'RiseTimeLimits',[0,1])
subplot 212
plot(t,y2,'r')
stepinfo(y2,t,1,'RiseTimeLimits',[0,1])
n= length(y1); wt= 1;
Tobj= 0; obj1= 0; obj2= 0;
ae1= abs(1-y1);  ae2= abs(1-y2); %IAE
ae= abs(1-y1)+abs(1-y2)+wt*abs(u1-0.1486)+wt*abs(u2+0.1038); % IAEU
% ae= t.*abs(1-y1)+abs(1-y2)+wt*abs(u1-0.1486)+wt*abs(u2+0.1038); %ITAEU
% ae= (1-y1).^2+(1-y2).^2+wt*(u1-0.1486).^2+wt*(u2+0.1038).^2; % ISEU
for i= 2:n
   stepsize= t(i)-t(i-1);
   Tobj= Tobj+0.5*(ae(i-1)+ae(i))*stepsize;
   obj1= obj1+0.5*(ae1(i-1)+ae1(i))*stepsize;
   obj2= obj2+0.5*(ae2(i-1)+ae2(i))*stepsize;
```

end

[obj1 obj2 Tobj]

buf= [t y1 y2 u1 u2];

Appendix B2: MATLAB code for Simulate the top and bottom composition of distillation column process using NPID controller with decoupling (WD).

```
clear all
% With decoupling
x= [ 0.6846  0.0863  0.5417  -0.1426  -0.0355  -0.2167]; %fval=  12.3707IAEU
x= [ 0.4406  0.2228  0.5024  -0.1271  -0.0304  -0.0397]; %fval= 23.6527 ITAEU
x= [ 0.6009  0.1057  0.6995  -0.1737  -0.0433  -0.2727]; %fval = 6.7545 ISEU
simulink_model= 'NPID_WD2_Wd';
simulink_model= 'NPID_WD2_Wod';
load_system(simulink_model);
% Call NPID gains
simOut= sim(simulink_model,'SaveOutput','on');
data= simOut.find('data');
t= data.Time;
y1= data.Data(:,1);
y2= data.Data(:,2);
u1= data.Data(:,3);
u2= data.Data(:,4);
subplot 211
plot(t,y1,'b')
stepinfo(y1,t,1,'RiseTimeLimits',[0,1])
subplot 212
plot(t,y2,'r')
stepinfo(y2,t,1,'RiseTimeLimits',[0,1])
n= length(y1); wt= 1;
Tobj= 0; obj1= 0; obj2= 0;
```

```
ae1= abs(1-y1);  ae2= abs(1-y2); %IAE
% ae= abs(1-y1)+abs(1-y2)+wt*abs(u1-0.1486)+wt*abs(u2+0.1038); % IAEU
% ae= t.*abs(1-y1)+abs(1-y2)+wt*abs(u1-0.1486)+wt*abs(u2+0.1038); %ITAEU
ae= (1-y1).^2+(1-y2).^2+wt*(u1-0.1486).^2+wt*(u2+0.1038).^2; % ISEU
for i= 2:n
   stepsize= t(i)-t(i-1);
   Tobj= Tobj+0.5*(ae(i-1)+ae(i))*stepsize;
   obj1= obj1+0.5*(ae1(i-1)+ae1(i))*stepsize;
   obj2= obj2+0.5*(ae2(i-1)+ae2(i))*stepsize;
end
[obj1 obj2 Tobj]
buf= [t y1 y2 u1 u2];
```

Appendix B3: MATLAB code for Simulate the top and bottom composition of distillation column process using FOPID controller with decoupling (WD).

```
clear all
% With decoupling
 x= [ 0.4740  0.1026  0.3629  -0.0610   -0.0808  -0.2865   0.9154  0.7037   0.7456
0.9516]; %fval =13.0855 IAEU
 x= [ 0.0985  0.1878  0.4485  -0.0700  -0.0436   -0.0981   0.8736  0.7817    0.5002
0.7133]; %fval =24.3871 ITAEU
x= [ 0.3713  0.0656 -0.0003   0.2663  -0.1688   -0.4284    0.9976 0.4809    0.9958   0.4262
         ]; %fval =6.6998ISEU
simulink_model= 'FOPID_WD2_Wd';
simulink_model= 'FOPID_WD2_Wod';
load_system(simulink_model);
% Call FOPID gains
simOut= sim(simulink_model,'SaveOutput','on');
data= simOut.find('data');
t= data.Time;
y1= data.Data(:,1);
```

```
y2= data.Data(:,2);
u1= data.Data(:,3);
u2= data.Data(:,4);
subplot 211
plot(t,y1,'b')
stepinfo(y1,t,1,'RiseTimeLimits',[0,1])
subplot 212
plot(t,y2,'r')
stepinfo(y2,t,1,'RiseTimeLimits',[0,1])
n= length(y1); wt= 1;
Tobj= 0; obj1= 0; obj2= 0;
ae1= abs(1-y1);  ae2= abs(1-y2); %IAE
ae= abs(1-y1)+abs(1-y2)+wt*abs(u1-0.1486)+wt*abs(u2+0.1038); % IAEU
ae= t.*abs(1-y1)+abs(1-y2)+wt*abs(u1-0.1486)+wt*abs(u2+0.1038); %ITAEU
ae= (1-y1).^2+(1-y2).^2+wt*(u1-0.1486).^2+wt*(u2+0.1038).^2; % ISEU
for i= 2:n
   stepsize= t(i)-t(i-1);
   Tobj= Tobj+0.5*(ae(i-1)+ae(i))*stepsize;
   obj1= obj1+0.5*(ae1(i-1)+ae1(i))*stepsize;
   obj2= obj2+0.5*(ae2(i-1)+ae2(i))*stepsize;
end
[obj1 obj2 Tobj]
buf= [t y1 y2 u1 u2];
```

Appendix B4: MATLAB code for Simulate the top and bottom composition of distillation column process using PID controller without decoupling (WoD).

```
clear all
x= [0.1580    0.0039    0.1265   -0.2233 -0.0105   -0.3695]; %fval = 22.2616 IAEU
x= [0.4734    0.0020    0.6016   -0.1085 -0.0110   -0.3221]; %fval = 31.6696 ITAEU
x= [0.2826    0.0223    0.3611   -0.2359 -0.0063   -0.4540]; %fval = 8.2788 ISEU
```

```
simulink_model= 'PID_WoD2_Wd';
simulink_model= 'PID_WoD2_Wod';
load_system(simulink_model);
% Call PID gains
simOut= sim(simulink_model,'SaveOutput','on');
data= simOut.find('data');
t= data.Time;
y1= data.Data(:,1);
y2= data.Data(:,2);
u1= data.Data(:,3);
u2= data.Data(:,4);
subplot 211
plot(t,y1,'b')
stepinfo(y1,t,1,'RiseTimeLimits',[0,1])
subplot 212
plot(t,y2,'r')
stepinfo(y2,t,1,'RiseTimeLimits',[0,1])
n= length(y1); wt= 1;
Tobj= 0; obj1= 0; obj2= 0;
ae1= abs(1-y1);  ae2= abs(1-y2); %IAE
ae= abs(1-y1)+abs(1-y2)+wt*abs(u1-0.1486)+wt*abs(u2+0.1038); % IAEU
ae= t.*abs(1-y1)+abs(1-y2)+wt*abs(u1-0.1486)+wt*abs(u2+0.1038); %ITAEU
ae= (1-y1).^2+(1-y2).^2+wt*(u1-0.1486).^2+wt*(u2+0.1038).^2; % ISEU
for i= 2:n
   stepsize= t(i)-t(i-1);
   Tobj= Tobj+0.5*(ae(i-1)+ae(i))*stepsize;
   obj1= obj1+0.5*(ae1(i-1)+ae1(i))*stepsize;
   obj2= obj2+0.5*(ae2(i-1)+ae2(i))*stepsize;
end
```

```
[obj1 obj2 Tobj]
buf= [t y1 y2 u1 u2];
```

Appendix B5: MATLAB code for Simulate the top and bottom composition of distillation column process using NPID controller without decoupling (WoD).

```
clear all
x= [ 0.5339  0.0039  0.7891  -0.1161   -0.0099  -0.2992]; %fval= 22.5879 IAEU
x= [ 0.9595  0.2886  0.1954  -0.0073   -0.0082  -0.0198]; %fval=32.8064 ITAEU
x= [ 0.3125  0.0156  0.3301  -0.2332   -0.0080  -0.4951]; % fval= 8.1969 ISEU
simulink_model= 'NPID_WoD2_Wd';
simulink_model= 'NPID_WoD2_Wod';
load_system(simulink_model);
% Call NPID gains
simOut= sim(simulink_model,'SaveOutput','on');
data= simOut.find('data');
t= data.Time;
y1= data.Data(:,1);
y2= data.Data(:,2);
u1= data.Data(:,3);
u2= data.Data(:,4);
subplot 211
plot(t,y1,'k')
stepinfo(y1,t,1,'RiseTimeLimits',[0,1])
subplot 212
plot(t,y2,'r')
stepinfo(y2,t,1,'RiseTimeLimits',[0,1])
n= length(y1); wt= 1;
Tobj= 0; obj1= 0; obj2= 0;
ae1= abs(1-y1);  ae2= abs(1-y2); %IAE
ae= abs(1-y1)+abs(1-y2)+wt*abs(u1-0.1486)+wt*abs(u2+0.1038); % IAEU
```

```
ae= t.*abs(1-y1)+abs(1-y2)+wt*abs(u1-0.1486)+wt*abs(u2+0.1038); %ITAEU
ae= (1-y1).^2+(1-y2).^2+wt*(u1-0.1486).^2+wt*(u2+0.1038).^2; % ISEU
for i= 2:n
   stepsize= t(i)-t(i-1);
   Tobj= Tobj+0.5*(ae(i-1)+ae(i))*stepsize;
   obj1= obj1+0.5*(ae1(i-1)+ae1(i))*stepsize;
   obj2= obj2+0.5*(ae2(i-1)+ae2(i))*stepsize;
end
[obj1 obj2 Tobj]
buf= [t y1 y2 u1 u2];
```

Appendix B6: MATLAB code for Simulate the top and bottom composition of distillation column process using FOPID controller without decoupling (WoD).

```
clear all
x= [.3748  0.0362   0.7398     0.0320  -0.0214  -0.2835  0.7500  0.7415  0.4851  0.8583];
%fval =23.6993 IAUE
 x= [.2091  0.8434   0.9669  -0.0059  -0.0133  -0.0451  0.3664  0.8467  0.7274  0.9500];
%fval =28.8029 ITAUE
x= [.2106  0.0156   0.1006   0.0293  -0.1036  -0.2912  1.0000  0.2970  0.6455  0.6317];
         %fval =8.2932 ISEU
simulink_model= 'FOPID_WoD2_Wd';
simulink_model= 'FOPID_WoD2_Wod';
load_system(simulink_model);
% Call FOPID gains
simOut= sim(simulink_model,'SaveOutput','on');
data= simOut.find('data');
t= data.Time;
y1= data.Data(:,1);
y2= data.Data(:,2);
u1= data.Data(:,3);
u2= data.Data(:,4);
```

```
subplot 211
plot(t,y1,'k')
stepinfo(y2,t,1,'RiseTimeLimits',[0,1])
subplot 212
plot(t,y2,'r')
stepinfo(y2,t,1,'RiseTimeLimits',[0,1])
n= length(y1); wt= 1;
Tobj= 0; obj1= 0; obj2= 0;
ae1= abs(1-y1);  ae2= abs(1-y2); %IAE
ae= abs(1-y1)+abs(1-y2)+wt*abs(u1-0.1486)+wt*abs(u2+0.1038); % IAEU
ae= t.*abs(1-y1)+abs(1-y2)+wt*abs(u1-0.1486)+wt*abs(u2+0.1038); %ITAEU
ae= (1-y1).^2+(1-y2).^2+wt*(u1-0.1486).^2+wt*(u2+0.1038).^2; % ISEU
for i= 2:n
   stepsize= t(i)-t(i-1);
   Tobj= Tobj+0.5*(ae(i-1)+ae(i))*stepsize;
   obj1= obj1+0.5*(ae1(i-1)+ae1(i))*stepsize;
   obj2= obj2+0.5*(ae2(i-1)+ae2(i))*stepsize;
end
[obj1 obj2 Tobj]
buf= [t y1 y2 u1 u2];
```

Appendix C: Appendixes related to steady state analysis of a DC system

Appendix C1: MATLAB code for steady state operation of top and bottom composition of distillation column process without decoupling (WoD).

```
%Steady state analysis of the distillation column without decoupling
clear all
s=tf ('s');
g11=12.8*exp(-1*s)/(16.7*s+1);
g12=-18.9*exp(-3*s)/(21*s+1);
g21=6.6*exp(-7*s)/(10.9*s+1);
g22=-19.4*exp(-3*s)/(14.4*s+1);
G= [g11 g12; g21 g22];
t=0:0.02:150;
```

```
u1=0.1*ones(size(t));
u2=zeros(size(t));
U=[u1;u2];
% plots the simulated time response of the dynamic system model G
y=lsim(G, U, t);
plot(t, y(:,1))
plot(t, y(:,2))
```

Appendix C2: MATLAB code for steady state operation of top and bottom composition of distillation column process with decoupling (WD).

```
clear all
%Steady state analysis of the distillation column with decoupling
S=tf('s');
g11=12.8*exp(-s)/(16.7*s+1);
g12=-18.9*exp(-3s)/(21*s+1);
g21=6.6*exp(-7s)/(10.9*s+1);
g22=-19.4*exp(-3s)/(14.4*s+1);
G=[g11 g12; g21 g22];
m11=1
m12=(24.66*s)+(1.48exp(-2s))/(21*s+1);
m12=(4.89*s)+(0.34exp(-4s))/(10*s+1);
m22=1
M=[m11 m12; m21 m22];
F=G*M
t=0:0.02:150;
u1=0.1*ones(size(t));
u1=zeros(size(t));
U=[u1;u2];
%plots the simulated time response of the dynamic system model F
y=lsim(F, U, t);
plot(t, y(:,1))
plot(t, y(:,2))
```

Appendix D: Appendixes related to the DC system controllers

Appendix D1: PID controller of Distillation column MATLAB /Simulink model.

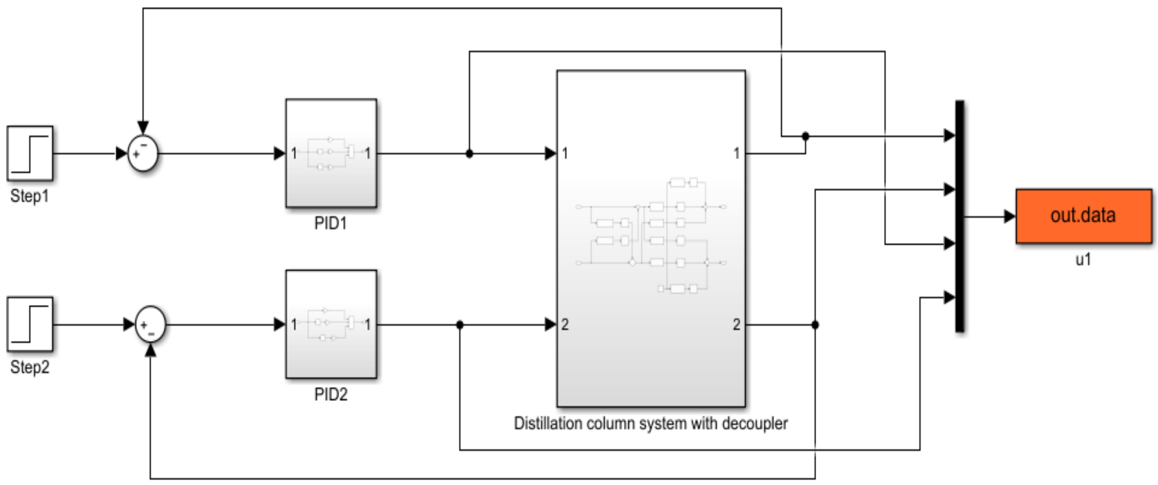

Figure D1.1 MATLAB Simulink model of distillation column with PID control system.

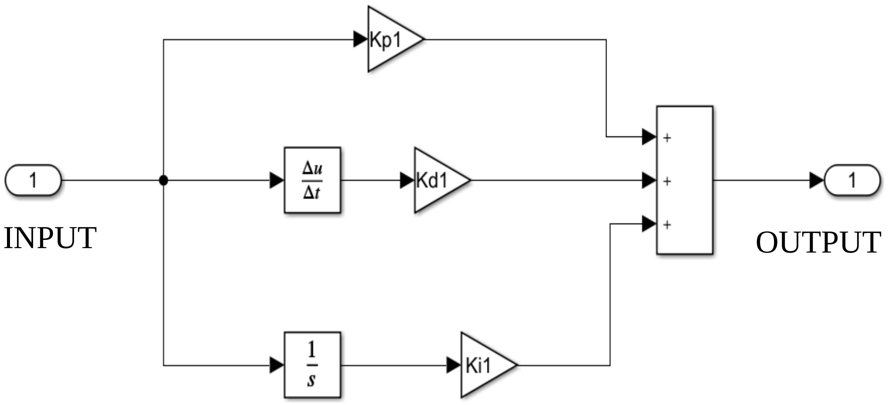

Figure D1.2: MATLAB Simulink model of PID control.

Appendix D2: NPID controller of Distillation column MATLAB /Simulink model.

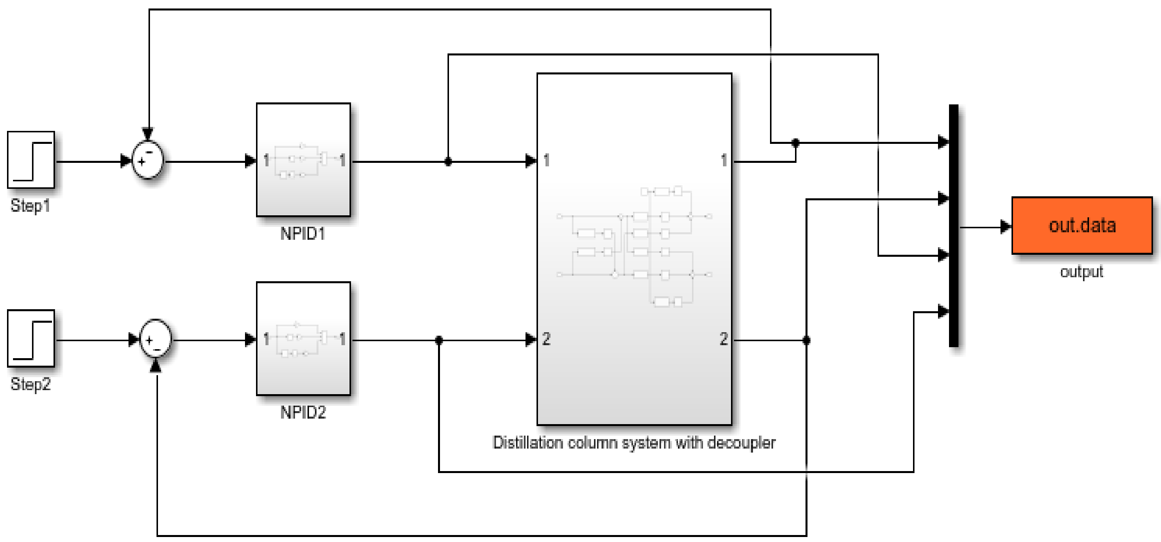

Figure D2.1 MATLAB Simulink model of distillation column with NPID control system.

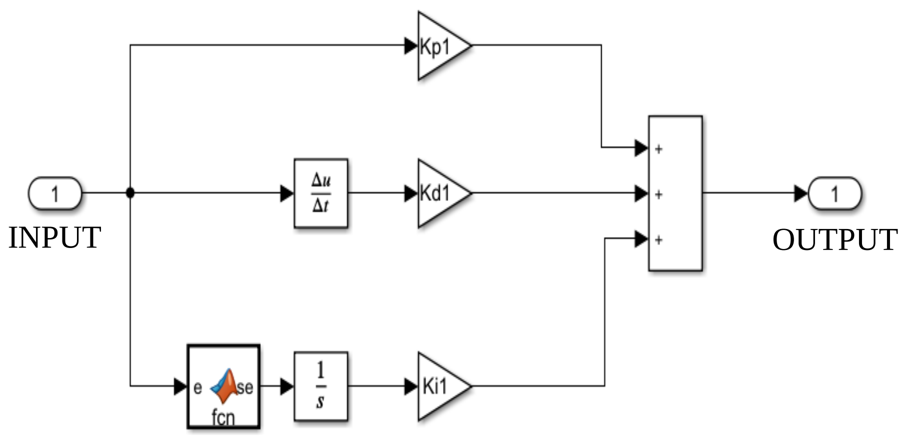

Figure D2.2: MATLAB Simulink model of NPID control.

Implementation of nonlinear gain using MATLAB code

```
function se= fcn(e)
dyr = 1;
se= exp(-e^2/(2*dyr^2))*e;
```

Appendix D3: FOPID controller of Distillation column MATLAB /Simulink model.

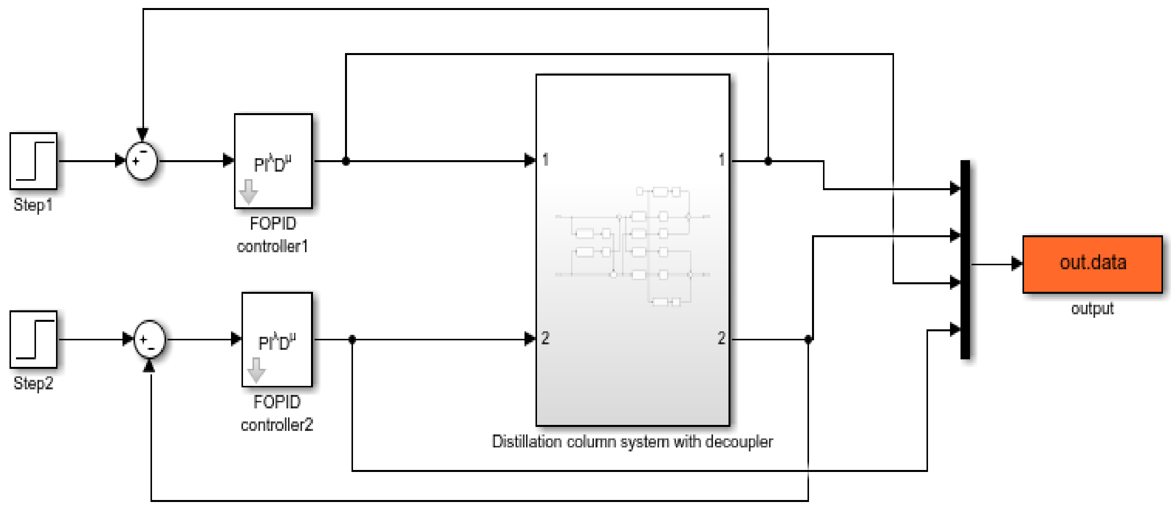

Figure D3.1 MATLAB Simulink model of distillation column with FOPID control system.

Appendix E: Appendixes related to optimization of the DC controllers

Appendix E1: Tuning the PID controller gain using performance criteria of IAEU, ITAEU, and ISEU with decoupling (WD).

No of Optimiza	K_{p1}	K_{i1}	K_{d1}	K_{p2}	K_{i2}	K_{d2}	**Fitness value**
			J_1 = IAEU				
1	0.6098	0.0604	0.5725	-0.1649	-0.0154	-0.2674	12.8438
2	0.6107	0.1364	0.5456	-0.0814	-0.0157	-0.0250	14.1450
3	0.5645	0.2915	0.7341	-0.1901	-0.0198	-0.2647	14.5353
4	0.6148	0.0971	0.6183	-0.0857	-0.0099	0.0885	16.1616
5	**0.4924**	**0.1316**	**0.5372**	**-0.1705**	**-0.0233**	**-0.2717**	**12.7566**
6	0.4891	0.1278	0.5711	-0.1394	-0.0170	-0.1152	12.9417
7	0.4923	0.0887	0.6450	-0.1311	-0.0165	-0.1039	12.8295
8	0.5549	0.0847	0.4802	-0.1538	-0.0489	-0.2212	15.0278
9	0.4409	0.0861	0.4103	-0.1513	-0.0237	-0.2543	13.0148
10	0.6148	0.0971	0.6183	-0.0857	-0.0099	0.0885	16.1616
			J_2 = ITAEU				
1	0.4247	0.2049	0.5498	-0.0779	-0.0167	0.0587	27.6853
2	0.4157	0.1576	0.3886	-0.1141	-0.0217	-0.1436	27.3966
3	0.5490	0.1510	0.6116	-0.1295	-0.0159	-0.2538	29.0481
4	0.6445	0.0892	0.5520	-0.1255	-0.0161	-0.0910	27.5220
5	0.5000	0.1511	0.5000	-0.1172	-0.0221	-0.1453	26.0382
6	0.4258	0.1480	0.3694	-0.1361	-0.0214	-0.1435	26.7316
7	0.6555	0.0654	0.4510	-0.1404	-0.0173	-0.1301	27.7559
8	0.5511	0.2485	0.6640	-0.0408	-0.0095	0.2431	30.7215
9	**0.4796**	**0.1679**	**0.5191**	**-0.1158**	**-0.0196**	**-0.0617**	**25.8887**
10	0.4468	0.2254	0.6220	-0.1261	-0.0149	-0.0138	27.1986
			J_3 = ISEU				
1	0.6167	0.2820	0.9173	-0.1521	-0.0203	-0.4078	7.7658
2	0.7706	0.1791	0.7416	-0.1423	-0.0236	-0.2648	7.5297
3	0.5223	0.0990	0.5951	-0.1927	-0.0287	-0.3583	6.8006

4	**0.5302**	**0.0812**	**0.7214**	**-0.1809**	**-0.0237**	**-0.3249**	**6.7631**
5	0.5473	0.0781	0.4284	-0.1672	-0.0245	-0.1959	6.9043
6	0.5473	0.0781	0.4284	-0.1672	-0.0245	-0.1959	6.9043
7	0.5518	0.2424	0.8994	-0.2151	-0.0194	-0.2423	7.5797
8	0.5185	0.0851	0.5287	-0.1866	-0.0248	-0.3146	6.7746
9	0.5783	0.1340	0.6732	-0.1661	-0.0224	-0.2266	6.9196
10	0.8140	0.3735	0.7572	-0.1212	-0.0187	-0.0311	9.1792

Appendix E2: Tuning the PID controller gain using performance criteria of IAEU, ITAEU, and ISEU without decoupling (WoD)**.**

No of Optimization	**K_{p1}**	**K_{i1}**	**K_{d1}**	**K_{p2}**	**K_{i2}**	**K_{d2}**	**Fitness value**
J_1 = IAEU							
1	0.8047	0.0923	0.5858	-0.0298	-0.0063	-0.2619	24.2702
2	0.6776	0.4848	0.6709	0.0398	-0.0062	0.1978	29.7167
3	0.2141	0.0496	0.1506	-0.2981	-0.0119	-0.4748	24.4442
4	0.8047	0.0923	0.5858	-0.0298	-0.0063	-0.2619	24.2702
5	**0.1580**	**0.0039**	**0.1265**	**-0.2233**	**-0.0105**	**-0.3695**	**22.2616**
6	0.2141	0.0496	0.1506	-0.2981	-0.0119	-0.4748	24.4442
7	0.1656	0.0084	0.1086	-0.2636	-0.0145	-0.4072	23.6290
8	0.9969	0.0156	0.4662	-0.0139	-0.0057	-0.0155	23.6672
9	0.9158	0.1455	0.7427	-0.0155	-0.0068	-0.1400	24.5045
10	0.5405	0.0165	0.6706	-0.1282	-0.0087	-0.4377	23.4144
J_2 = ITAEU							
1	0.9742	0.2428	0.3013	0.0215	-0.0080	0.0439	37.2464
2	0.5261	0.1215	0.6385	-0.0831	-0.0078	-0.1984	48.1428
3	0.9953	0.1997	0.2776	-0.0465	-0.0123	-0.0777	36.6869
4	**0.4734**	**0.0020**	**0.6016**	**-0.1085**	**-0.0110**	**-0.3221**	**31.6696**
5	0.5261	0.1215	0.6385	-0.0831	-0.0078	-0.1984	48.1428

6	0.9953	0.1997	0.2776	-0.0465	-0.0123	-0.0777	36.6869
7	0.9974	0.1972	0.4268	-0.0283	-0.0083	-0.0856	35.6873
8	0.9909	0.2341	0.6508	0.0097	-0.0067	-0.1569	38.0602
9	0.9938	0.4416	0.3037	0.0059	-0.0056	0.0376	42.5948
10	0.5261	0.1215	0.6385	-0.0831	-0.0078	-0.1984	46.1428
J_3 = ISEU							
1	0.5607	0.0156	0.8080	-0.1313	-0.0052	-0.1007	9.0424
2	0.3647	0.0205	0.5917	-0.2158	-0.0107	-0.4696	8.3120
3	0.3438	0.0254	0.8284	-0.2197	-0.0019	-0.3316	8.8458
4	**0.2826**	**0.0223**	**0.3611**	**-0.2359**	**-0.0063**	**-0.4540**	**8.2788**
5	0.8506	0.0544	0.4589	-0.1025	-0.0088	-0.2731	9.6888
6	0.7479	0.1087	0.7913	-0.1468	-0.0059	-0.4003	9.5615
7	0.3363	0.0507	0.7551	-0.1333	-0.0051	-0.0997	9.4888
8	0.8489	0.1975	0.8016	-0.0595	-0.0048	-0.2066	10.7574
9	0.7031	0.0159	0.6058	-0.0106	-0.0056	0.0444	10.7323
10	0.4337	0.1369	0.7287	-0.1720	-0.0060	-0.4670	9.3287

Appendix E3: Tuning the NPID controller gain using performance criteria of IAEU, ITAEU, and ISEU with decoupling (WD).

No of Optimization	**K_{p1}**	**K_{i1}**	**K_{d1}**	**K_{p2}**	**K_{i2}**	**K_{d2}**	**Fitness value**
J_1 = IAEU							
1	0.6643	0.1962	0.6859	-0.1396	-0.0370	-0.1534	13.0946
2	0.5407	0.1323	0.6535	-0.0730	-0.0204	0.1179	13.7943
3	0.5597	0.0916	0.3029	-0.1797	-0.0084	-0.1008	19.4516
4	**0.6846**	**0.0863**	**0.5417**	**-0.1426**	**-0.0355**	**-0.2167**	**12.3707**
5	0.3393	0.1186	0.8683	-0.1404	-0.0599	-0.2140	15.3624
6	0.5791	0.0782	0.3099	-0.1341	-0.0361	-0.1965	12.8860
7	0.3393	0.1186	0.8683	-0.1404	-0.0599	-0.2140	15.3624

8	0.5791	0.0782	0.3099	-0.1341	-0.0361	-0.1965	12.8860
9	0.5499	0.1838	0.6249	-0.1232	-0.0368	-0.1733	12.7767
10	0.4658	0.2512	0.5874	-0.1475	-0.0361	-0.1409	13.2016
J_2 = ITAEU							
1	0.4403	0.2017	0.4581	-0.1493	-0.0380	-0.1216	24.5021
2	0.5411	0.2320	0.6580	-0.1636	-0.0810	-0.3546	26.4923
3	0.3993	0.1756	0.3105	-0.1320	-0.0303	-0.1188	24.8653
4	**0.4406**	**0.2228**	**0.5024**	**-0.1271**	**-0.0304**	**-0.0397**	**23.6527**
5	0.4267	0.2652	0.6072	-0.1021	-0.0566	-0.4049	31.0551
6	0.5552	0.2091	0.6338	-0.1335	-0.0242	-0.0389	24.2867
7	0.5077	0.1909	0.4650	-0.1347	-0.0492	-0.1456	24.2802
8	0.5208	0.2337	0.6409	-0.1330	-0.0293	-0.1252	24.3694
9	0.3869	0.1464	0.2208	-0.1371	-0.0284	-0.1700	26.3887
10	0.4982	0.1971	0.4800	-0.1324	-0.0433	-0.1050	24.1612
J_3 = ISEU							
1	0.8777	0.3148	0.9526	-0.2481	-0.0397	-0.2823	9.1623
2	0.5555	0.3814	0.8869	-0.1372	-0.0202	0.1419	8.3174
3	0.5563	0.3061	0.9275	-0.1482	-0.0233	0.0671	7.8980
4	0.6266	0.1256	0.4052	-0.1592	-0.0355	-0.2635	6.8632
5	**0.6009**	**0.1057**	**0.6995**	**-0.1737**	**-0.0433**	**-0.2727**	**6.7545**
6	0.5973	0.0993	0.7346	-0.1668	-0.0305	-0.1524	6.8981
7	0.6081	0.1621	0.5460	-0.1482	-0.0427	-0.2303	6.8985
8	0.6238	0.1257	0.5180	-0.1613	-0.0363	-0.1739	6.8419
9	0.6408	0.0950	0.5841	-0.1812	-0.0567	-0.4255	6.8749
10	0.5708	0.1228	0.4230	-0.1643	-0.0344	-0.2417	6.9032

Appendix E4: Tuning the NPID controller gain using performance criteria of IAEU, ITAEU, and ISEU without decoupling (WoD).

No of Optimization	K_{p1}	K_{i1}	K_{d1}	K_{p2}	K_{i2}	K_{d2}	**Fitness value**
J_1 = IAEU							
1	0.7066	0.0127	0.7822	-0.0937	-0.0097	-0.2257	23.1898
2	0.9434	0.0500	0.6855	-0.0690	-0.0104	-0.1987	24.6315
3	0.3944	0.0162	0.7720	-0.1979	0.0022	-0.1259	32.5280
4	0.7092	0.0082	0.7689	-0.0961	-0.0090	-0.2880	22.7332
5	0.8940	0.1538	0.5104	-0.0553	-0.0091	0.0657	28.8389
6	**0.5339**	**0.0039**	**0.7891**	**-0.1161**	**-0.0099**	**-0.2992**	**22.5879**
7	0.4438	0.0150	0.5762	-0.1415	-0.0098	-0.3949	23.4484
8	0.6709	0.0039	0.7755	-0.1035	-0.0096	-0.3594	22.7640
9	0.9958	0.1333	0.5070	0.0107	-0.0080	0.0973	26.5996
10	0.7811	0.0423	0.4808	-0.0400	-0.0074	-0.1022	24.0996
J_2 = ITAEU							
1	0.9890	0.3460	0.7676	0.0226	-0.0053	-0.2304	45.4604
2	0.8931	0.5666	0.7711	0.0104	-0.0077	0.1223	44.5324
3	0.9832	0.4122	0.7265	0.0869	-0.0137	-0.4636	104.3170
4	0.8359	0.1930	0.6952	-0.0400	-0.0093	-0.1645	38.6331
5	0.9961	0.2893	0.5682	-0.0192	-0.0058	-0.2231	44.1785
6	**0.9595**	**0.2886**	**0.1954**	**-0.0073**	**-0.0082**	**-0.0198**	**32.8064**
7	0.9993	0.1978	0.6141	-0.0417	-0.0102	-0.1035	36.1073
8	0.9528	0.1563	0.4256	-0.0596	-0.0109	-0.1208	38.5913
9	1.0000	0.6480	0.4900	-0.0444	-0.0212	-0.0498	50.2671
10	0.9986	0.1707	0.6078	-0.0480	-0.0116	-0.1295	37.3383
J_3 = ISEU							
1	0.4293	0.0193	0.5368	-0.1589	-0.0062	-0.4221	8.4465
2	0.4833	0.0087	0.7474	-0.1371	-0.0061	-0.2652	8.6567
3	0.6052	0.0069	0.3934	-0.1556	-0.0062	-0.4635	8.7903

4	**0.3125**	**0.0156**	**0.3301**	**-0.2332**	**-0.0080**	**-0.4951**	**8.1969**
5	0.9748	0.1936	0.6680	-0.0386	-0.0036	-0.0411	11.6363
6	0.4924	0.0217	0.6163	-0.1380	-0.0084	-0.3803	8.5828
7	0.2663	0.0108	0.0907	-0.2271	-0.0079	-0.4443	8.3011
8	0.3062	0.1599	0.7366	-0.2634	-0.0064	-0.4746	9.7923
9	0.3255	0.0392	0.4942	-0.2304	-0.0027	-0.4591	8.5255
10	0.7489	0.0234	0.6964	-0.0642	-0.0051	-0.1365	9.5820

Appendix E5: Tuning the FOPID controller gain using performance criteria of IAEU, ITAEU, and ISEU with decoupling (WD).

No of Optimizatio	K_{p1}	K_{i1}	K_{d1}	K_{p2}	K_{i2}	K_{d2}	λ_1	λ_2	μ_1	μ_2	**Fitness value**
J_1 = IAEU											
1	0.5166	0.1555	0.4514	0.3676	-0.3511	-0.1822	0.8131	0.2171	0.7002	0.5429	19.4421
2	**0.4740**	**0.1026**	**0.3629**	**-0.0610**	**-0.0808**	**-0.2865**	**0.9154**	**0.7037**	**0.7456**	**0.9516**	**13.0855**
3	0.5958	0.2741	0.5576	0.0704	-0.1620	-0.4418	0.8140	0.5633	0.8254	0.8714	15.4657
4	0.0156	0.2519	0.5321	-0.2333	0.2904	-0.4050	0.8726	0	0.5031	0.2415	42.1314
5	0.6802	0.1679	-0.2277	0.0744	-0.1706	-0.3562	0.6397	0.4785	0.0089	0.8957	19.4693
6	0.0303	0.5106	0.8266	0.2259	-0.3486	0.0314	0.7505	0.1349	0.6400	0.0313	25.4295
7	0. 6622	0.2602	0.4910	0.0697	-0.1260	-0.3737	0.8055	0.5860	0.8783	0.7454	14.7969
8	0.6170	0.0607	-0.2266	-0.3454	-0.0217	0.2676	0.9602	0.9240	0.0177	0.0128	13.9480
9	0.1703	0.5745	0.2917	0.1900	-0.0715	-0.4454	0.2360	0.8776	0.9260	0.3437	18.9649
10	0.3679	0.2177	0.3089	0.6014	-0.3242	-0.3717	0.6812	0.2759	0.8387	0.2044	19.7026
J_2 = ITAEU											
1	**0.0985**	**0.1878**	**0.4485**	**-0.0700**	**-0.0436**	**-0.0981**	**0.8736**	**0.7817**	**0.5002**	**0.7133**	**24.3871**
2	0.1175	0.2441	0.5979	0.4579	-0.4575	-0.1546	0.8738	0.1532	0.6146	0.4914	32.9301
3	0.0072	0.1222	0.6447	0.0339	-0.0583	-0.2074	0.8665	0.6395	0.2775	0.9389	31.8640
4	0.2934	0.1715	0.3269	0.0323	-0.0575	-0.2935	0.9381	0.9037	0.9349	0.4228	25.5924
5	0.5175	0.1688	0.4574	-0.0350	-0.0369	-0.1981	0.9575	0.8206	0.9113	0.6857	25.4927
6	0.3827	0.2365	0.5182	0.3278	-0.2544	-0.1481	0.8834	0.2842	0.9219	0.3985	32.7330
7	0.4340	0.1372	0.3103	0.1805	-0.2038	-0.1890	0.9594	0.3079	0.9197	0.6654	30.9844
8	0.1955	0.3073	0.7099	0.0405	-0.0718	-0.3557	0.7710	0.6619	0.8469	0.6477	33.7571
9	0.1955	0.3073	0.7099	0.0405	-0.0718	-0.3557	0.7710	0.6619	0.8469	0.6477	33.7571

10	0.1274	0.1853	0.3732	0.1022	-0.0513	-0.3169	0.8268	0.9028	0.5512	0.3603	27.5769
					J_3 = ISEU						
1	0.0184	0.4530	0.0463	0.6554	-0.3564	-0.4776	0.2704	0.3181	0.8855	0.2930	8.6621
2	0.3706	0.0594	0.1053	0.3241	-0.1156	-0.4450	0.9740	0.5727	0.1496	0.2277	6.8097
3	0	0.3530	0.4401	0.0840	-0.0305	-0.2438	0.5192	0.9457	0.4763	0.1535	7.1844
4	0.8312	0.0281	-0.4104	-0.1368	-0.0166	-0.0179	0.8403	0.7523	0.2881	0.5704	9.9955
5	**0.3713**	**0.0656**	**-0.0003**	**0.2663**	**-0.1688**	**-0.4284**	**0.9976**	**0.4809**	**0.9958**	**0.4262**	**6.6998**
6	0.7820	0.0674	0.0265	-0.2115	0.0318	-0.0434	0.0637	0.0014	0.8888	0.4801	16.3645
7	0.1444	0.1469	0.4948	-0.0234	-0.0672	-0.0719	0.9352	0.5654	0.4130	0.6669	7.5960
8	0.0273	0.2147	0.4627	0.0098	-0.4998	0.4050	0.7305	0.0607	0.4328	0.0656	11.1338
9	0.0997	0.3109	0.1070	0.1996	-0.0274	-0.3805	0.3932	0.9793	0.6821	0.0974	7.4936
10	0.3843	0.2221	-0.0134	0.5786	-0.3608	-0.4455	0.3087	0.3024	0.1277	0.3763	8.2737

Appendix E6: Tuning the FOPID controller gain using performance criteria of IAEU, ITAEU, and ISEU without decoupling (WoD).

No of Optimizatio	**K_{p1}**	**K_{i1}**	**K_{d1}**	**K_{p2}**	**K_{i2}**	**K_{d2}**	**λ_1**	**λ_2**	**μ_1**	**μ_2**	**Fitness value**
					J_1 = IAEU						
1	0.4398	0.0273	0	0.1233	-0.1196	-0.4039	0.5672	0.4028	0.6098	0.7518	24.4113
2	0.5107	0.2747	0.6757	0.2639	-0.1727	-0.2338	0.4692	0.2698	0.6805	0.6860	25.7166
3	0.3241	0.2688	0.6852	0.1634	-0.0627	-0.2095	0.5333	0.4832	0.5264	0.4450	24.2606
4	0.7692	0.3977	-0.4945	0.3211	-0.1320	-0.2389	0.1257	0.3231	0.0297	0.3003	27.3889
5	0.0091	0.0677	0.2849	-0.2472	0.0296	-0.1890	0.5943	0.0043	0.7383	0.9970	27.3341
6	0.6309	0.1327	0.3950	0.1809	-0.1433	-0.1328	0.6316	0.2441	0.9033	0.7332	27.1871
7	**0.3748**	**0.0362**	**0.7398**	**0.0320**	**-0.0214**	**-0.2835**	**0.7500**	**0.7415**	**0.4851**	**0.8583**	**23.6993**
8	0.9340	0.0716	0.4902	0.7058	-0.3003	-0.4846	0.1235	0.2386	0.9421	0.2358	25.9335
9	0.3211	0.7210	0.5820	0.2475	0.0936	0.1224	0.2745	0.0017	0.9043	0.4331	34.6520
10	0.0734	0.1816	0.9003	0.0426	-0.0732	-0.1712	0.5678	0.3301	0.6459	0.8292	26.5310
					J_2 = ITAEU						
1	0.6377	0.2761	0.4946	0.7175	-0.3855	-0.3827	0.7844	0.1459	0.9421	0.2013	37.0198
2	0.9805	0.6218	0.7270	0.5473	-0.4060	-0.1793	0.8352	0.1355	0.8419	0.4898	34.0461
3	0.3457	0.9063	0.7413	0.2153	-0.1761	-0.0918	0.5543	0.2000	0.8268	0.6664	33.6823
4	0.9893	0.1727	0.5470	0.0343	-0.0304	-0.0591	0.6322	0.5268	0.8383	0.6537	29.8769
5	**0.2091**	**0.8434**	**0.9669**	**-0.0059**	**-0.0133**	**-0.0451**	**0.3664**	**0.8467**	**0.7274**	**0.9500**	**28.8029**

6	0.6076	0.5898	0.6351	0.7275	-0.3838	-0.3820	0.5724	0.1656	0.9421	0.2145	32.2394
7	0.8809	0.6393	0.7026	0.5803	-0.3748	-0.2115	0.8664	0.1648	0.7950	0.3648	35.2174
8	0.4362	0.9844	0.8468	0.3576	-0.2962	-0.0975	0.5387	0.1365	0.8513	0.6972	34.1271
9	0.4768	0.0578	0.9116	-0.2028	0.1506	0.1718	0.8876	0.0095	0.6881	0.8568	51.7582
10	0.9950	0.0786	0.5509	0.1664	-0.0849	-0.2748	0.7906	0.4452	0.9332	0.6098	33.8130
J_3 = ISEU											
1	0.4725	0.1470	0.1319	0.4186	-0.3170	-0.3291	0.2439	0.1833	0.5983	0.5693	9.1445
2	0.3606	0.0481	0.3497	-0.0185	-0.0743	0.0364	0.4033	0.2353	0.5070	0.2193	11.3341
3	0.3658	0.0451	0.2063	0.1765	-0.0493	-0.4547	0.6618	0.6231	0.6230	0.4112	17.8112
4	0.2287	0.0732	0.3265	0.4207	-0.4349	-0.2673	0.2700	0.1098	0.5146	0.6578	9.0934
5	0.9998	0	-0.4014	0.0788	-0.2400	0.1066	0.2445	0.0598	0.0039	0.1055	12.0588
6	**0.2106**	**0.0156**	**0.1006**	**0.0293**	**-0.1036**	**-0.2912**	**1.0000**	**0.2970**	**0.6455**	**0.6317**	**8.2932**
7	0.5957	0.1052	0.2086	0.0973	-0.0533	-0.2599	0.6130	0.4685	0.6237	0.4842	9.2114
8	0.2996	0.1630	0.3974	0.3805	-0.3398	-0.2866	0.1706	0.1624	0.4459	0.5853	9.1767
9	0.4344	0.2507	0.3788	-0.1437	0.0000	0.0708	0.3647	0.3086	0.5429	0.3498	12.8025
10	0.1529	0.0697	0.0523	0.1380	-0.2588	-0.1085	0.2737	0.0782	0.7241	0.7811	10.1730

Appendix F: Appendixes related to steady state and parameter of DC

Appendix F1: Steady state operating condition of a nine (9) inch diameter and eight (8) trays of wood and berry distillation column system.

Table F1.1 Typical steady state operating condition [24].

Steam	Flow [lb/min]	Composition [wt.% methanol]
Overhead	1.18	96.0
Reflux	1.95	96.0
Bottoms	1.27	0.5
Feed	2.45	46.5
Steam	1.71	----
		Temperature [^{o}F]
	Reflux	151.7
	Feed	168.0
	Steam	233.0
	Condensate	277.5
	Reboiler	209.6
	Plate 1	203.6
	Plate 2	194.4
	Plate 3	181.2
	Plate 4	172.9
	Plate 5	164.1
	Plate 6	156.8
	Plate 7	152.1
	Plate 8	148.5
	Condenser	143.9

Appendix F2: Parameters values for of a nine (9) inch diameter and eight (8) trays of wood and berry distillation column system.

Table F2.1. Parameters values for the simulation of distillation column [20], [57].

Description	**Symbol**	**Value**	**Unit**
Flow rate of liquid distillate.	D_L	27.8	lbmol/min
Composition of liquid distillate.	X_D	0.899	mol fraction
Flow rate of vapor distillate.	D_V	200	lbmol/min
Composition of vapor distillate.	Y_D	0.947	mol fraction
Liquid holdup in reflux drum.	M_D	8.056	lbmol
Reflux flow rate.	R (U_1)	400.864	lbmol/min
Flow rate of liquid Feed.	F_L	800	lbmol/min
Composition of liquid feed.	Z_L	0.60	mol fraction
Flow rate of vapor feed.	F_L	200	lbmol/min
Composition of vapor feed.	Z_V	0.53	mol fraction
Composition of bottom product,	X_B	0.481	mol fraction
Liquid holdup in column base,	M_B	4.897	lbmol
Vapor boil-up rate,	V_B (U_2)	428.66	lbmol/min
Hydraulic time constant,	β	3.6	Second
Relative volatility,	α	2.0	_
Total number of trays,	NT	8	_
Feed tray location,	NF	3	_
Internal liquid flow rate	Ln	_	_
Reference value of internal flow rate	Ln_0	_	_
Reference molar holdup for nth tray	Mn_0	_	_